

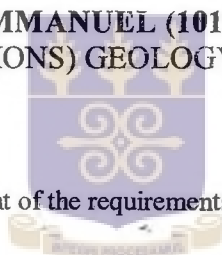
**Hydrochemical and Isotopic Characterization of Groundwater in the
Buem, Voltaian and Togo Formations of the Volta Region, Ghana.**

A thesis presented to the

**GEOLOGY DEPARTMENT, UNIVERSITY OF GHANA
LEGON**

BY

**NTI EMMANUEL (10120836)
B.Sc. (HONS) GEOLOGY, 1998**



In partial fulfillment of the requirements for the degree of

MASTER OF PHILOSOPHY

In

GEOLOGY

June, 2005



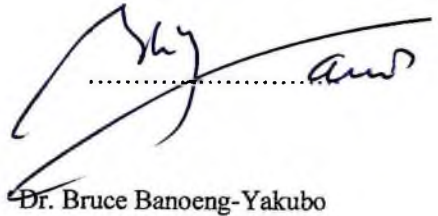
G 379689
TD319-G45N87
bltc c.1

I hereby declare that, except for references to other people's work; which have been duly acknowledged, this dissertation is the result of my own research work carried out in the Department of Geology under the supervision of Dr. Bruce Banoeng-Yakubo.



.....

Nti Emmanuel
Student



.....

Dr. Bruce Banoeng-Yakubo
Supervisor



Specially dedicated to God Almighty and all manner of persons who contributed to the success of this work.



ACKNOWLEDGEMENTS

Various contributions from a number of personalities and groups without which this work would not have been possible need to be acknowledged.

- My supervisor, Dr. Bruce Banoeng-Yakubo. You directed every step I took and offered useful criticisms. Thank you, Doctor.
- I cannot forget the special input of DANIDA-ENRECA, for making funds available for the collection and analysis of my samples. I say a big thank-you.
- It is with a deep sense of gratitude that I mention Prof. Danso and Mr. Sarquah of Ecological Laboratory of the University of Ghana. You put your shoulder to the wheel in getting my samples analyzed.
- I express special appreciation to all the Lecturers of the Geology Department especially, Dr. David Atta-Peters, Dr. Thomas Armah, Dr. Jacob Kutu, Dr. Frank Nyame and Dr. Johnson Manu for their sound support.
- I appreciate the role played by Dr. Boateng and Mr. Julius Awuni of Community Water and Sanitation Agency (CWSA), Ho in helping me get access to information on some boreholes in the study area.
- A special mention is made of the non-teaching staff of the Geology Department especially Mr. John Mensah for his special role in this work. Thank you John.
- Credit is given to Harrison Komladzei of CSIR-Accra for helping me with my maps.
- Finally, I sincerely thank my course mates for their tolerance and care.

TABLE OF CONTENTS

ACKNOWLEDGEMENTS.....	iv
TABLE OF CONTENTS.....	v
LIST OF TABLES	viii
LIST OF FIGURES.....	ix
CHAPTER ONE.....	1
INTRODUCTION.....	1
1.1 Background and Justification of Study.....	1
1.2 Objective of Study.....	3
1.3 Methodology.....	3
1.3.1 Desk study and Field Data Collection.....	4
1.3.2 Laboratory Data Analysis.....	4
1.3.3 Results Presentation and Interpretation.....	5
CHAPTER TWO.....	5
LITERATURE REVIEW.....	6
CHAPTER THREE.....	17
STUDY AREA.....	17
3.0 Introduction.....	17
3.1 Location.....	17
3.2 Topography and Drainage	17
3.3 Climate and Vegetation	20
3.4 Soils, Geology and Hydrogeology	22
3.4.1 Soil.....	22
3.4.2 Geology.....	23
3.4.2.1 The Buem Formation.....	25
3.4.2.2 The Voltaian System	26
3.4.2.3 The Togo Formation.....	28
3.5 Hydrogeology	29
3.5.1 Togo and Buem Formations	29
3.5.2 The Voltaian System	31
3.6 Socio-economic Activities.....	32
CHAPTER FOUR.....	33

METHODOLOGY	33
4.1 Desktop and field data collection	33
4.2 Field data collection.....	34
4.2.1 Collection of major ion sample	35
4.2.2 Collection of stable isotope sample.....	35
4.2.3 pH measurements	35
4.2.4 Electrical Conductivity measurements	36
4.2.5 Alkalinity measurements	36
4.3 Laboratory data analysis.....	37
4.3.1 Major and minor ions analysis.....	38
4.4 Methodology For The Presentation And Interpretation Of Results	41
4.4.1 Calculation of Carbon Dioxide Partial Pressure in the Sub-surface	41
4.4.2 Statistical Methods	42
4.4.2 Graphical Methods	42
CHAPTER FIVE	45
RESULTS AND DISCUSSION.....	45
5.1 Hydrochemistry	45
5.1.1 pH distribution.....	47
5.1.2 Electrical Conductivity (EC) distribution.....	53
5.1.3 Total dissolved solids (TDS) distribution.....	57
5.1.4 Groundwater Temperature distribution	61
5.1.5 Sodium distribution	63
5.1.6 Potassium distribution	70
5.1.7 Calcium distribution	73
5.1.8 Magnesium distribution.....	80
5.1.9 Bicarbonate distribution.	85
5.1.10 Sulphate distribution.....	91
5.1.11 Chloride distribution.....	93
5.1.12 Nitrate distribution.....	95
5.2 Hydrochemical facies	96
5.2.1 Hydrochemical Facies in the study area.....	97
5.2.1.1 Calcium+Magnesium-Bicarbonate facies.....	98

5.2.1.2 Calcium-Bicarbonate facies.....	102
5.2.1.4 Magnesium-Bicarbonate facies.	109
5.2.1.5 Calcium+Magnesium-Chloride Facies.....	110
5.4 Environmental Isotopes.....	111
5.4.1 Relationship between oxygen-18 and deuterium.....	111
5.4.2 Relationship between Deuterium and Altitude.....	116
5.4.3 Relationship between Oxygen-18 and Hydrochemistry.....	117
CHAPTER SIX.....	120
CONCLUSION AND RECOMMENDATION.....	120
6.1 Conclusion.....	120
6.2 Recommendations.....	124
REFERENCES.....	126
APPENDIX A.....	140
APPENDIX A2.....	141
APPENDIX B.....	142



LIST OF TABLES

Table 1.1	The classification of the Voltaia Formation.....	30
Table 5.1	The summary of the physico-chemical parameters in the various Formation.....	45
Table 5.2	The statistical summary of the water types in the Buem Formation.....	116
Table 5.3	The statistical summary of the water types in the Voltaian Formation ...	116
Table 5.4	The statistical summary of the water types in the Togo Formation.....	116
Table 5.5	The analytical results of deuterium/ oxygen-18, Formation, sample location, temperature, depth and chemical parameters.....	138



Figure 3.1 Inset: Map of Ghana showing the study area.	19
Figure 3.2 Geological map of the study area.	24
Figure 5.2a The scatter plot of pH and Total dissolved ions in the study area.	49
Figure 5.2b The scatter plot of pH and Bicarbonate in the study area.	49
Fig 5.3 Scatter plot of pH and carbon dioxide partial pressure in the study area.	51
Fig 5.4 Scatter plot of EC and TDS in the study area.	55
Fig 5.5 Scatter plot of EC and HCO_3^- in the study area.	55
Figure 5.6 a,b,c and d Scatter plot of EC (Type I) and Ca, Mg, Na and HCO_3^- in the area.	56
Figure 5.7 a,b,c and d Scatter plot of Ca, Mg, Na and HCO_3^- against EC (Type II) in the area.	57
Fig 5.8a Scatter plot of TDS against HCO_3^- in the study area.	59
Fig 5.8b Scatter plot of TDS against Na/Na+Ca in the study area.	60
Figure 5.9 Scatter plot of TDS and Na in the various aquifers in the area.	61
Figure 5.10 Scatter plot of TDS and Ca in the various aquifers in the area.	62
Figure 5.11 Scatter plot of TDS and Mg in the various aquifers in the area.	62
Figure 5.12 Scatter plot of depth of borehole and water temperature in the study area.	64
Figure 5.13 a,b,c. Scatter plot of sodium (Group I) and TDS , EC and HCO_3^- in the study area.	67
Figure 5.14 Scatter plot of sodium (group II) and (a) TDS (b) EC (c) HCO_3^- (d) Ca in the study area.	68
Figure 5.15 Scatter plot of sodium (group III) and (a) TDS (b) EC (c) HCO_3^- (d) Ca in the study area.	69
Figure 5.15 e Scatter plot of sodium (group III) and Cl in the study area.	70
Figure 5.16 Scatter plot of potassium and TDS in the study area.	72
Figure 5.17 Scatter plot of potassium and EC in the study area.	73
Figure 5.18 Scatter plot of potassium and HCO_3^- in the study area.	73
Figure 5.19a Scatter plot of Calcium and pH of the group I type in the study area.	75
Figure 5.19b Scatter plot of Calcium and TDS of the group I type in the study area.	75
Figure 5.20 Scatter plot of Calcium and HCO_3^- of the group I type in the study area.	76
Figure 5.21 Scatter plot of Calcium and Na of the group I type in the study area.	77

Figure 5.22 Scatter plot of Calcium and pH of the group II type in the study area. ...	78
Figure 5.23 Scatter plot of Calcium and TDS of the group II type in the study area. .	79
Figure 5.24 Scatter plot of Calcium and HCO ₃ of the group II type in the study area.	79
Figure 5.25 Scatter plot of Calcium and Na of the group II type in the study area. ...	80
Figure 5.26 Scatter plot of Calcium and Mg of the group II type in the study area. ..	81
Figure 5.27 Scatter plot of Magnesium and pH in the study area.	82
Figure 5.28 Scatter plot of Magnesium and TDS in the study area.	83
Figure 5.29 Scatter plot of Magnesium and Bicarbonate in the study area.	83
Figure 5.30 Scatter plot of Magnesium and Sodium in the study area.	85
Figure 5.31 Scatter plot of bicarbonate and total dissolved solids in the area.	87
Figure 5.32 Scatter plot of bicarbonate and pH in the area.	88
Figure 5.33 Scatter plot of HCO ₃ ⁻ and Na in the study area.	90
Figure 5.34 Scatter plot of HCO ₃ ⁻ and Ca in the study area.	90
Figure 5.35 Scatter plot of HCO ₃ ⁻ and Mg in the study area.	91
Figure 5.36 Scatter plot of Ca and SO ₄ ²⁻ in the study area.	93
Figure 5.37 Scatter plot of pH and sulphate in the study area.	94
Figure 5.38 Scatter plot of TDS and chloride in the study area.	95
Figure 5.39 Scatter plot of Na and chloride in the study area.	96
Figure 5.40 Piper plot of samples in the study area.	99
Figure 5.41 Fingerprint diagram of samples in the Ca+Mg-HCO ₃ facies.	101
Figure 5.42b Scatter plot of pH and Ca, Na and Mg of the Ca+Mg-HCO ₃ facies. ...	103
Figure 5.43 Fingerprint diagram of groundwater of the Calcium-Bicarbonate facies	104
Figure 5.44a Scatter plot of bicarbonate and Ca, Na and Mg of the Ca-HCO ₃	105
Figure 5.44b Scatter plot of EC and Ca, Na and Mg of the Ca-HCO ₃ facies.	105
Figure 5.45 Fingerprint diagram of groundwater of the Sodium-Bicarbonate facies	109
Figure 5.46 Scatter plot of TDS and Ca, Na and Mg of the Na-HCO ₃ ⁻ facies in the study area.	109
Figure 5.47 Scatter plot of pH against Ca, Na and Mg in the Na-HCO ₃ facies.	110
Figure 5.48 Scatter plot of sodium and chloride of the Sodium-Bicarbonate facies.	110
Figure 5.49 Scatter plot of Delta Deuterium and delta Oxygen-18 of groundwater samples in the study area.	115
Figure 5. 50 Distribution of delta Deuterium values in the study area.	116

Figure 5.51 Scatter plot of Del Deuterium and altitude of samples site in the study area. 118


Figure 5.52 Scatter plot of Delta Deuterium and temperature of samples in the study area. 119

Figure 5.53 Scatter plot of Delta Oxygen-18 and sodium, calcium and magnesium in the study area..... 119

Figure 5.54 Scatter plot of Delta Oxygen-18 and electrical conductivity in the study area. 120



Variation in groundwater chemistry and isotopic composition has been observed in the northern part of the Volta Region. The geology of the study area consists of quartz schist, quartzitic sandstone, shales, mudstones and siltstone. The extent to which the water chemistry and isotopic composition has been affected by geology is however not known. This study therefore seeks to determine the general chemical character of the groundwater in relation to the different lithologies and determine the source(s) and origin of recharge to the aquifer systems. This study combines geology with the physico-chemical and isotopic data of groundwater samples systematically obtained from boreholes in the area.



The distribution of physico-chemical parameters define three hydrochemical zones controlled mainly by mineralogy and degree of weathering in the various lithologies: The quartz schist and quartzitic sandstone aquifer is dominated by slightly acidic (mean pH is 5.9) and relatively low TDS; the shale aquifer by near neutral (mean pH is 6.8) and medium TDS; and mudstones and siltstone aquifer by neutral (mean pH is 7.2) and relatively high TDS. However, apart from the slightly acidic water occurring in some parts of the south, which falls below the accepted lower limit of 6.5 (WHO, 1993), the chemical composition of the groundwater in the area is generally of acceptable chemical quality.

The quartz schists, quartzitic sandstones and shales aquifers are characterized by Calcium+Magnesium-Bicarbonate, Calcium-Bicarbonate and Magnesium Bicarbonate water types. These water types are controlled mainly by dissolution of

plagioclase feldspar, sericites and minor carbonate materials. Sodium-Bicarbonate facies on the other hand is found in the mudstone and siltstone aquifers and influenced mainly by cation exchange and/or dissolution of albite-rich plagioclase.

The relationship between deuterium and oxygen-18 shows two classes of water. The relatively enriched samples are confined to the south while the depleted samples are in the north indicating, probably, continental or latitude effect. However, all the samples lie along the global meteoric water line suggesting that groundwater recharge in the area is by rainfall with no evaporation prior to infiltration. This may indicate rapid flow towards the potentiometric surface.



CHAPTER ONE

INTRODUCTION

1.1 Background and Justification of Study.

Groundwater is a major source of drinking water supplies in the Jasikan, Kadjebi and Nkwanta districts of the Volta region. Greater part of the area lies within the Buem Formation which is made up of shales, sandstones and quartzitic sandstones. However, at the fringes, the Voltaian siltstones and mudstone and the Togo shales and quartzites do occur. Almost all the communities in the area depend entirely on hand pump-fitted or mechanized boreholes for their daily source of water supply especially during the dry season when all the ephemeral streams have gone dry. Moreover, parts of the study area are known to have water-borne diseases such as guinea worm and bizzihara caused by the drinking of contaminated surface water bodies. The reliance of the local population on unwholesome surface water has greatly affected their productivity and a resultant rise in the poverty level.

Because groundwater is generally believed to be of acceptable quality and requires little or no treatment in the area, it is adjudged a better alternative source of potable water for the local population. This has prompted the involvement of the Government of Ghana and other bodies such as Danish International Development Agency (DANIDA), Canadian International Development Agency (CIDA), Catholic Relief Agency, Evangelical Presbyterian Church (E.P.C) among others to provide hand-dug wells and boreholes for communities in the area. The exploitation of the groundwater

resources in the area started as far back as the colonial times with the sinking of large diameter wells. Currently, there are over 500 boreholes in the study area (CWSA, 2000). These boreholes are of various depths ranging from 24 to 88m tapping different aquifers.

The provision of groundwater by the various agencies has churn out a lot of invaluable data such as lithological data, aquifer characteristics and water quality data which, when given due attention, could enable a better understanding of the water chemistry and groundwater occurrence in the area. Since a major component of the groundwater development is the quality of the groundwater, for an aquifer to be a reliable source of groundwater, not only must predictable quantities of water be available, but also the water must be of predictable and wholesome chemical composition. Though, the quality of groundwater in the area is generally good, there are localities where the quality is slightly affected by the taste, odour and hardness. These physical characteristics are mostly caused by the chemical composition of the water which generally depend on the geology (Hem, 1989). It is however not known the extent to which the chemical composition is affected by the geology. With the upsurge in the number of boreholes and increase in the population, there is the possibility of change in the water quality with time.

Though it is part of almost all the drilling programs in the area to assess the quality of groundwater before its use, little or no attempt has been made to monitor changes in water quality from time to time. Moreover, knowledge of the source(s) of recharge and the various processes and conditions that give rise to the composition of the water in the area is scanty. Obviously, this is a major setback to the rational management of

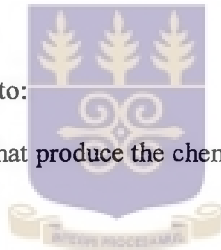
the groundwater resource in the study area. As a result, this present work seeks to combine geological and hydrochemical information to determine the areal distribution of groundwater types based on the major ions and the various processes that influence the water composition. Furthermore, the study will integrate hydrochemical and stable isotopic data to ascertain the causes of hydrochemical variations and determine the source(s) of recharge to the aquifer system in the area.

1.2 Objective of Study

The main aim of this research is to determine the general chemical character of the groundwater in relation to the different lithologies and establish the hydrochemical facies of the area.

The specific objectives include to:

- a. identify the processes that produce the chemical and isotopic compositions of the groundwater and
- b. determine the source(s) and origin of recharge to the aquifer systems.



1.3 Methodology

The systematic way of carrying out the research can broadly be divided into four main parts. These are:

1. Desk study of all available data
2. Field data collection

3. Laboratory data analyses and
4. Results presentation and interpretation

1.3.1 Desk study and Field Data Collection

Geological and topographical maps of the study area were obtained from the Geological Survey Department (GSD) and Ghana Survey Department, Accra respectively.

Borehole data which consisted of borehole lithological logs, pumping test results and water quality results were downloaded from the database section of the Community Water and Sanitation Agency (CWSA) office at Ho to obtain the borehole attribute data and verify whether the communities selected on the topographical map really have boreholes that could be sampled.

Seventy-one (71) water samples with their coordinates recorded using a Garmin 12 GPS device were systematically taken according to lithologies and distance from each other. The water samples comprise sixty-seven (67) groundwater and four (4) surface water from rivers. On site measurement of the physical parameters and laboratory analysis were done with standard instruments as described in Chapter Four.

1.3.2 Laboratory Data Analysis

Laboratory analysis of sodium, potassium, lithium, ammonium, calcium, magnesium, fluoride, chloride, bromide, nitrite, nitrate, phosphate and sulphate was done at the Ecological Laboratory, University of Ghana, Legon using dual- column DX-120 ion

University of Ghana <http://ugspace.ug.edu.gh>
chromatograph. On the other hand, oxygen-18 and deuterium isotopic analysis were carried out at the Geological Institute, University of Copenhagen and Institute of Physics and Astronomy, University of Aarhus, Denmark respectively. A VG Sira 10 Mass Spectrometer and Euro Vector elemental analyzer (EA; EuroPyrOH-310) were used in the determination of oxygen-18 and deuterium respectively.

1.3.3 Results Presentation and Interpretation

Field measured pH and alkalinity were used to calculate the partial pressure of carbon dioxide for all the water samples. The results for field determination of chemical and physical characteristics and other borehole attributes were presented in a tabular form and simple statistics performed using Ms Excel 2003 program. Also, compositional diagrams were constructed among the various physico-chemical parameters to observe the relationships. Moreover, the major cation and anion data were plotted on the fields of a Piper diagram and Finger print diagram to visualize the difference in the major-ion chemistry along the flow path. Furthermore, isotopic data were interpreted by comparing it with the Global Meteoric Water Line (GMWL)(Craig, 1961).

LITERATURE REVIEW

Knowledge of work done on the subject in the area of research or elsewhere is relevant in any scientific work. This will help to be make meaningful inferences and draw useful conclusions. This chapter therefore dwells on work done by various authors in the study area, in the country and around the world, and pinpoints the relevant conclusions that were drawn from them.

Groundwater occurs in many different geological formations. Nearly all rocks in the upper part of the earth's continental crust, whatever their type, origin or age, possess pores or voids. In unconsolidated granular materials, the voids are the spaces between the grains which may become reduced by compaction and cementation (Chapman, 1992). Groundwater in consolidated formations occurs in weathered and fractured zones (Acheampong ,1995; and Winograd and Thordarson, 1968). Raju and Reddy (1998) also noted that the occurrence, movement and control of groundwater, particularly in hard rocks, are governed by different factors such as topography, lithology, weathering and structures such as fractures and faults.

Lerner (1997) broadly defined recharge as the water that reaches the aquifer from any direction. Despite the fact that various sources of recharge exist, Lerner *et al.* (1990) suggested the recharge mechanism common to all of them as: direct, indirect and localized recharge. They defined direct recharge as the water added to the

groundwater reservoir in excess of soil-moisture deficits and evapotranspiration by direct vertical percolation through the vadose zone. Indirect recharge is the percolation to the water table through the beds of surface-water courses. Finally, they defined localized recharge as an intermediate form of recharge resulting from the horizontal surface concentration of water in the absence of well-defined channels.

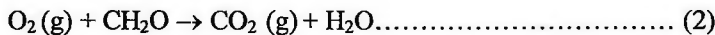
Several workers have attempted to find sources of recharge to aquifers. Groundwater recharge at the water-table of the Midwestern Basins and Arches aquifer system in parts of Indiana, Ohio, Michigan and Illinois of the U.S is primarily from infiltration of precipitation and the associated flow away from the water table within the saturated zone (Eberts *et al.* 2000). Freeze and Cherry (1979) summed up the fact that nearly all groundwater originates as rain that infiltrates through the soil. Before rainwater reaches its final destination underground, it interacts with the atmosphere, the soil environment and aquifer material.

Appelo and Potsma (1993) in discussing the constituents of rainwater stated that, the composition of rainwater is determined by the source of the water vapour and by the ions that are acquired by the water or lost from it during transport through the atmosphere. Ridder (1978) in the study of precipitation in the Netherlands concluded that, as the distance from the coast increases, the concentration of ions that are derived from seawater decreases. In the investigation of the rainwater in the US and Europe, Likens *et al.* (1977) realized a conspicuous enrichment of NO_3^- and SO_4^{2-} and concluded that these ions originated mainly from industrial and traffic fumes containing gaseous NO_x and SO_2 . As a result, Freeze and Cherry (1979) reported that the pH of precipitations in industrial areas is frequently as low as between 3 and 4. The dissolved solids in rainwater range from several milligrams per litre in

continental nonindustrial areas to several tens of milligrams per litre in coastal areas (Feth *et al.*, 1964 and Whitehead and Feth, 1964). This makes the pH of precipitation in nonurban and nonindustrial areas to be normally between 5 and 6 (Freeze and Cherry, 1979). The most important interaction of precipitation with the atmosphere results in the formation of weak carbonic acid by reaction with carbon dioxide (Hem, 1992).



Further interaction of the percolating water with the soil environment produces large amount of acid as a result of oxidation of organic matter that consumes much or all of the available dissolved oxygen (Freeze and Cherry, 1979), according to the equation 2 below:



Thus the partial pressure of carbon dioxide in the soil zone is increased. This is usually within the range 10-100 times than that in the atmosphere (Deutsch, 1997; Bolt and Bruggenert, 1978) and makes the resulting water a more aggressive weathering agent (Deutsch, 1997).

Due to the dissolution of some gases such as carbon dioxide (CO₂), oxygen (O₂), sulphur dioxide (SO₂) in rainwater, it becomes slightly to moderately acidic and an oxidizing solution that can quickly cause chemical alterations in soil or geologic materials into which it infiltrates (Freeze and Cherry, 1979). Water is commonly referred to as a universal agent. Consequently, when water which is low in dissolved substances comes in contact with reactive aquifer materials, there is a reaction, driven by disequilibrium established between the water and the solid phases or soil gases (Deutsch, 1997). The extent of this reaction is influenced by physical, chemical and

biological parameters (Davis and DeWiest, 1996). As rain falls on land, fractionation of water instantly begins. Some infiltrate into the soil and taken up by roots of plants while another moves deeper under the influence of gravity. Part of the subsurface where the empty spaces are partly filled with water and partly with air is known as the unsaturated or vadose zone. At greater depth, all the empty spaces are completely filled with water - saturation zone (Jury, Gardner and Gardner, 1991; Chapman, 1992; Fetter, 1994). Since the vadose zone is made up of a solid, liquid and gaseous phase, it is one of the most important components in the study of groundwater chemistry.

The interaction of precipitation with geologic materials releases ionic substances into solution (Freeze and Cherry, 1979; Deutsch, 1997; and Rao, 2003). The type and quantity of ions in solution depend on several factors. Appelo and Postma (1993) gave some of the factors as:

- I. Evaporation and evapotranspiration
- II. Selective uptake of ions by vegetation
- III. Decay of organic matter
- IV. Rate of dissolution
- V. Precipitation of minerals
- VI. Mixing of different water qualities and
- VII. Anthropogenic factors.

Cheboterev (1955) concluded that the composition of groundwater depends on distance along the flow path and age of water. Chapman (1992) also stated that the type and concentrations of salts depend on the geological environment, source and movement of the water. The chemical composition of groundwater is influenced by the surface and subsurface geology (Stallard and Edmand, 1983). Lyons *et al.* (1992)

University of Ghana <http://ugspace.ug.edu.gh>
concluded that the direction of flow influences the chemical composition of groundwater. The natural chemical composition of groundwater is the result of time-, temperature-, and pressure- dependent reactions among dissolved constituents in the water and minerals in the rock and soil. Helgesen *et al.* (1993) pointed out that the chemistry of groundwater is a product of any or all of the following factors: chemistry of the water entrapped in the interstices of the sedimentary rock during deposition; changes accompanying diagenesis; the lithology and structure of the soil and rock through which it has passed; the rate of flow and position along a flow path; and interchange with water from the surface or from adjacent rock units. Appelo and Postma (1993) stated that the chemical composition of groundwater is the combined result of the composition of the water that enters the groundwater reservoir and the reactions with the minerals present in the rock that may modify the water composition. They further noted that, apart from the natural processes controlling the groundwater quality, the effect of pollution such as nitrate from fertilizers and acid rain, also influences the groundwater chemistry.

By comparing the concentrations of different species in terrestrial waters in the United States (US) in a frequency plot, Davies and DeWiest (1966) were able to show that the distribution curves for different species have variable gradients and concluded that the solubility and availability of the minerals in the rocks place an upper limit on the concentration of the species in natural water. Gibbs (1970), in the study of the chemical composition of the surface waters of the world concluded that their composition is a function of rain and seawater chemistry, rock weathering and evaporation. Deutsch (1997), also, pointed out that the relative concentrations of dissolved constituents are determined by the available supply from the solid phases

and solubility of secondary minerals from weathering processes. MacDonald *et al.* (2003) noted that the chemical composition of groundwater of the Permian aquifer of Dumfries is affected basically by the infiltrating rainfall and modified by the dissolution of varying carbonate materials in the breccia, sandstone and surficial deposits. The chemical composition of the water of the alluvial plain of Tucuman province is strongly influenced by the interaction with the basinal sediments and hydrologic characteristics such as the flow pattern and time of residence. Furthermore, dissolution of soluble salts, cation exchange, calcite precipitation, weathering of aluminosilicates and gas exchange with the atmosphere also contribute to the water composition (Garcia *et al.*, 2001). The major factors controlling the distribution of hydrochemical facies in the Gaza Strip of Palestine are sand dunes and rainfall (Al-Agha *et al.*, 2004). Raji and Alagbe (1997) by investigating the hydrochemical facies of parts of Nigerian Basement Complex pointed out that apart from the lithology, the chemistry of the groundwater is affected by the rainfall and its proximity to the sea. Acheampong and Hess (1995) pointed out that silicate dissolution and cation exchange reactions are the main processes controlling solute behavior in the Southern Voltaian Sedimentary basin of Ghana. Milde *et al.* (1983) pointed out that natural processes influencing the genesis and occurrence of groundwater, however, show extreme variety from place to place in chemical composition. Groundwater composition varies from one location to another. Even within the same locality, groundwater compositions are not the same (Garcia *et al.*, 2001).

Many sedimentary rocks are made up of mixed assemblages of minerals derived from various sedimentary, igneous or metamorphic sources (Freeze and Cherry, 1979). Fetter (1994), noted that sedimentary rocks are typically composed of silicate, carbonate and/or clay minerals which may be deformed or undeformed. Since individual strata in a sedimentary terrain commonly comprise of mixed mineralogical assemblages, Freeze and Cherry, 1979, pointed out that, large difference exist in the chemistry of groundwater from bed to bed and from region to region. Despite the large variation in the chemical composition of groundwater in a sedimentary formation, many workers have used the concept of hydrochemical facies to categorize groundwater (Back, 1961, 1966; Morgan and Winner, 1962 and Seaber, 1962). Hydrochemical facies can be used to describe the bodies of groundwater in an aquifer that differ in their chemical composition (Fetter, 1994). Thomas *et al.* (1996) noted that the chemical composition of the water in the basin fill aquifer in Smith Creek Valley which is made up of poorly sorted heterogeneous sediments at the margin but sequentially change into well-sorted coarse to heterogeneous sediments to fine-grained playa sediments near the center of the basin evolve from Na-Ca-HCO₃, Na-HCO₃ to Na-Cl. Al-Agha *et al.* (2004) in their study of the clayey sandstone and silt aquifers of the Gaza Strip of Palestine concluded that two main hydrochemical facies, namely Ca+Mg-CO₃+HCO₃ and Na+K-Cl+SO₄, are predominant in the area. The groundwater chemistry of the Permian aquifer of the Dumfries, Scotland, composed of sandstone and breccia units is dominated by the Ca-Mg-HCO₃⁻ type (MacDonald *et al.*, 2003). Raji and Alagbe (1997) in studying the hydrochemical facies in parts of the Nigerian Basement Complex observed that an appreciable percentage of the water had facies in which no single cation-anion pair exceeds 50% in any study area. Garcia *et al.* (2001) concluded that the groundwater types in the alluvial plains of the Tucuman

province in Argentina are Na-HCO₃ and Na-SO₄+Cl types. Apambire *et al.* (1997) showed that two main water types occur in the Birrimian metasediment, metavolcanics and the associated granitoids of the Upper regions of Ghana, namely, the type I and II. They pointed out that the dominant ions found in type I are calcium, magnesium and bicarbonate while calcium, sodium and bicarbonate are found in type II due mainly to the dissolution of the aquifer. Acheampong *et al.* (1995) concluded that the water types found in the South Voltaian Basin in the Afram Plains area of Ghana, made up of sandstones, conglomerate and shales are mainly Ca+Mg-HCO₃, Na+K-HCO₃ and Na-HCO₃.

Stable isotopes have become an important tool in the study of geologic processes that affect surface and groundwater and serve as conservative tracers of water origin (Guendouz *et al.*, 2003). Akiti (1986) also stated that environmental isotopes have proved to be valuable in studying the infiltration process and locating recharge areas. Krabbenhoft *et al.* (1990) indicated that stable isotope of water are excellent tracers of recharge of surface water to groundwater, particular in areas where there is shallow water table. Freeze and Cherry (1979) noted that ¹⁸O and ²H serve mainly as indicators of groundwater source areas and as evaporation indicators in surface water bodies. Based on a survey of D/H variations of meteoric groundwater in the Albuquerque, New Mexico area, Yapp (1985) proposed not fewer than three separate sources of groundwater namely; seepage from the Rio Grande in the center of the basin, runoff from the Sandia and Manzano mountains along the eastern margin of the basin and a poorly understood perhaps older groundwater whose relationship with surface recharge are unknown. McLean *et al.* (2000) used stable isotopic data to

identify different recharge sources for the different groundwater types in the Lower Namoi River Catchment.

Due to the complexities in groundwater recharge in most landscapes, the meteoric signal can be significantly modified. Darling and Bath (1988) in their study of the unsaturated zone of the English Chalk observed that seasonal isotope variation in rainwater are attenuated to less than 5 % at a depth of about 5 m making the isotopic composition of the unsaturated zone very close to the long term weighted mean for rainfall and local recharge. Similar observations were made by Eichinger *et al.* (1984) in their study of the seepage velocity of water in the unsaturated Quaternary gravel near Munich. They noted that at a depth of 9 m the amplitude of variation of the precipitation input was reduced to less than 10 %.

The property that makes stable isotopes effective in groundwater studies is the tendency of some pair of isotopes to fractionate or separate into light and heavy fractions readily (Fetter, 1994). Friedman (1953) first noted that a change in concentration of H_2^{18}O was accompanied by a change in ^2H in precipitation. Craig (1961) showed that the partitioning of ^{18}O and ^2H by meteorological processes occurs in a predictable fashion. Urey (1947) concluded that isotope fractionation can be represented as an exchange of isotope between any two molecular species or phases participating in a reaction.

Before water reaches its final destination underground, it would have undergone various processes such as evaporation from the oceans, rainout, re-evaporation and runoffs. Due to the complexity of the hydrological cycle, it will be surprising that ^{18}O

and ^2H behave all that predictably. Craig (1961) in his study of continental precipitation found out that $\delta^{18}\text{O}$ and $\delta^2\text{H}$ values correlate on a global scale and define a relationship known as the Global Meteoric Water Line given by the equation:

$$\delta\text{D} = 8\delta^{18}\text{O} + 10\text{‰} \dots\dots\dots(3)$$

He further noted that deviation from the meteoric water line can be interpreted as being caused by precipitation that occurred during a warmer or colder climate than at present or by geochemical changes that occurred when water was underground. Gonfiantini *et al.* (1974) realized that the isotopic composition of the groundwater of the Chatt-el-Honda in Algeria fall along the Global Meteoric water line but shows wide scattering. They separated the samples into shallow and deep waters and realized that the deep groundwaters are isotopically lighter than the shallow groundwaters. They concluded that the deep groundwaters are ancient and originated from rains of a different climatic regime.

Mayo and Klauk (1991) in the investigation of the isotopic composition of the groundwater and surface water in the Great Salt Lake area found that most of the samples grouped on the global meteoric water line; however, deviations occurred due to evaporation and heating in thermal springs.

All the groundwater samples in the Midwestern Basins and Arches aquifer system plotted on or slightly above the meteoric water line indicating that groundwater in the area originated as atmospheric precipitation. Most of the groundwater in the aquifer system has an isotopic composition similar to the surface water in the area and concluded that they were likely recharged under similar climatic condition as present. However, few groundwater samples were found to be relatively light and they deduced that they were probably recharged in an era when the climate colder than the

present (Eberts and Lori, 2000). Based on the plot of δD versus $\delta^{18}O$ of the groundwater from the Albuquerque, New Mexico, Lambert and Balsley (1996) observed two groups that defined non-overlapping end members that are well aligned along the meteoric water line:

- a. the eastern domain having $\delta D > -86\text{‰}$ and $\delta^{18}O > -12\text{‰}$
- b. the central basin having $\delta D < -95\text{‰}$ and $\delta^{18}O > -13.2\text{‰}$

They proposed three sources of the central basin samples:

- a. May be mixing effect between baseline Rio Grande water and deuterium-depleted groundwater found typically at the greatest depth
- b. May represent recharge from river seepage under conditions of higher runoff
- c. Palaeorecharge

Kortatsi and Sekpey (1993) pointed out that the oxygen- and hydrogen- isotopic compositions of the groundwater from the Keta Basin are slightly isotopically enriched as compared to the groundwater in the Upper West Region and Upper East Region of Ghana. The oxygen- and hydrogen- isotope compositions of the samples collected from the shallow and deep groundwater of the Keta Basin plot along a seawater mixing line or evaporation line (Jorgensen and Banoeng-Yakubo, 2001). Based on isotopic data, Akiti (1986) concluded that the high chloride content of the groundwater of the Accra plains originated from the dissolution of evaporites salts in the soil. Acheampong and Hess (1995) noted that all the groundwater samples when plotted on $D/^{18}O$ diagram, lie on or close to the global meteoric water line and concluded that the groundwater in the South Voltaian Sedimentary Basin is recharged by meteoric water.

CHAPTER THREE

STUDY AREA

3.0 Introduction

Research needs to be placed in geographical and geological perspective to make interpretation meaningful. It involves knowing the study area including its geographical boundary and the physical conditions that pertain in the area. This chapter focuses on the location of the study area, topography and drainage, climate, vegetation, geology and hydrogeology.

3.1 Location

The study area covers the entire northern half of the Volta Region within the Jasikan, Kadjebi and Nkwanta Districts. It is within latitudes $8^{\circ}50'N$ and $7^{\circ}07'N$ and longitudes $0^{\circ}55'E$ and $0^{\circ}14'E$, and a geographical areal extent of 6625km^2 . The area is bounded on the east by The Republic of Togo, in the west by the Volta Lake, in the south by southern part of Volta Region and in the north by the Northern Region (Fig.3.1).

3.2 Topography and Drainage

The study area can be divided into two topographical regions. These are the heavily dissected and mountainous Togo-Buém ranges and the generally flat Voltaian Basin.

The Togo-Buém ranges form part of the fold mountains that flank the Voltaian basin on the east known as the Akwapim-Togo Ranges. It is a combination of slightly dissected and heavily dissected mountainous with sharp transition. The flat grounds are noted for their positive topographic features such as hills and ridges which were formed as a result of denudational processes. These hills form continuous ridges which change into ranges. The elevations of these ranges vary from 75 meters in the river valleys to 180 meters at Kadjebi. Occurring in the eastern part of the study area, is the mountainous heavily dissected features which were formed as a result of tectonic and erosional activities. They comprise the large Baglo-Kute range, Tutukpene range and the Shiare-Chilinga range all showing features of horst uplift and bounded on the east and west by submeridional fault (Lashmanov, 1965; Blay, 1971). Usually the ranges are separated by hilly plains, a classic example is Tutukpene and the Shiare-Chilinga ranges that are separated by hilly plains. These reliefs were not only tectonic but lithological as well, as the highlands are covered by highly resistant Togo quartzites and the quartzites-like sandstones and the flat grounds by less resistant sandstones, phyllites and sericite schists. Usually the ridges are separated by river valleys of tectonic origin, dissected by deep ravines.

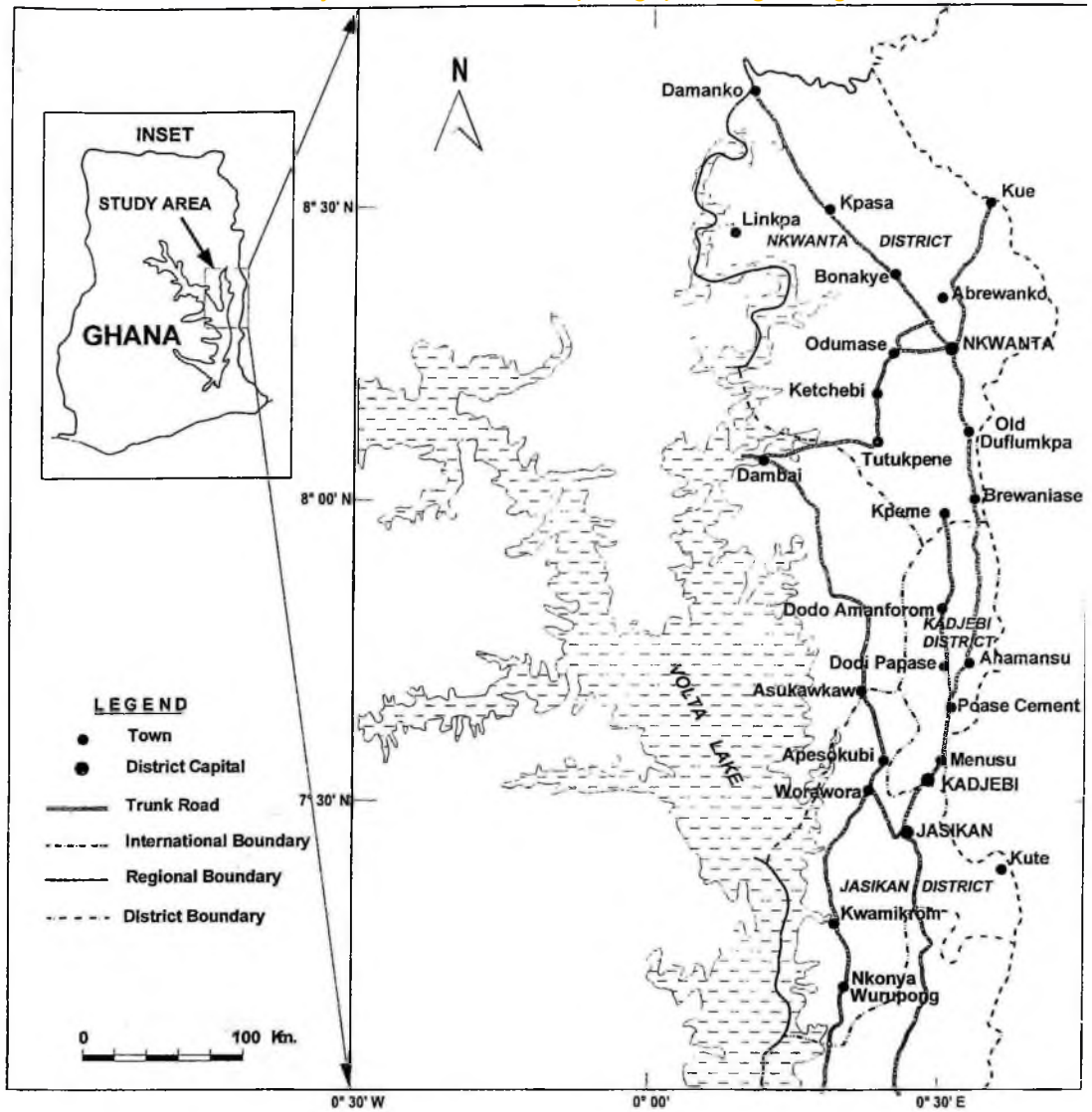


Figure 3.1 Inset: Map of Ghana showing the study area.

Some cone-like tops rise above the forest boundary and are heavily grassed, thus hampering erosion. Slopes are very steep, normally exceeding 35° to 40°. The average height of the ranges is 450m above sea level; height increases to between 600m and 900m on or near the border with Togo.

On the other hand, the Voltaian basin occupies the top western margin of the area. It is made up of gently dipping or flat-bedded rocks that are easily eroded (Dickson and Benneh, 1980). Dickson et al further stated that the erosion resulted in an almost flat and extensive plain that is between 60m and 150m.

The drainage system is fairly dense and belongs to the Oti river basin, which eventually joins the White Volta. Big rivers such as Konsu, Che, Kpassa, Dzindzi, Sabon and Chai Wulubong take their source from the hills. They are swift and deep with many rapids and waterfall. A classic example is the Sabon river that cut the rocks in its flowing path and form many rapids. Only few of the big rivers are perennial. However most of them dry up and ceases to flow in the dry season. The valleys in the uplands are V-shaped, steep sided (35 to 50°), a badly developed flood plain and a minor bed deposit development. Running in the plains, the rivers becomes quite, have distinct beds and pronounced flood-plains which attains up to 100m in some places.

2.3 Climate and Vegetation

The study area falls in the wet semi-equatorial climatic zone which is defined by two air masses namely, tropical continental and tropical maritime air masses. Due to the

University of Ghana <http://ugspace.ug.edu.gh>
relative movement of these air masses, two rainfall maxima are defined in this zone. The first rainy season is from May to June, with the heaviest rainfall in June. The second rainy season is from September to October. The mean annual rainfall in this climatic zone ranges between 1250mm and 2000mm. The dry seasons are pronounced with the temperature of about 30°C occurring between March and April and a lower temperature of 26°C in August. The mean annual temperature is approximately 27°C. Average monthly relative humidities are highest (75-80%) during the two rainy seasons and lowest (70-80%) during the rest of the year (Dickson and Benneh, 1985).

The area falls within 2 vegetative zones. These are:

- I. Guinea Savannah and
- II. Moist-semi deciduous forest

Occurring at the northwestern part of the area is the Guinea Savannah. The boundary between it and the moist-deciduous forest is not permanent; the marginal areas of the moist-deciduous forest may become part of it through man's activities. It is made up of trees such as the dawa dawa, acacia, and the shea tree, which have become adapted to the environment. They are few and widely scattered except along the margin of the moist-deciduous forest where the trees often grow quite close together. Grasses grow in tussocks and can reach a height of 3m or more. Plants look green in the wet season but change from green to yellow and the trees begin to shed their leaves soon after the rains.

The moist semi-deciduous forest on the other hand, is found in the whole of Jasikan and Kadjebi and the southern part of the Nkwanta districts. It occurs in the wet semi-

equatorial climatic region where the rainfall is between 1250mm and 1750mm and the dry seasons are clearly marked (Dickson and Benneh, 1980). It is composed of three layers or strata of trees referred to as the upper, middle and lower layers. Within the forest, it is difficult to distinguish between the lower and middle layers because they have more or less continuous canopies. Below the lower layer is found the undergrowth with the ground vegetation.

Many of the trees of the upper and middle layers exhibit deciduous characteristics during the long dry season (November to march) when the influence of the Harmattan is greatly felt.

3.4 Soils, Geology and Hydrogeology

3.4.1 Soil

As with the geology, three (3) types of soils occur in the study area. These are:

- a) Forest ochrosols
- b) Lithosols
- c) Groundwater lateritic soil

The Forest Ochrosol soils range in colors from brown to orange. They are porous, well drained and generally loamy. They contain greater quantities of nutrients and are generally alkaline. The soils support many tree crops including cocoa.

Furthermore, the lithosols soil occurs on the Togo Series on steep slopes made up of hard resistant Togo quartzites. They are immature, shallow and generally poor in nutrients.

The groundwater lateritic soil on the other hand, develops over the Voltaian shales. Their principal characteristic is the presence, at generally shallow depths below the surface of the soil, of a more or less cemented layer of ironstone called iron pan, through which rainwater does not penetrate easily. Thus the top layers of the soil become waterlogged right up to the surface in the rainy season, but dries out in the dry season. However, if the underlying iron pan is not a continuous sheet and therefore allows better downward drainage, water logging in the rainy season occurs only in the lower layers of the soil, just above the iron pan, and not right up to the surface. The texture of the soil is silty or sand loam. The color ranges from combinations of yellow and brown to yellow and gray. The soil is poor in organic matter and nutrients and the deficiency increases from south to north.

3.4.2 Geology

The area under study is characterized by a complex geology. Most parts of the area fall in the slightly metamorphosed sedimentary and ubiquitous rocks of the infracambrian sandy-mudstone Buem Formation. Also occurring at the northwestern and eastern flanks are the gently dipping beds of the Voltaian Formation and the metamorphosed upper Proterozoic sandy- clayey Togo quartzites, schists, phyllites and shales respectively (Fig. 3.2).

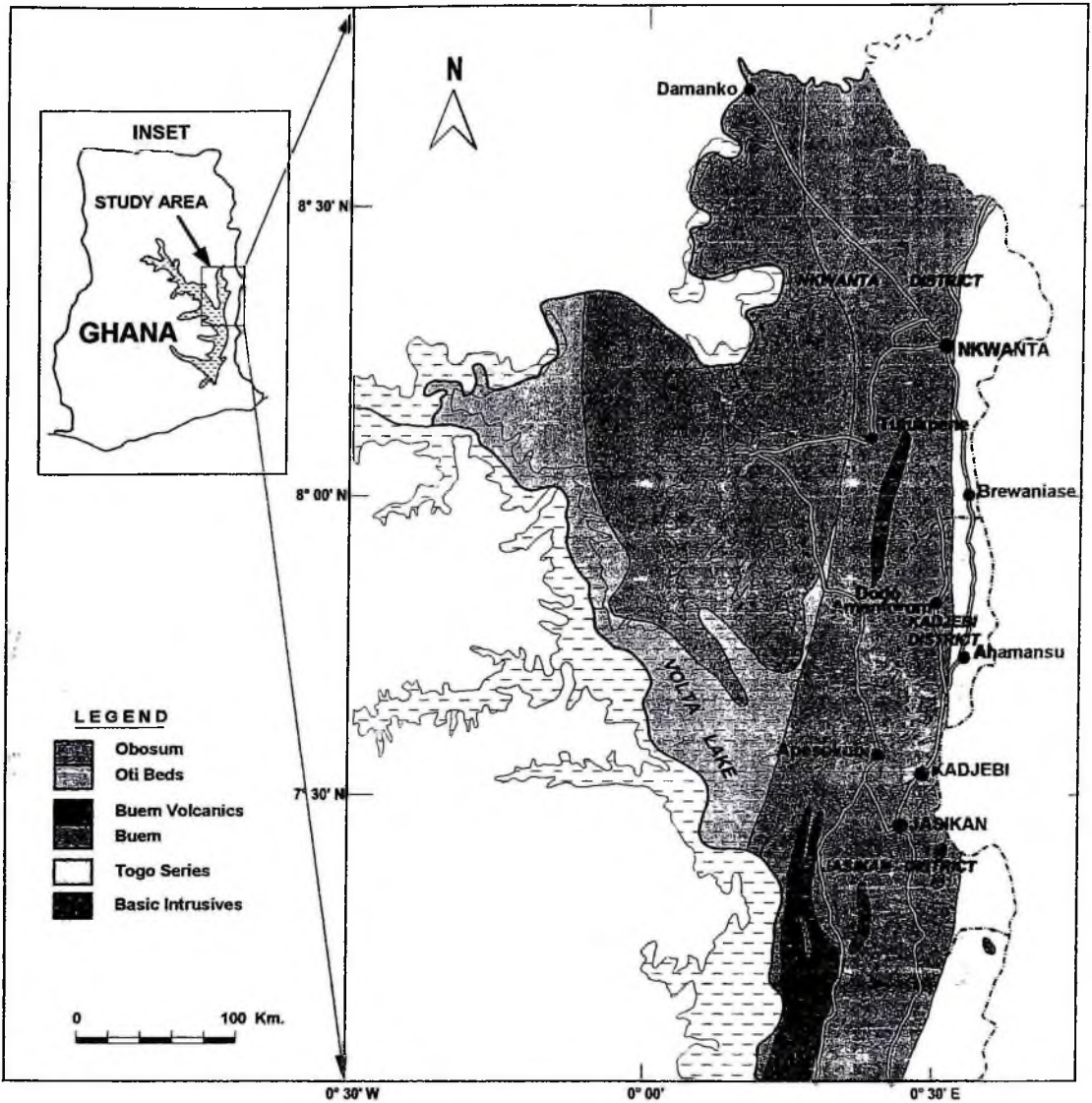


Figure 3.2 Geological map of the study area.

3.4.2.1 The Buem Formation

About 90% of the area under review occurs in the Buem Formation. It occurs to the western, northern and northwestern part of the Togo Series. Different workers have given different opinion about the age and the association of this Formation (Koert, 1910; Robertson, 1921; Kitson, 1928 and Junner, 1940). This controversy is believed to arise partly from the complex nature of the geology and tectonics. However, the classification that is generally accepted is that the Buem is younger than the Togo but older than the Voltaian (Bates, 1955; Geological Map of Ghana, 1958). The Formation is believed to have been deposited in a tectonic-generated north-south oriented, probably narrow and quite deep basin (Blay, 1971).

Lithologically, the formation in the Nkwanta area can be divided into three groups (Lashmanov, 1965). These are the lower, middle and upper suites. The lower suite is composed of tillites with bands and patches of mudstones, siltstones, polymictic and oligimictic quartz sandstone gritstone, siliceous rocks, conglomerate and limestone. The middle suite conformably overlay the fragmentary rocks of the lower subgroup. It consists of fine and medium grained oligomictic quartz sandstone, variegated mudstone and siltstone, gritstone, inequigranular sandstone and fine pebble conglomerate in minor quantity. The upper suite which is less common in the Nkwanta area but occupies larger areas in the southern part of Ghana consists of effusive basalt and andesite-basalt rocks with occasional siltstone and mudstone varieties. Moving further south around Jasikan area, Blay (1971) separated the Buem Formation into two parts, namely the sandstone group and minor intrusives at the upper part. The upper intrusives are made up of serpentinites and gabbros with

numerous haematite. The sandstone group consists of mainly grey-gritty coarse-grained feldspathic sandstone, arkosic gritty sandstone, greywacke and whitish-grey, gritty quartz veined quartzitic sandstone with minor shale intercalations. There are also pink, purple and pale yellow thinly bedded and massive shale, micaceous sandy shale, siltstone and greywacke.

The minerals in the sandstone in the Nkwanta area are either entirely quartz or quartz and little plagioclase weathering to kaolinite, zircon, apatite, garnet, tourmaline and rutile. The feldspathic sandstone on the other hand consists mainly of plagioclase and quartz with little microcline. The mudstone also consists of quartz, feldspar and sericite flakes. Finally, the siltstone is made up of quartz, plagioclase, leucoxene, zircon, ilmenite and ore minerals. The formation is highly folded along N-S lines and the beds generally dip to the east at 10° - 90° with an average of about 60 - 65° . Normally, the formation is unmetamorphosed but in the fault along the Buem-Togo contact, it is frequently sheared and schistose masses of basic igneous rocks (dolerite and gabbro) intrude the Formation particularly in the vicinity of the Buem-Togo contact (Junner and Service, 1936).

3.4.2.2 The Voltaian System

The Voltaian Formation which occurs in the northwestern portion of the area is made up, predominantly, of quiet, shallow marine deposits with marginal lagoonal areas periodically cut off from the sea. The deposits consist of sandstones, siltstone, shale, mudstones and conglomerates (Kesse, 1985). Mineralogically, Bobrov and Pentelkov (1964) noted that the mudstones and siltstones are made up of clay materials, quartz

and plagioclase feldspar. Various workers have given different classification to the Voltaian at different places. A summary is shown in Table 3.1.

The Voltaian System has a total thickness of between 3000-4000m (Watt, 1977) and rests unconformably on the Lower Proterozoic Birimian Formation and related granitoids and also on the Lower to middle Proterozoic Tarkwaian System.

Table 3.1 Classification Of The Voltaian Formation (Kesse, 1985)

Cooper (1926)	Junner and Service (1936)		Junner and Hirst (1946)	Soviet Geological Team (1964)	Annan Yorke (1980)	Wright (1985)
	Formation	Approximate thickness in metres				
a) Siliceous Sandstone Group	Group A - Massive, quartz sandstone	75	Upper Voltaian	Massive sandstone	Massive cross-bedded sandstone	Continental conglomerate and sandstone
b) Thinly bedded sandstone and sandy shale Group	Group B - Green, micaceous and feldspathic sandstone with spotted carbonate	60-75		Thin bedded sandstone	Thin bedded sandstone. Tamale red beds	
c) Mudstone Group	Group C - Olive, purple, brown and grey shales with a few thin beds of arkosic sandstone.	120-140	Middle Voltaian	Obosum beds	Tamale red beds	Siltstone, sandstone, greywackes, dolomitic limestones
d) Calcareous sandstone Group	Group D - White thinly bedded quartz sandstone containing clay pellets, with a thin bands of pebbly quartz grit and conglomerate at the base	30		Oti beds	Green-gray Lower series	
e) Clay shale Group			Lower Voltaian	Basal sandstone	Basal sandstone	Shales, sandstones and limestones

There are varied opinions about the age of the Voltaian Formation. Robertson (1921) inferred the age of Proterozoic. Others thought the Formation is Lower and even Upper Paleozoic (Koert, 1910; Kitson, 1928; Junner, 1928 and Furon, 1963). But all the investigators agreed that the Formation is younger than the Birrimian (both Lower and Upper Proterozoic) and Tarkwaian (Upper Proterozoic).

3.4.2.3 The Togo Formation

The Togo formation occurs on the eastern margin of the study area. It forms the range of mountains and hills known in the study area as the Shiare-Kilinga ridge of the Akuapim-Togo Range (Lashmanov, 1965). The Formation further runs through the region in a NE-SW direction into the Republic of Togo. The rocks of the Togo Formation are broadly composed of metamorphosed arenaceous and argillaceous group in the Baglo area (Blay, 1971). Lashmanov (1965) in the Nkwanta area also divided the rocks into three subseries namely, Lower, Middle and Upper suites.

Despite the difference in classification, there is a general agreement as to the types of lithologies in the area. Blay (1971) gave the various lithologies in the Togo as quartzites, schists, phyllites and shales. The quartzites occur in the extreme east and consist of various members including quartz-schist, quartz-sericite schist, cataclastic quartzite and micaceous quartzite. Moving further westwards occurs the schist and phyllites of the middle and upper suites. Mineralogically, the schist consists predominantly of quartz and sericites. Chlorite sometimes occurs in subordinate amounts. The phyllites also consist mainly of sericites with minor amount of chlorite, plagioclase and quartz believed to be derived from the metamorphism of argillaceous materials.

The boundary between the Togo and the Buem is believed to be tectonic rather than sedimentary (Blay, 1971; Junner, 1940) and marked in the western margin by major thrust faults. The Togo Series have been subjected to intense directed pressure metamorphism resulting in intense folding, fracturing and faulting which occur both

locally and regionally. Blay (1971) noted two major joint sets in the quartzites trending NE and NW. The general trend of the fault is also given as NE-SW. Isoclinal folding with axial planes of the fold inclined to the ESE at 30°-60° is the rule. Recumbent folds with dips of less than 30° sometimes occur. Metamorphism in the Togo Series ranges from greenschist to amphibolite facies.

3.5 Hydrogeology

The rocks of the study area range from consolidated sediments to metamorphic rocks with little or no porosity. Groundwater occurrence and flow is thus associated with the development of secondary porosity and distribution and rate of recharge and discharge.

3.5.1 Togo and Buem Formations

Due to the consolidated nature of the Togo and Buem Formations located in the study area, groundwater accumulation is restricted to fractures, joints, fissures and weathered zones. The main source of recharge to the aquifers is the infiltration of rain and associated flow within the saturated zone. Due to multiplicity of factors such as mineralogy, degree of rock deformation and rainfall distribution, variable overburden thickness pertains in the area. Available data indicate that the thickness of the weathered zone ranges between 1 and 28.5m with an average and median of 4.9 and 3m, respectively.

The weathered zone consists of lateritic soil, sand, sandy clay, gravelly clay and clay. Not much is known about the hydraulic characteristics of this layer, but a good yield

University of Ghana <http://ugspace.ug.edu.gh>

is obtained where it is thick and permeable enough to store and transmit water. The massive bedrocks range from highly weathered, through moderately weathered to fresh bedrocks. Specifically, they act as confining units restricting flow between the overburden and the fractured rocks beneath. As a result the aquifers are either confined to semi-confined. However, where the fractures are well developed in any of the rock units, high yielding wells can be obtained. Appendix A1 illustrates a typical borehole at Ahubrase JSS showing the geology and hydrogeologic properties in the Buem Formation.

The yields of boreholes range between 9 and 1260 l/min with an average and median of 100 and 78 l/min, respectively. Kesse (1985) reports that the average yield is about 150l/min and yields range from 15-525 l/min.

The average depth of boreholes in the area is 60m. However, CWSA Drilling report (2002) gives the borehole depth range of 22-60m with a mean of 42m. On the basis of available aquifer-test data, the calculated transmissivity values range between 0.2 and 11.4 m²/day. The specific capacities of the boreholes in the area vary from 0.04 to 1.23 m³/h/m with an average of 0.47 m³/h/m. No observation-well data is available for the estimation of the storativity of the aquifers. The contact of the quartzite and the argillaceous rocks in the valleys usually yields numerous springs which are sources of the perennial drainage in the area.

The chemical analyses of water from these rocks show that the water is generally usable for most purposes. The hardness is mainly temporary and is about 190mg/l.

The average chloride concentration is about 16 mg/l. Iron and Manganese concentrations as high as 40 mg/l have been reported in few cases.

3.5.2 The Voltaian System

The Voltaian rocks are generally well consolidated and inherently impermeable except in a few isolated places, eg in a long belt between Kete Krachi and Sang where the strata may possibly be permeable. The sandstone, quartzite and arkose produce sandy superficial deposits from weathering with variable thickness. The thicknesses of the weathered zone in the study area range between 2 and 9m with an average of 3m. Because of the thinness of the overburden it is not a good aquifer. Appendix A2 shows a stratigraphic section of a borehole at Kabre Akura in the Voltaian Formation. As in the Buem and Voltaian Formations, the main source of recharge to the aquifers is infiltrating rainfall. Due to thinness of the weathered zone, large areas are covered by shallow ephemeral lakes and ponds during the wet season but disappear during the dry season. The yield of this Formation in the study area has a mean of 35 l/min and ranges between 0 and 280 l/min. The average depth of boreholes in the area is 49m and between 28 and 75m.

The transmissivity values obtained during pumping test range between 2.5 and 39.6 m²/day (Gills, 1969). The specific capacities of the wells in the area vary from 0.11 to 1.97 m³/h/m. No observation-well data is available for the estimation of the storativity of the aquifers.

University of Ghana <http://ug.edu.gh>
Total dissolved solids (TDS) concentrations up to 1560 mg/l have been noted in water samples from this area. In the Kete Krachi area, boreholes have much higher yield than elsewhere in the Voltaian basin. The average yield of successful boreholes is about 146.3 l/min with a range from 13.3-273 l/min (Kesse, 1985).

3.6 Socio-economic Activities

The study area has a total population of 314,559 with a majority of them living in the rural areas. The ratio of male to hundred females is 101.7 in the Jasikan, 106 in the Kadjebi and 97.9 in the Nkwanta districts (PHC, 2000).

The area is linked by first, second and third class road. The roads linking the various communities in the area are mainly feeder roads.

The main occupation of the inhabitants is farming. They cultivate crops such as cassava, maize, plantain, yam and cocoa. The women engage themselves in the processing of gari.

CHAPTER FOUR

METHODOLOGY

Hydrochemical and isotopic studies like all scientific studies, require systematic and standardized approach. This involves the careful and proper handling of equipments, samples and reagents to avoid unnecessary errors. This is necessary to ensure that objectives outlined can be achieved. This chapter deals with the methods used in the research in the data collection process. It also describes the equipments used, the laboratory data analyses, the limitation of the methods used and the presentation.

The steps followed in this research are:

- I. Desktop and field data collection
- II. Laboratory data analyses
- III. Results presentation and interpretation

4.1 Desktop and field data collection

Groundwater composition and characteristics is dependent largely on geology, hydrology and geography (Raji and Alagbe, 1997). Therefore, before fieldwork was undertaken, a thorough study on all relevant information about the study area was done. This involved the geology, hydrology, geography and socio-economic activities of the area.

The geological map of the area was digitized from the geological map of the Volta Region and borehole drilling reports obtained from the database section of the

Community Water and Sanitation Agency (CWSA), Ho and CSIR, Accra respectively. The hydrogeological information was also obtained from CWSA, Ho, while the geography from the Geography Departmental library, University of Ghana, Legon. The socio-economic activity on the other hand was partly obtained from the Population Impact Project (PIP) office and partly from observation on the field.

4.2 Field data collection

Field sampling sites were randomly selected, taking into consideration the geology and availability of hand pump-fitted boreholes. In all, seventy-one (71) water samples, consisting of sixty-seven (67) groundwater samples from existing boreholes that cover the entire area and four (4) surface water samples. The depth of the boreholes ranged between twenty-eight (28) and eighty-eight (88) meters.

Before a sample was taken, the position of the borehole was taken with a Garmin GPS placed on the head of the borehole. The unit of measurement is degree decimal and WGS 84 was used as a reference. The accuracy of the instrument is $\pm 10\text{m}$. After that, the borehole was pumped until the Electrical Conductivity (EC), pH and temperature of the water remained relatively constant.

Four (4) different water samples were taken. The type of analysis to be performed on the sample, the borehole ID and date of collection were indicated on the sample bottle for easy identification. The first portion was used to fill the sample bottles for $D/^{18}\text{O}$ analysis. The second portion was poured into a filtration instrument to filter samples

to be used in major ion determination. The third portion was used in the determination of on-site physical parameters. The last portion was used in the determination of alkalinity.

4.2.1 Collection of major ion sample

The water sample was poured into filtration equipment using a 0.45 μ m acetate filter membrane. It was manually pumped until the 200mL glass bottle was full. Two sterilized and thoroughly rinsed High Density Polyethylene (HDPE) sample bottles were filled with the filtered water. The sample for cation analysis was then acidified with a 30% nitric acid (HNO₃) to reduce the pH to less than or equal to two (pH \leq 2) to avoid the precipitation of substances especially calcium. The two bottles were firmly capped and placed in cool storage in an ice chest.

4.2.2 Collection of stable isotope sample.

The only precaution that was ensured in the collection of the stable isotope sample was that, a representative water sample was obtained and sample bottle filled to the brim. It was then firmly capped and placed in cool storage.

4.2.3 pH measurements

A WTW Multi 340i meter was used in the measurement of the pH of the water samples. Before the instrument was used in the measurement, it was calibrated with standard solutions of pH 4.00 and 7.00. It was then rinsed with the water from the

borehole that was to be sampled and dipped in the water sample until the pH readings remained stable at 25°C. The accuracy of the measurement is ± 0.1 .

4.2.4 Electrical Conductivity measurements

The WTW Cond 315i conductivity meter was used to measure the electrical conductivity of the water sample. It consists of a 6V alkaline-manganese, type AA battery-powered meter and a WTW Tetracon 325 standard-conductivity cell. The instrument after being calibrated with a standard solution of 0.03M KCl was rinsed with the water from the borehole being sampled. The probe was dipped in the sample until the meter readings of conductivity and temperature remained stable. The accuracy of the EC measurements was $\leq 0.5\%$ of measured value ± 1 digit. That of the temperature was ± 0.1 . After each measurement the conductivity cell was cleaned with deionised water.

4.2.5 Alkalinity measurements

The alkalinity of the water indicates its ability to neutralize acids. It is also a measure of the total acid-neutralizing capacity of the water sample (Deutsch, 1997). It is controlled by the sum of titrable bases and taken as an indication of the concentration of carbonates, bicarbonates and hydroxides (Chapman, 1992). The alkalinity measurements were obtained in the field to avoid carbon dioxide degassing and subsequent calcite precipitation in the sample bottle prior to laboratory analysis. It

was determined according to the procedure described in the instrument manual (Hach, 1997) as below:

A 50ml water sample was placed in a graduated beaker. The content of one phenolphthalein indicator powder pillow was added and swirled to mix. The solution remained colorless for all the samples since the water samples were acidic. The content of one Bromcresol Green-Methyl Red indicator powder pillow was added to the sample to give blue-green colour. It was then titrated against 1.6N H₂SO₄ using Hach digital titrator until an endpoint colour of light pink was obtained (Fig. 4.3). According to Hach (1997) the alkalinity of the sample was calculated as:

$$\text{Total alkalinity} = \# \text{ of digits} \times \text{digit multiplier} \dots\dots\dots(4)$$

In this case the multiplier was 2, since the alkalinity in the study area was generally between 200-800 mg/L.

4.3 Laboratory data analysis

Dissolved minerals and gases in groundwater are determined by well-standardized methods of laboratory analysis. The laboratory analysis in this study is divided into two parts namely:

- I. Major and minor ions analysis
- II. Stable deuterium (D) and oxygen 18 (¹⁸O) isotopic analysis.

4.3.1 Major and minor ions analysis

Groundwater is never pure; It contains at least small amount of dissolved gases and other substances. The composition of groundwater is dependent on many factors such as, the initial composition of the water, the partial pressure of the gas phase, the type of soil it flowed through and the pH and the Eh of the solution. Hydrochemically, natural waters contain a number of different dissolved inorganic constituents. These are major, minor and trace ions. The major ions include sodium, potassium, calcium, magnesium, sulphate, chloride and bicarbonate. Examples of minor ions are iron, manganese, fluoride, nitrate, strontium and boron. Trace elements present include arsenic, lead, cadmium and chromium which have concentrations of a few microgram per litre.

For the purposes of this study, only the major and some minor ions of the samples were analyzed. This was done at the Ecological laboratory of the University of Ghana, Legon using a dual-column DX-120 ion chromatograph with the Peaknet software. The ions analysed for were sodium, potassium, lithium, ammonium, calcium, magnesium, fluoride, chloride, bromide, nitrite, nitrate, phosphate and sulphate.

The operation of the ion chromatograph is based on the well-established principle of ion exchange chromatography and the use of electrical conductance in the determination of ions in solution after their initial separation. The equipment is made up of a dual eluant reservoir (A and B), pump, sample injection valve, a pair of guard

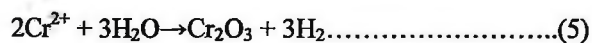
and separator columns, Dual Self Regenerating Suppressor (SRS) column, conductivity cell and conductivity meter and a recorder. When a sample is injected into the system, the pump elutes some eluant at the rate of 1ml/min to ensure that the sample was present in the electrolyte background. The eluants are mainly aqueous acids for cation analysis and aqueous bases for anion determination.

The acid used in the reservoir B was a diluted 20 mN H_2SO_4 , while the base in the reservoir A was a mixture of 3.5N Na_2CO_3 and 1.6N $NaHCO_3$. The sample in the eluant background then moved into the separator column by passing through the guard column. The double separators were switched in turns in the analysis of either cations or anions. The separators are made of a low-capacity exchange separator resin, using strong acid for cation analysis and strong base for anion determination. The resins are stable over a wide range of pH.

The presence of separated cations and anions in an electrolyte background presents a major setback for the use of electrical conductance for quantifying eluted ionic species. However, this problem was solved by the use of the Self-Regenerating Suppressors (SRS) column. The main function of the SRS was to convert relatively high conductive eluant ions into species of low or zero conductance so as to aid the conductivity cell to pick only the conductivity of the sample in question.

4.3.2 Laboratory stable isotopic analyses

The oxygen isotope ratio was determined by acidification with 100% phosphoric acid and equilibration of 5mL of the sample with CO₂ gas as described by Epstein and Mayeda (1953). The analyses were carried out on a VG Sira 10 mass spectrometer with an automatic inlet. The deuterium D measurement on the water samples were carried out on a Euro Vector elemental analyser (EA; EuroPyrOH-3100) with a Euro Vector liquid autosampler (LAS; Euro AS-300) couple to a Micromass IsoPrime isotope ratio mass spectrometer (IRMS). The method uses the continuous flow technique where a constant flow of helium carries the water samples from EA to the mass spectrometer. The syringe fitted to the liquid autosampler pulls up to 0.5µl of water from small sealed sample vial. The water sample then enters the EA by heated injector port held at 160°C. At delivery, the syringe penetrates a septum sealing the heated injector from the atmosphere. In the furnace (105°C), the following pyrolytic reaction takes place reducing the water vapour into hydrogen:



Hereafter the hydrogen gas molecules are transported through a GC-column transforming the H₂ pulse to an adequate form for the integration software, and further through an open split to the mass spectrometer. The results for both isotopes are expressed in per mill (‰) deviation from the Vienna Standard Mean Ocean Water (VSMOW) standard using the standard δ- notation. Reproducibility is better than 0.1‰ for δ¹⁸O and about 1‰ for δD.

4.4 Methodology For The Presentation And Interpretation Of Results

Collected and analysed data need to be in a form that can easily bring out meaning and facilitate interpretation. This section shows the calculation of the partial pressure of carbon dioxide from the pH and alkalinity, statistical analysis and graphical methods used for interpretation

4.4.1 Calculation of Carbon Dioxide Partial Pressure in the Sub-surface

Inorganic carbon concentration in groundwater is a function of both solution pH and partial pressure of carbon dioxide gas in equilibrium with water. Because of this equilibrium, if any two of these variables can be measured in a sample of water, then the third variable can be solved for.

The relationship among these three properties is used to calculate carbon dioxide partial pressure in equilibrium with groundwater using field measured values for pH and alkalinity. The equation is as follows:

$$P_{CO_2} \text{ (atm)} = \frac{(\gamma_{CO_3^{2-}})(10^{-pH})^2 \text{ Alkalinity (mg/l CaCO}_3)}{10^{-18.2} \left[2 + \frac{10^{-pH}}{10^{-10.3}} \right] (5 \times 10^4)} \dots\dots\dots(6)$$

$\gamma_{CO_3^{2-}}$ = activity coefficient of CO_3^{2-} Alkalinity = total inorganic alkalinity

$\gamma_{CO_3^{2-}}$ = (0.6-1) (Calculated from Davis or Debye-Huckel equation for groundwater with TDS less than 10,000 mg/l). (Deutsh, 1997)

The mean, standard deviation and coefficient of correlation are the simple statistical analyses carried out in this study. The mean and standard deviation of the hydrochemical parameters determined are presented in Table 5.1 in Chapter 5.

The mean and standard deviation of a group of related numerical values are useful in water quality analysis. They give a clearer picture by way of summary of parameters measured over an entire area.

The mean and standard deviation of parameters were computed using the Ms Excel 2003 program.

On the other hand, coefficient of correlation searches for relationships among measured parameters. These relationships are assigned values between 0 and 1. The closer the value is to 1 the better the relationship. Just as mean and standard deviation, the coefficient of correlation among parameters were computed using the Ms Excel 2003 program.

4.4.2 Graphical Methods

Graphical methods are used to help in interpretations. Various techniques for graphical representation of analyses have been proposed. The graphical methods employed in in this study include Compositional diagrams, Piper plots and Schoeller Semilogarithmic diagram.

The relationships among measured and calculated parameters are clearly noticed by the use of Compositional diagrams or Scatter plots. Although these diagrams cannot prove that one variable causes the other, they do indicate the existence of a relationship, as well as the strength of that relationship. It involves plotting one property on the ordinate axis and the other on the abscissa. The purpose of the scatter diagram is to display what happens to one variable when another variable is changed. The diagram is used to test a theory that the two variables are related. The type of relationship that exists is indicated by the slope of the diagram.

Piper diagram displays the relative concentration of the major cations and anions. It consists of two separate triangular plots and a central diamond plot where the points from the two trilinear plots are projected. In the triangular plots, the axes run from 0 to 100 on each of the three sides. In the right triangle, the axes increase in a counter clockwise direction. The axis restarts to zero at each apex; in the left triangle, the axes increase in a clockwise direction--restarting at zero at each apex. For each sample, there are three variables to determine the plotting position in each triangular plot, for example the axes may be the three major cations (left) and anions (right) and the variables are the cation/anion composition of the sample. Each of the three cation/anion variables, in milliequivalents, is divided by the sum of the three values, to produce a percent of total cations. For example, if $\text{Ca} = 0.80 \text{ meq}$, $\text{Mg} = 0.26 \text{ meq}$, and $\text{Na} + \text{K} = 0.89 \text{ meq}$, then $\% \text{Ca} = 41$, $\% \text{Mg} = 13$, and $\% [\text{Na} + \text{K}] = 46$.

The data points in the center field are located by extending the points in the lower triangles to the point of intersection in the center field. The axis values at the top and

bottom of the center field are 100; the axis values on the left and right side of the center field are 0.

The Schoella semilogarithmic diagram (Schoella, 1955, 1962) also known as fingerprint diagram allows major ions of many samples to be represented on a single graph in which samples with similar pattern can easily be discriminated. The Schoella diagram shows the total concentration of major ions in log-scale.

RESULTS AND DISCUSSION

Groundwater, before reaching its destination picks up physico-chemical signatures that reflect the various processes it had undergone. A conscientious study of these signatures can facilitate the understanding of the history or may be used to predict quality. This chapter presents the results of both laboratory and field physico-chemical analyses of groundwater from the study area. Subsequently, the processes that gave rise to the observed compositions are discussed. Furthermore, based on the major ion compositions, water types in the various formations in the study area are presented. Finally, the isotopic results and the possible source of recharge are given.

5.1 Hydrochemistry

The summary of the physico-chemical parameters of the samples in the various Formations are presented in Table 5.1. The interpretation and discussion of the physico-chemical parameters as they are in the various Formations are given below.

5.1.1 pH distribution

Groundwater pH is a fundamental property that describes the acidity or alkalinity of groundwater and largely controls the formation of many organic and inorganic substances dissolved in groundwater (Derickson, 2003).

The pH of water is a commonly determined property and in the area, it ranges from 4.69 to 7.78 with an average and standard deviation of 6.42 and 0.75 respectively at 25 °C. The minimum pH occurs at Guaman in the Jasikan District while the maximum occurs at Kabre Akura in the Nkwanta District. pH of between 6.2 and 7.4 occurs in the northwestern, central eastern and the southern tip of the area. Moderately acidic water of between 4.69 and 5.6 occurs to the northwest of the lower half of the study area. Despite the moderately acidic nature of some of the samples, they fall within the pH range of natural water, that is between 4.5-8.5 (Hounslow, 1995; Langmuir, 1997). However, 44% of the samples falls below the lower limit of the recommended range (6.5-8.5) for domestic use (WHO, 1993).

The plots of pH versus total dissolved ions (TDI), bicarbonate ion (HCO_3^-) and electrical conductivity (EC) of samples show high positive correlation and reveal two classes of water (Fig. 5.2 a, b and c):

- I. pH of less than or equal to 6.5 and relatively low TDI, bicarbonate and electrical conductivity and

II. pH greater than 6.5 and medium to relatively high TDI, bicarbonate and electrical conductivity.

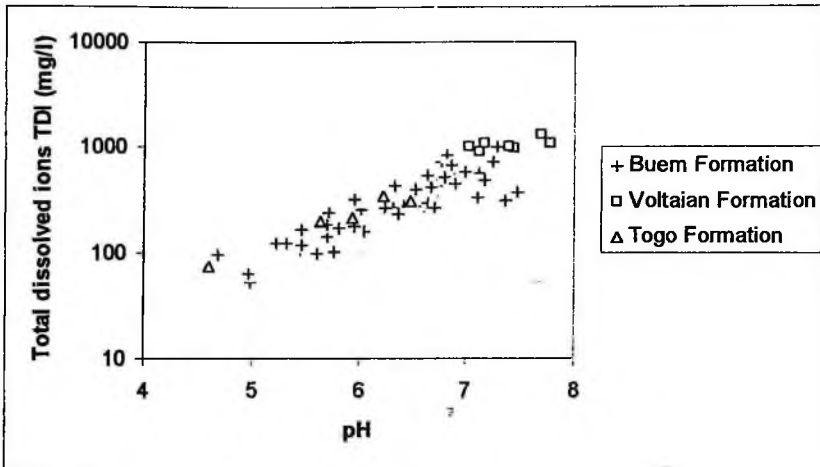


Figure 5.2a The scatter plot of pH and Total dissolved ions in the study area.

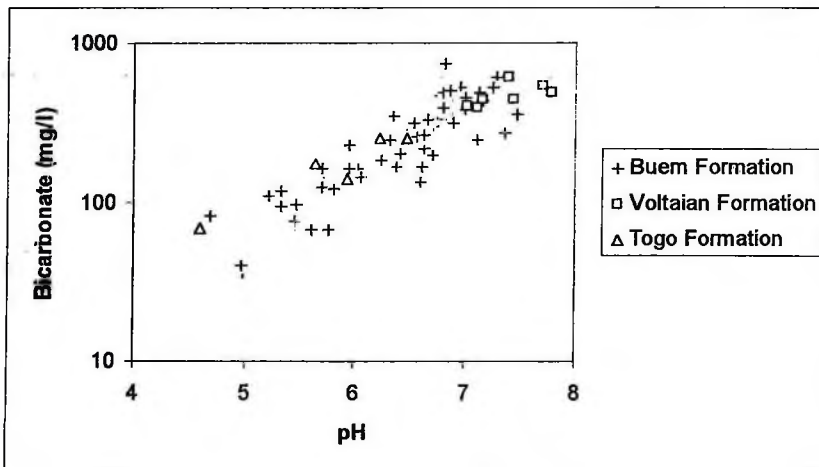


Figure 5.2b The scatter plot of pH and Bicarbonate in the study area.

The first group of low pH groundwater occurs in quartzitic sandstones interlayered with minor amounts of shales aquifers of the Buem Formation and quartz schist of the

Togo Formation, while the second group is groundwater from mainly the shales, slates, phyllites, mudstone and siltstone aquifers of the Buem and Voltaian Formations.

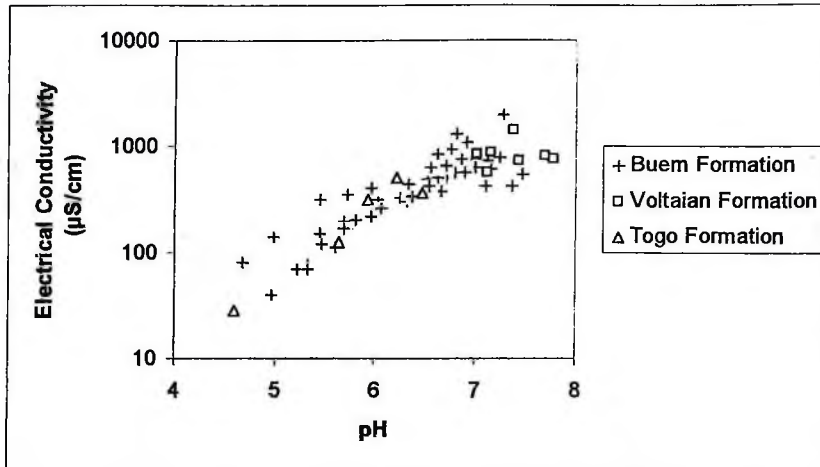


Figure 5.2c The scatter plot of pH and Electrical conductivity in the study area.

The calculated partial pressures of carbon dioxide (P_{CO_2}) values of all the samples are above that of the earth's atmosphere of ($10^{-3.5}$). This indicates that the groundwaters in these Formations become charged with carbon dioxide during infiltration through the soil zones. Figure 5.3 reveals a strong negative correlation between pH and the partial pressure of carbon dioxide in the study area and consistent with groundwater compositions in the Japanese forest belt (Ohte and Asano, 1997). Ohte and Asano (1997) attributed this observation to the dissolution of carbon dioxide and geochemical weathering of aquifer materials. Figure 5.3 further shows that the low pH samples have high carbon dioxide partial pressures indicating probably that the

University of Ghana <http://ugspace.ug.edu.gh>

infiltrating water does not encounter reactive aquifer materials containing carbonate minerals or that the reaction is occurring under an open system. The main rock type in the area is sandstone which documentally contains quartz, plagioclase feldspars and sericite flakes (Lashmanov, 1965). These minerals are relatively stable and their reaction with the carbon dioxide-charged water is not likely to consume much hydrogen ions and this explains the low pH.

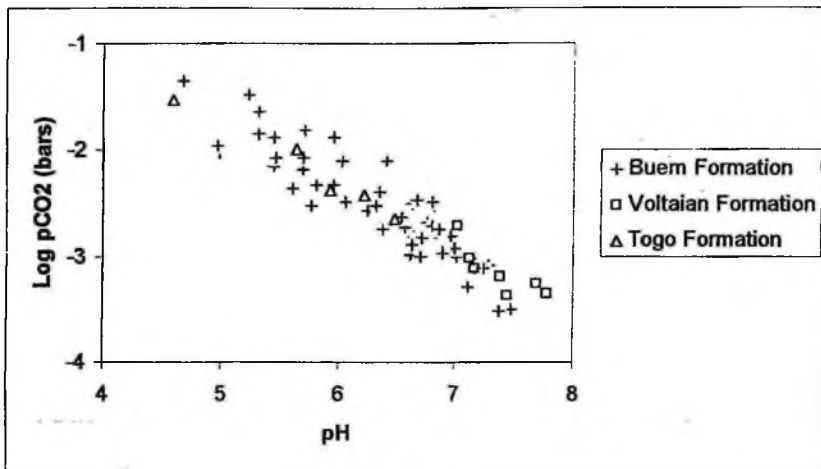


Fig 5.3 Scatter plot of pH and carbon dioxide partial pressure in the study area.

The results also indicate that, the relatively high pH groundwater have low carbon dioxide partial pressure values (Fig. 5.3). The bicarbonate and the total dissolved ions are all high in these aquifers. The main controlling factor on the pH in the aquifer is the presence of reactive materials such as carbonate and/or dissolution of anorthite-rich plagioclase feldspar in the aquifer. As the recharge water meets the carbonate materials and/ or anorthite-rich plagioclase feldspar, most of the carbon dioxide is consumed and releases greater amount of soluble ions in the aquifer into the water

giving rise to the relatively higher pH, high total dissolved ions, electrical conductivity and bicarbonate. This observation probably suggests that the reaction in the aquifer may be taking place under partially closed system (Appelo and Potsma, 1993).

The pH of the groundwater in the Voltaian Formation in this area (mean pH=7.3) is slightly higher than the pH in the South Voltaian Basin (mean pH=) (Acheampong and Hess, 1995). It falls within the pH range of 6.5-8.5 for domestic use (WHO, 1993).

The relatively high pH, high total dissolved ions, bicarbonate and electrical conductivity of the groundwaters in the Voltaian Formation aquifers probably indicate a dissolution reaction of the carbon dioxide-charged water with the aquifer materials, composed mainly of plagioclase feldspar and sercites in the mudstones and siltstones. This reaction consumes hydrogen ions and releases ions that increase the total dissolved ions (TDI) and electrical conductivity. The calculated partial pressure of carbon dioxide is decreased as pH increases (Fig. 5.3) partly confirming dissolution reaction.

Another possible reason for the high pH and bicarbonate could be due to the dissolution of minor carbonate (calcite) materials in the mudstone and siltstone aquifers since the possibility that such minerals which are present in trace amount may contribute significantly to the water chemistry cannot be discounted:

In the Togo Formation on the other hand, all the samples fall below the recommended limit of 6.5- 8.5 for drinking purposes (WHO, 1993). Nevertheless, the pH range is consistent with pH of groundwater in metamorphic bedrock (Galloway and Cowling, 1978; Reuss et al., 1987) demonstrating slower geological weathering. pH in this Formation is similar to most of the samples of the quartzitic sandstones in the Buem Formation indicating similar hydrochemical processes.

The relation between pH and partial pressure of carbon dioxide however shows a negative correlation (Fig 5.3) as in the other Formations. Decreasing carbon dioxide partial pressure results in the increase in the total dissolved solids indicating dissolution reaction under partially closed system.

Appelo and Potsma (1993) stated that groundwater pH is influenced by dissolution of CO_2 , oxidation of ammonia and pyrite. The general absence of fertilizer application and the lack of pyrites in the study area makes the dissolution of CO_2 and its interaction with aquifer materials the probable reason for the variation of groundwater pH in the area.

5.1.2 Electrical Conductivity (EC) distribution

The Electrical Conductivity (EC) of a solution is the ability of a substance to conduct electrical current due to the presence of ionic species in solution. Pure liquid water has a very low electrical conductivity of a few hundreds of a microsiemen per centimeter at 25°C. As ion concentrations increase, the electrical conductivity increases, therefore electrical conductivity provides an indication of the amount of dissolved salts in a solution. Thus, natural groundwater which contains a variety of dissolved minerals shows a wide range in electrical conductivity from 2 to 200,000 $\mu\text{S}/\text{cm}$ (Hem, 1989).

The EC of the groundwater in the study area ranges from 28.1 $\mu\text{S}/\text{cm}$ at Kromasi to 1946 $\mu\text{S}/\text{cm}$ at Dawa with a mean of 489.7 $\mu\text{S}/\text{cm}$. Its distribution generally follows that of pH, total dissolved solids and bicarbonate (Fig.5.2c, 5.4 and 5.5). The variation of EC in the study area can be grouped into three types:

- Type I: Electrical conductivity less or equal to 500 $\mu\text{S}/\text{cm}$
- Type II: Electrical conductivity between 500 and 1000 $\mu\text{S}/\text{cm}$ and
- Type III: Electrical conductivity greater than 1000 $\mu\text{S}/\text{cm}$.

The type I covers about 60% of the study area. It occurs in the central part of the area which is made up predominantly of partially crystalline sandstones interlayered with minor shales and slates. There is strong positive correlation between EC and sodium, magnesium, calcium and bicarbonate ions in this group (Fig 5.6 a,b,c and d). The plots further show that a regression line of best fit has a significant electrical conductivity intercepts with calcium, magnesium and sodium but passes almost

through the origin with bicarbonate. This observation probably suggests that the electrical conductivity is principally influenced by the dissolution of albite-rich plagioclase feldspars in this group which yields bicarbonate ions in the water. The relatively low electrical conductivity is therefore attributed to the dissolution of relatively stable albite-rich plagioclase feldspars that occur in the quartzitic sandstones interlayered with minor shales and slates aquifers.

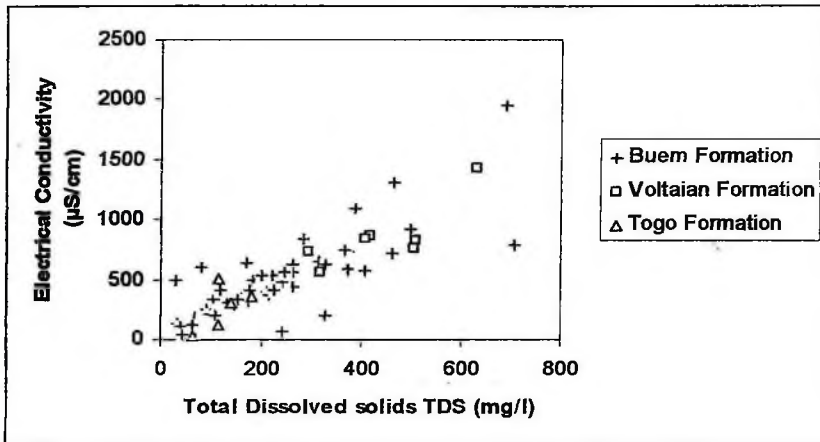


Fig 5.4 Scatter plot of EC and TDS in the study area.

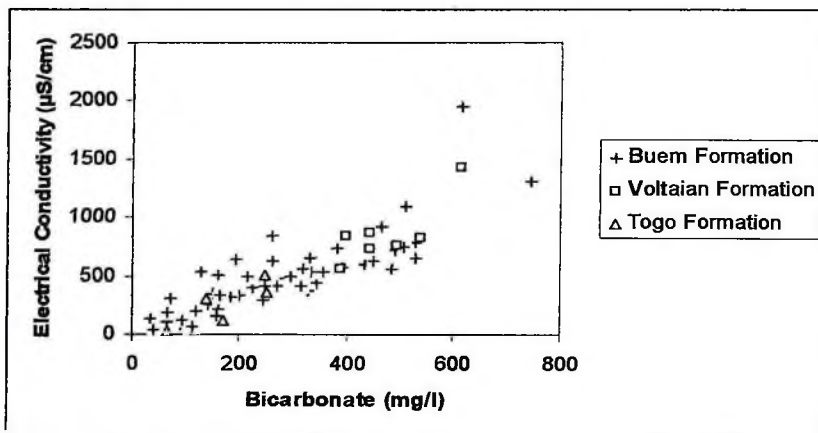


Fig 5.5 Scatter plot of EC and HCO_3^- in the study area.

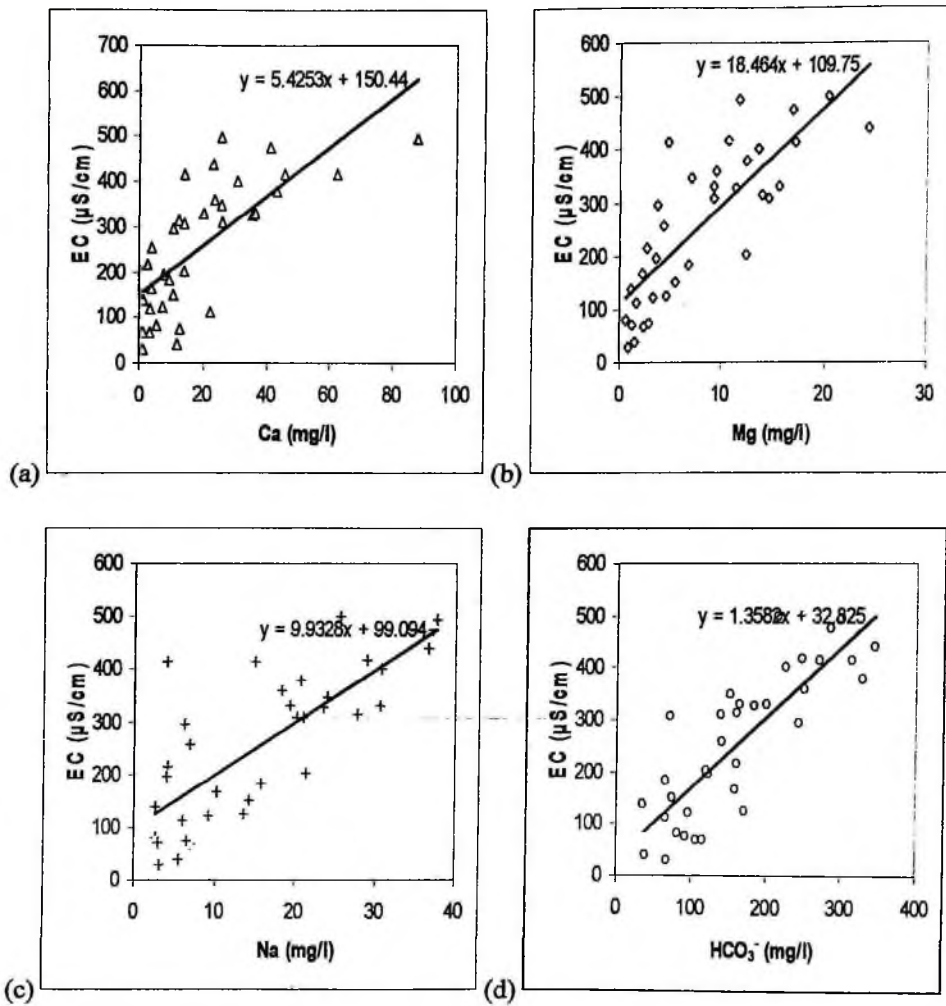


Figure 5.6 a,b,c and d Scatter plot of EC (Type I) and Ca, Mg, Na and HCO_3^- in the area.

The type II occurs in the mideastern and northwestern part of the study area where the shale/slate/phyllite and mudstone/siltstone aquifer occurs. It forms about 35% of the water samples. A positive correlation exists between EC and HCO_3^- .

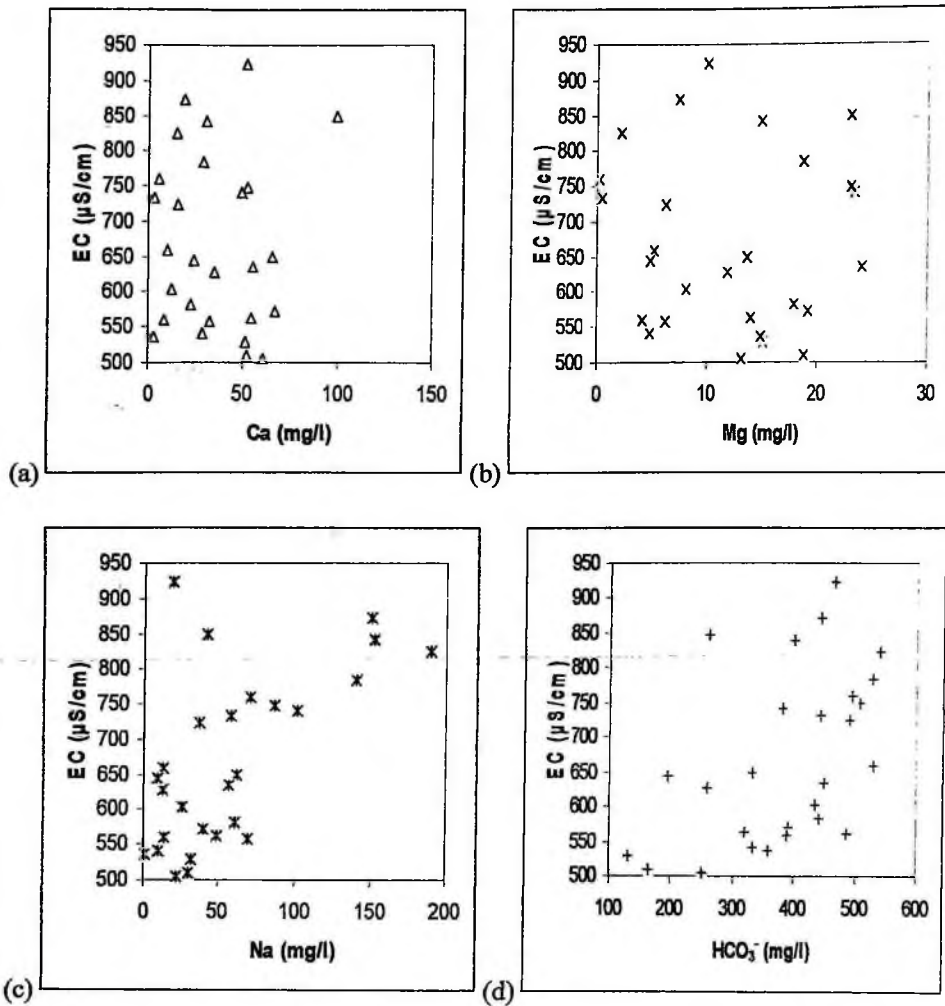


Figure 5.7 a,b,c and d Scatter plot of Ca, Mg, Na and HCO_3^- against EC (Type II) in the area.

There is however no clear pattern established between EC and the major cations (Fig.5.7 a,b and c). This probably indicate the occurrence of variable hydrogeochemical processes taking place in this aquifer influenced by geology.

Only 6% of the samples are of the type III and found generally in the northwestern portion of the study area. This group is found in the Buem and Voltaian siltstone and mudstone aquifers. The EC does not correlates with Ca, Mg, Na and HCO_3^- probably due to the small number of groundwater samples collected in this area.

5.1.3 Total dissolved solids (TDS) distribution.

Total dissolved solids (TDS) is the total quantity of dissolved materials in water and can be determined by weighing a dry residue after evaporation of a sample of groundwater or by estimation. The method selected for the determination of TDS depends on the objectives of the investigation (Briel, 1997). In this study however, the estimation method was used.

TDS in the study area ranges from a minimum of 29.55 mg/l at Kadjebi to a maximum of 706.63 mg/l at Alege Akura with an average of 238.04 mg/l. The distribution of the total dissolved solids generally follows that of electrical conductivity (Fig. 5.4), pH (Fig. 5.2 a) and bicarbonate (Fig. 5.8).

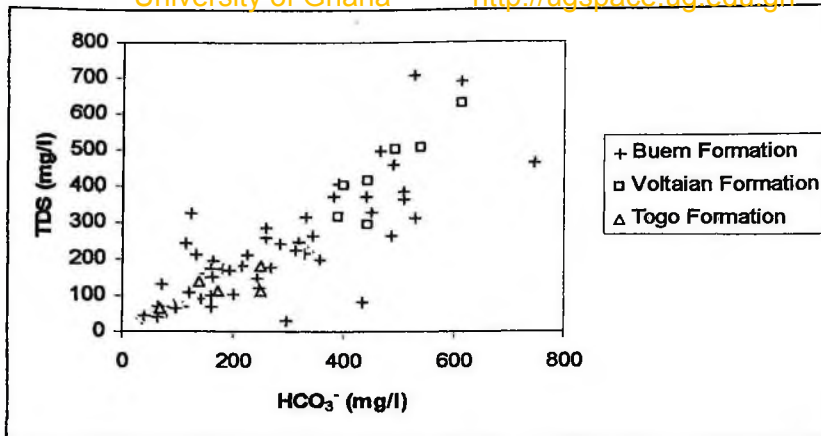


Fig 5.8a Scatter plot of TDS against HCO_3^- in the study area.

Figure 5.8b shows a plot of TDS against $\text{Na}/\text{Na}+\text{Ca}$ of groundwater in the study area (Gibbs, 1970). The chemistry of groundwater of high TDS of greater than 1000 mg/l is controlled mainly by evaporation and precipitation. Furthermore, TDS of between 100 and 1000 mg/l derives its composition from its interaction with rock units. On the other hand, TDS of less than 100 mg/l emanate from direct rainfall. Therefore, Figure 5.8b shows that 79% of the groundwater occurs in the in-flow from rock units zone while 21% in rainfall zone, indicating that majority of the groundwater in the study area probably acquired their chemical character by interacting with the aquifer materials while few of them from direct rainfall.

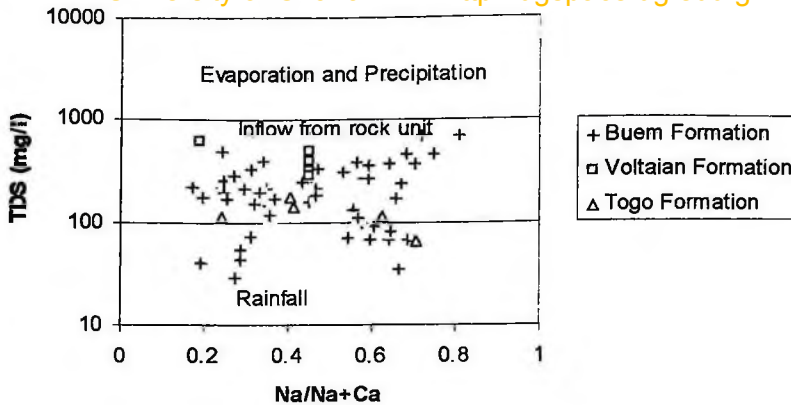


Fig 5.8b Scatter plot of TDS against Na/Na+Ca in the study area.

The scatter plot of the major cations against TDS is given in Figures 5.9, 5.10 and 5.11. They show the variation of TDS with Na, Ca and Mg ions in the various aquifers. The groundwater in the Buem quartzitic sandstones and shales/slate/phyllites and Togo phyllites and quartz-schist aquifers have TDS of less than 300 mg/l. On the other hand, TDS of greater than 300 mg/l occurs in the Buem and Voltaian mudstones. In the Buem quartzitic sandstones and shales/slate/phyllites and Togo phyllites and quartz-schist aquifers TDS correlates positively with all the major cations, probably confirming the dissolution of aquifer materials as the result of the water chemistry. All the water samples in the area have TDS of less than the permissible level of 1000 mg/l in drinking water (WHO, 1993), irrespective of the Formation. Generally, concentration of total dissolved solids concentrations in groundwater increase as it moves from the surface to the saturated zone and through the aquifer because of the dissolution of minerals (Freeze and Cherry, 1979). Additionally, processes such as evaporation, or evapotranspiration and hydrothermal

activities can increase the concentration of dissolved solutes. However, these processes become important in groundwater having total dissolved solids concentrations greater than 1000 mg/l. This probably indicates that mineral dissolution alone is responsible for solute increase in the groundwater of the area. The generally low TDS of less than 1000 mg/l in this Formation in the area indicates that the groundwater is not affected by industrial, mining, urban or agricultural activities as well as dissolution of readily soluble minerals (Lamb and Woodward, 1988). Furthermore, processes such as evaporation, or evapotranspiration and hydrothermal activities can be discounted as influencing the total dissolved solids. Since the total dissolved solids is a useful index of the chemical quality of groundwater, the samples in this Formation can be classified as fresh because its total dissolved solids is less than 1000 mg/l (Winslow and Kister, 1956; Helgesen et al., 1993).

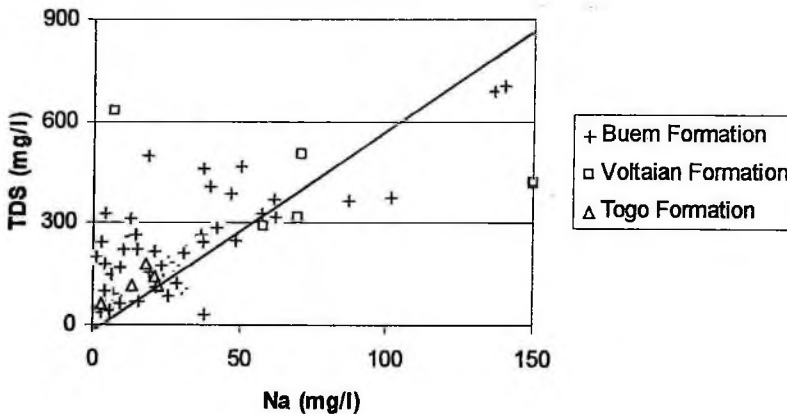


Figure 5.9 Scatter plot of TDS and Na in the various aquifers in the area.

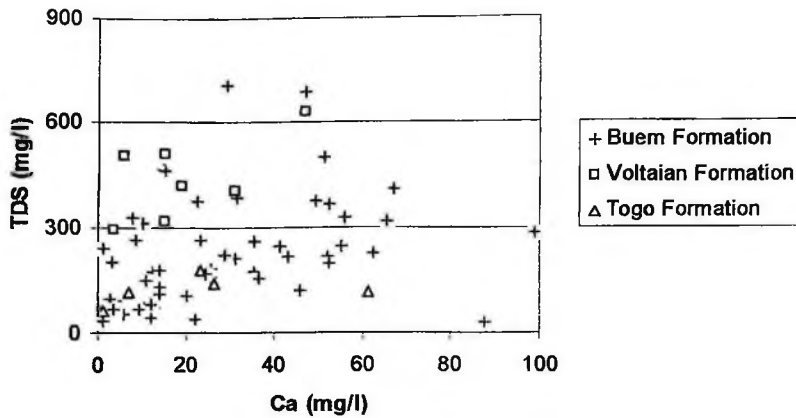


Figure 5.10 Scatter plot of TDS and Ca in the various aquifers in the area.

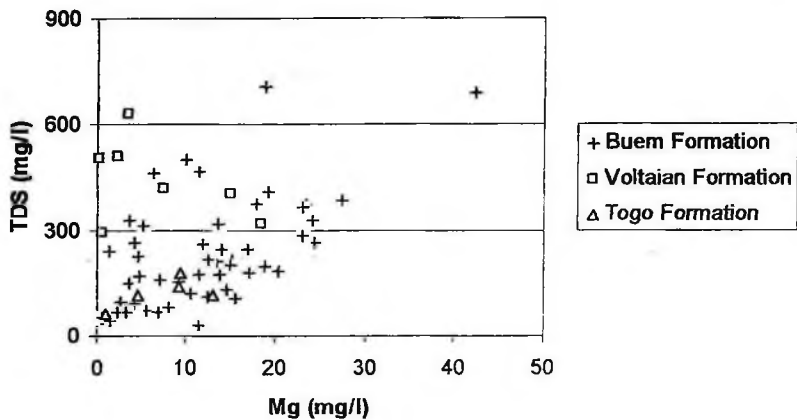


Figure 5.11 Scatter plot of TDS and Mg in the various aquifers in the area.

5.1.4 Groundwater Temperature distribution

Many characteristics of water such as electrical conductivity, pH and solubility of most dissolved constituents are affected by temperature. Also, temperature influences the rate of chemical reactions among dissolved substances. This therefore makes the

University of Ghana <http://www.uspjournal.org>
routine measurement of water temperature in the determination of water quality characteristics important.

The groundwater temperature in the area varies from 25.6°C at Obanda to 31.6°C at Sibi Central with an average of 28.3°C. The distribution does not depict any clear pattern, but, elevated temperatures are observed in the Voltaian Formation where the mudstones and siltstones aquifers occur. The mean groundwater temperature is close to the local mean annual temperature of 27°C showing shallow active groundwater circulation.

Temperature of groundwater is commonly in equilibrium with aquifer temperature. Therefore, the measured temperature of groundwater gives indication of the temperature attained at depth and provides information on the depth of circulation.

Bebout and Gutierrez (1981) observed that, the temperature of groundwater in South Louisiana, USA, increases with depth. However, in the study area no relationship exists between groundwater temperature and depth (Fig. 5.12). This is likely due to the roughly equal borehole depths and/ or inhomogeneity in aquifer characteristics.

The water temperature is poorly related to all the physico-chemical parameters as is shown in the low correlation coefficients (Appendix A-1) pointing to the shallow active water circulation in the area.

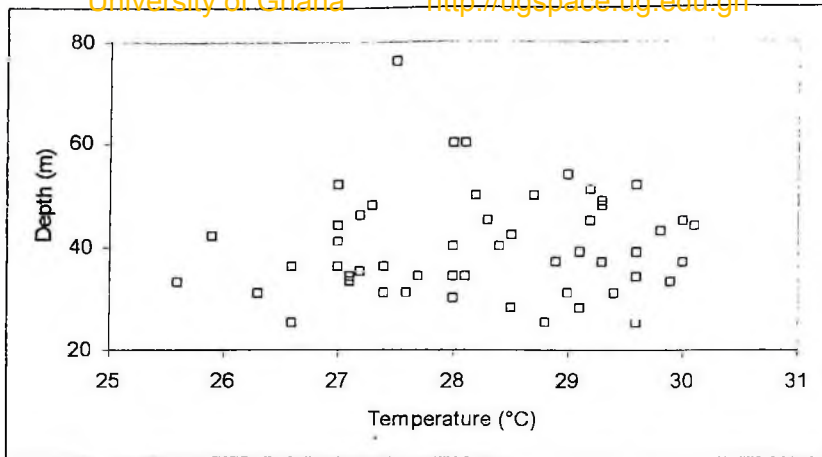


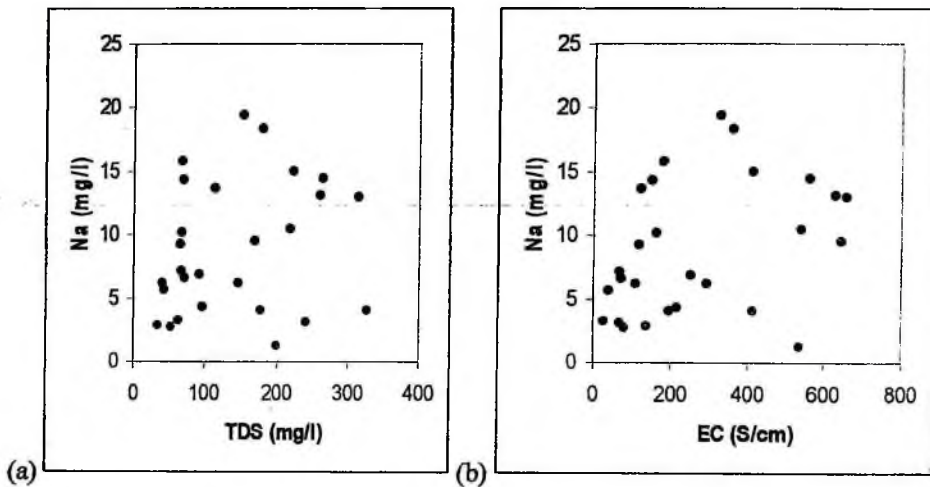
Figure 5.12 Scatter plot of depth of borehole and water temperature in the study area.

5.1.5 Sodium distribution

Sodium is the most abundant member of the alkali-metal group and the fourth most abundant metal in surface rocks. It occurs as a constituent of minerals found in some igneous and sedimentary rocks such as feldspars, clays and evaporites (Hem, 1989). Due to the highly soluble nature of sodium salts, a large amount of sodium is dissolved in natural water and remains soluble without undergoing precipitation reactions.

The concentration of sodium in the study area ranges between 1.2 mg/l at Nkwanta and 249.0 mg/l at Ebiteye #2 with an average and standard deviation of 39.4 mg/l and 48.1, respectively. The southeastern and northeastern parts of the study area made up mainly of quartzitic sandstones and sandstones aquifers have sodium concentration up

The second group of groundwater occurs mainly in the shale/ slate/ phyllite aquifers. Unlike the group I water, it is clear from Figure 5.14 a,b c that, sodium is strongly related to the total dissolved solids, electrical conductivity and bicarbonate. This indicates that sodium is a major contributor to ions in solution. This could be as a result of the interaction of the groundwater with a lithology of relatively high sodium content. Blay (1971) noted that the shale/ slate/ phyllite aquifers contain relatively high sodium composition as compared to quartzitic sandstone interlayered with minor shales aquifers.



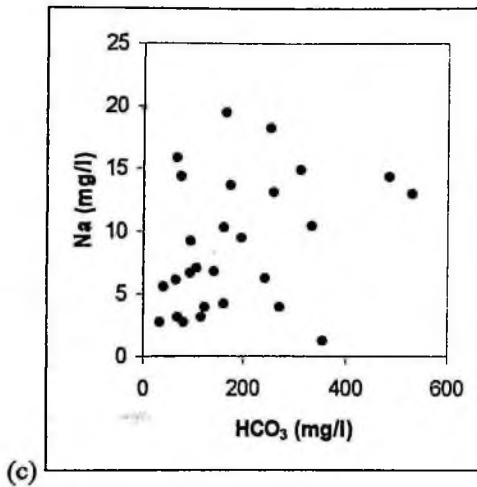
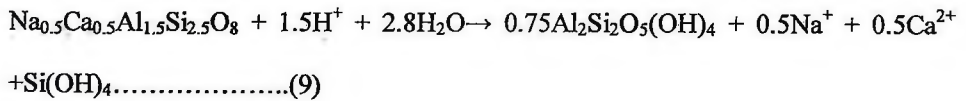


Figure 5.13 a,b,c. Scatter plot of sodium (Group I) and TDS , EC and HCO₃ in the study area.

The increase in sodium concentration corresponds to increase in calcium concentration (Fig. 5.14 d). It is therefore likely that the source of sodium is the dissolution of plagioclase feldspar given by the equation:



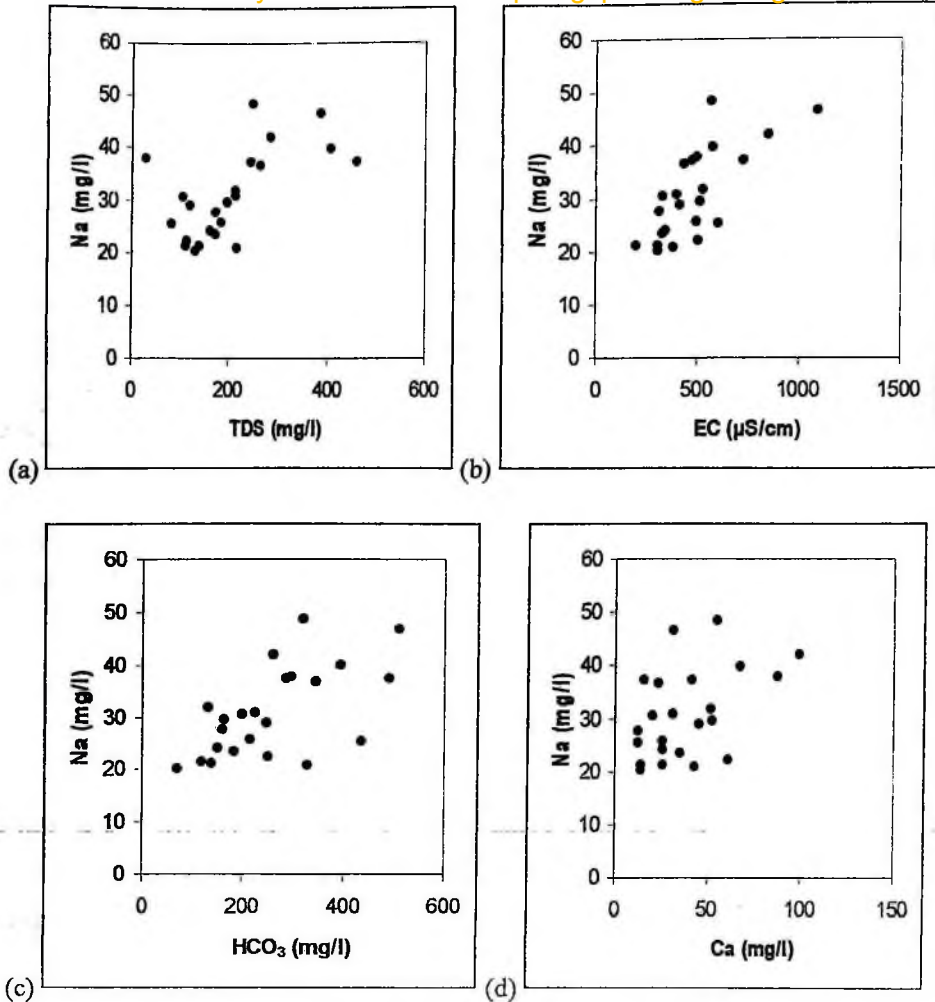


Figure 5.14 Scatter plot of sodium (group II) and (a) TDS (b) EC (c) HCO₃ (d) Ca in the study area.

The third group of groundwater occurs mainly in the siltstone and mudstone aquifers in the northwestern part of the study area which consists predominantly of clayey materials and subordinate amount of quartz, plagioclase feldspar and accessory apatite (Bobrov et al., 1964). Just like the group II groundwater, the plots of sodium against total dissolved solids, electrical conductivity and bicarbonate show a positive correlation (Fig. 5.15 a,b,c&d).

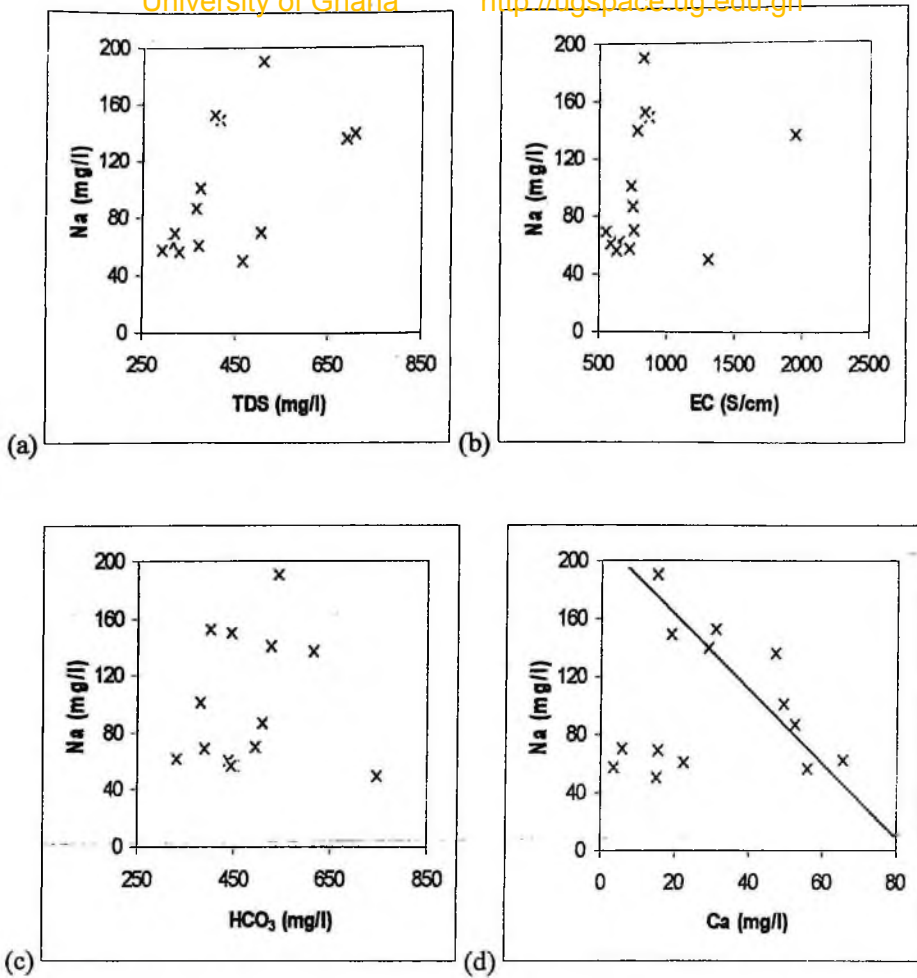


Figure 5.15 Scatter plot of sodium (group III) and (a) TDS (b) EC (c) HCO₃ (d) Ca in the study area.

The groundwaters of this group are relatively of high sodium concentration but low calcium and magnesium concentration. The relationship between sodium and chloride does not show a clearly defined pattern which indicates that halite dissolution is not a major process for sodium enrichment (Fig.5.14e). However the plot of sodium and

calcium shows a negative correlation (Fig. 5.14d). The possible reasons for this observable increase in the sodium concentration in this group are further dissolution of albite-rich plagioclase feldspars and cation exchange of calcium for sodium on clay surfaces.

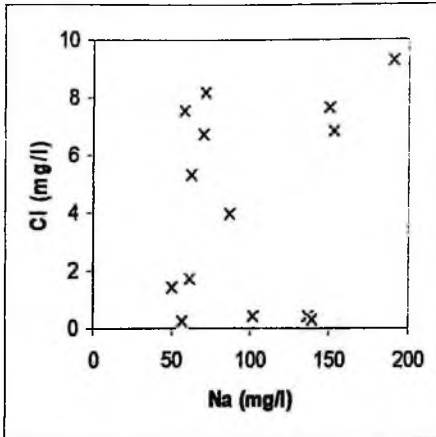
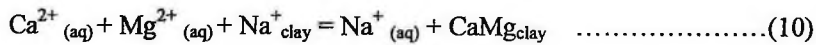


Figure 5.15 e Scatter plot of sodium (group III) and Cl in the study area.

Cation exchange of calcium for sodium on the siltstone and mudstone surface seems the likely process for sodium enrichment due to the negative correlation that exists between sodium and calcium (Fig. 5.14d) by the equation:



This process acts to increase the bicarbonate and may be responsible for the low calcium and magnesium concentrations in the siltstone and mudstone aquifers.

5.1.6 Potassium distribution

Potassium is the fifth most abundant metal in surface rocks and belongs to the alkali metal group. It is more abundant than sodium in sedimentary rocks but slightly less in igneous rocks. Notwithstanding the similarities in the chemical properties of potassium and sodium, they behave differently in natural systems. Sodium tends to continually remain in solution once it has been liberated from silicate mineral structures. Potassium on the other hand, is released with greater difficulty from silicate mineral and tends to be fixed to weathering products especially clay minerals. Just like sodium, it is an essential element for plant and animals and concentrated by plants (Hem, 1992).

The potassium concentration ranges from 0.13 mg/l at Nkwanta to 3.58 mg/l at Bonakye with an average of 1.71 mg/l. The concentration of potassium in the groundwater is generally low and contrasts with its content in the bulk rocks but consistent with its occurrence in natural water. Blay (1971) found the percentage composition of potassium in both the shales and sandstones to be more than hundred percent in excess with respect to sodium, calcium and magnesium. The potassium concentration of the groundwater in the shale/slate/ phyllites aquifers is however higher than the concentration in the sandstone aquifers which is in general agreement with the chemical analysis (Blay, 1971). The distribution of potassium generally follows that of sodium with higher concentrations occurring around Abotoase, Kwamekrom, Tutupene and Chiaso areas. Lower concentrations of less than 1.56

mg/l are however, found in the central and northeastern margin of the study area around Nkwanta township, Kadjebi and east of Jasikan.

Figures 5.16, 5.17 and 5.18 show that potassium concentration correlates poorly with total dissolved solids, electrical conductivity and bicarbonate, indicating that the dissolution of potassium-rich feldspar does not yield significant amount of potassium to the groundwater samples. The relatively high potassium in the Buem sandstones and shales aquifers according to Blay (1971) is expected to reflect in the groundwater by the dissolution of the potassium-rich feldspars that occur in the Buem sandstone and shale according to the equation:

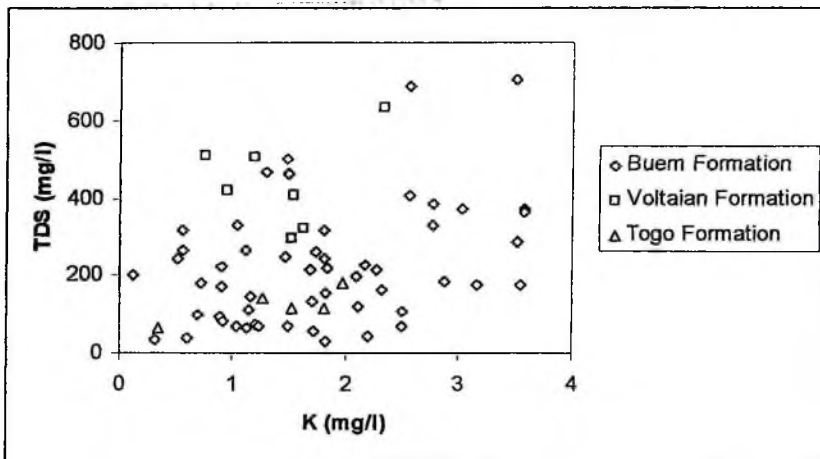
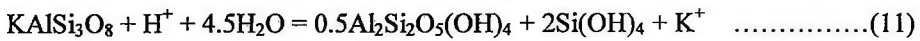


Figure 5.16 Scatter plot of potassium and TDS in the study area.

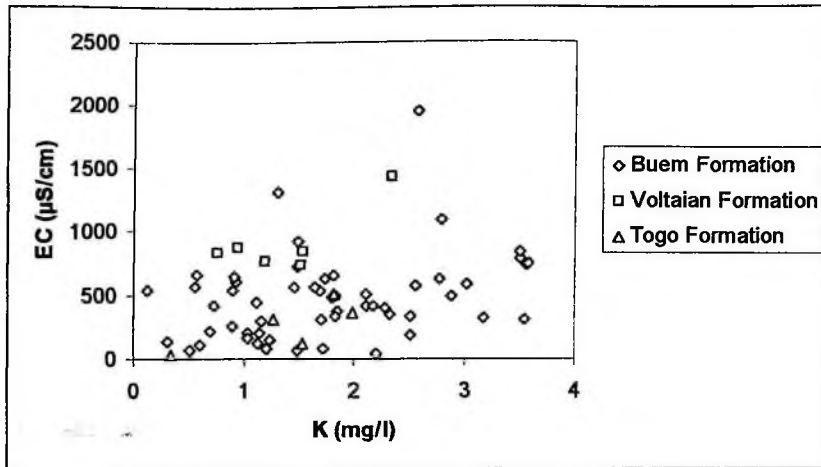


Figure 5.17 Scatter plot of potassium and EC in the study area.

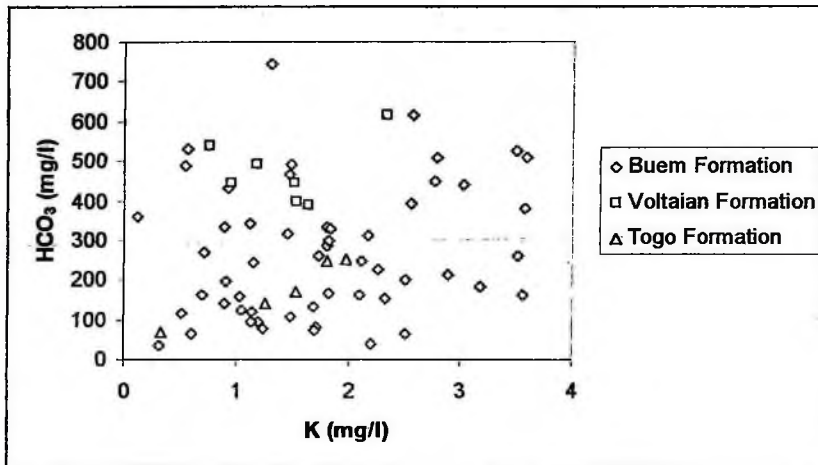


Figure 5.18 Scatter plot of potassium and HCO₃ in the study area.

This however, is not the case. The concentration of potassium in the groundwater in the area is quite low which is in general agreement with its concentration in natural water (Hem, 1992). This observation is partly due to the high degree of stability of potassium-bearing aluminosilicate minerals. Another plausible reason may be its

tendency to be fixed by clay minerals and to participate in the formation of secondary minerals (Mathess, 1982).

5.1.7 Calcium distribution

Calcium is the most abundant of the alkaline earth metals and the third most abundant metal at the earth's surface. It is a major constituent of many common rock forming minerals and an essential element for plant and animal life forms.

Calcium concentration in the study area ranges from 1.21 mg/l at Kadjebi to 98.9 mg/l at Chiaso with an average and standard deviation of 26.96 mg/l and 22.17 respectively. An estimated 70% of the area is of relatively low Ca concentration of less than 30 mg/l. However relatively high Ca concentration of greater than 30 mg/l occurs in pockets at central eastern and southern tip of the study area where the shales, slates and phyllites predominate in the aquifer.

Based on the calcium concentration and the type of aquifer, two classes of water are identified. These are:

Type I: Ca concentration of less than 30 mg/l and

Type II: Ca concentration of greater than 30 mg/l

The first group of groundwater has low calcium concentration of less than 30 mg/l and further reveals two sub water group when calcium is plotted against pH, TDS and

bicarbonate concentration (Figs. 19 a,b & 20) . The first sub group shows relatively low pH, TDS and bicarbonate and a low Ca.

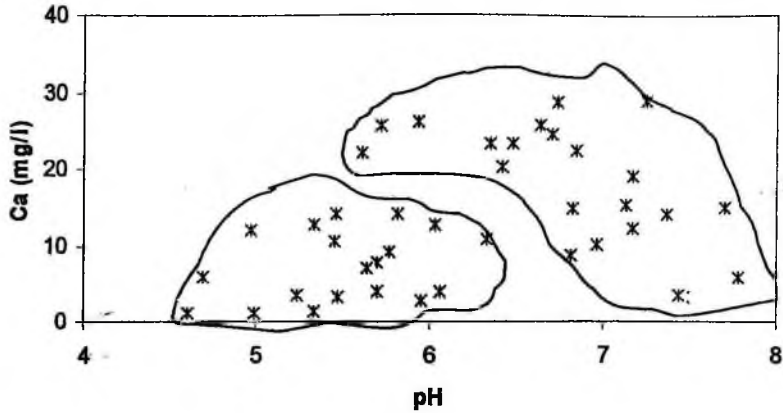


Figure 5.19a Scatter plot of Calcium and pH of the group I type in the study area.

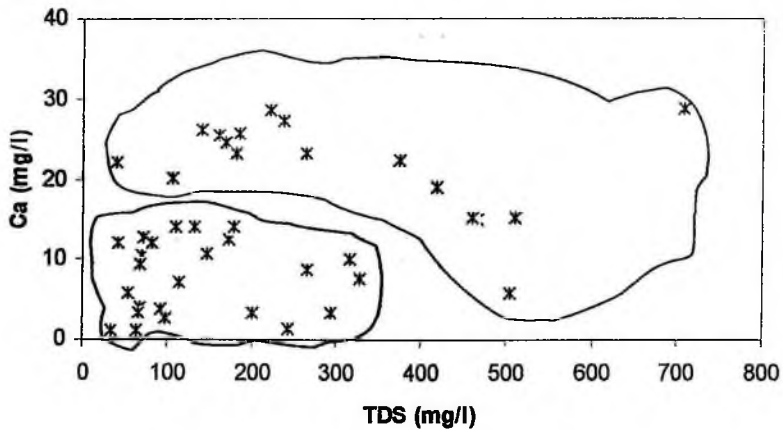


Figure 5.19b Scatter plot of Calcium and TDS of the group I type in the study area.

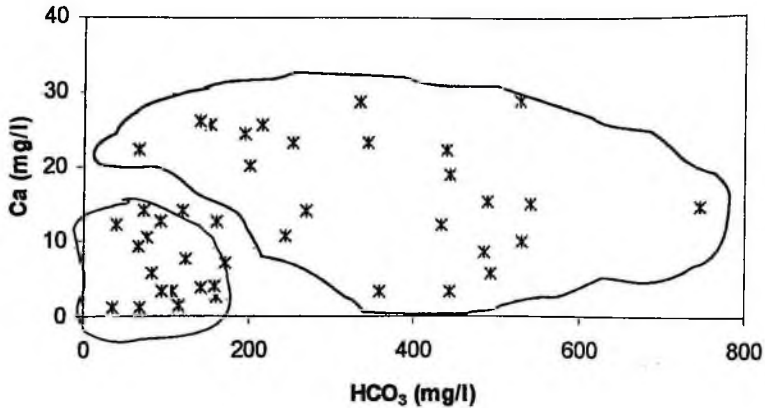


Figure 5.20 Scatter plot of Calcium and HCO_3 of the group I type in the study area.

This group is formed in aquifers made up predominantly of quartzitic sandstones but in some places intercalated with calcareous shales or slates. The plots show wide scattering of points in this sub-group, probably due to the multiple sources of calcium. Probable sources of calcium may be the dissolution of plagioclase feldspar in the quartzitic sandstone and dissolution of carbonate materials in the calcareous shales and slates.

The second sub-group shows generally low Ca but relatively high pH, TDS and bicarbonate. These samples occur in the Buem and Voltaian mudstones and siltstones. Bobrov and Pentelkov (1964) noted that the mudstones are composed predominantly of clayey materials and subordinate amount of quartz, plagioclase feldspar and accessory apatite. The relationships between calcium and pH, total dissolved solids and bicarbonate show negative correlation (Fig. 18,19& 20). Furthermore, as the calcium concentration decreases, sodium concentration increases (Fig. 5.21).

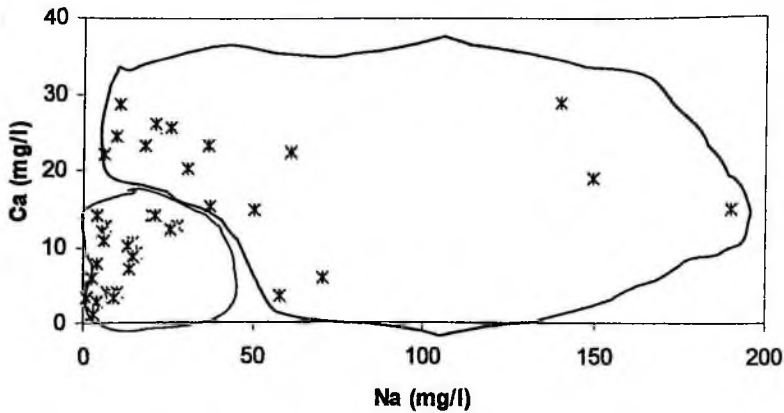
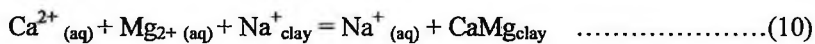


Figure 5.21 Scatter plot of Calcium and Na of the group I type in the study area.

The presence of mudstone and siltstone containing fine grained materials, and the negative correlation that exists between sodium and calcium concentration probably suggest cation exchange process to be accounting for the observed water chemistry (Foster, 1950; Back, 1966; Freeze and Cherry, 1979; Thorstenson et al., 1979; Chapelle and Knobel, 1983).



This process leads to increase in total dissolved solids and bicarbonate as observed in Figures 5.18 and 5.19.

Moreover, the low calcium concentration may be due to the precipitation of calcite. Precipitation of calcite would lead to decreasing bicarbonate, which is not the case in

this study area. The precipitation of calcite is therefore discounted. The cation exchange process seems more likely to explain the water chemistry, because of the presence of the clayey material and the increase in total dissolved solids, pH and bicarbonate (Appelo and Postma, 1993).

In the second group, which has calcium concentration greater than 30 mg/l, a wide range in pH, total dissolved solids, electrical conductivity and bicarbonate give uniform calcium concentration (Figs. 5.22,23& 24).

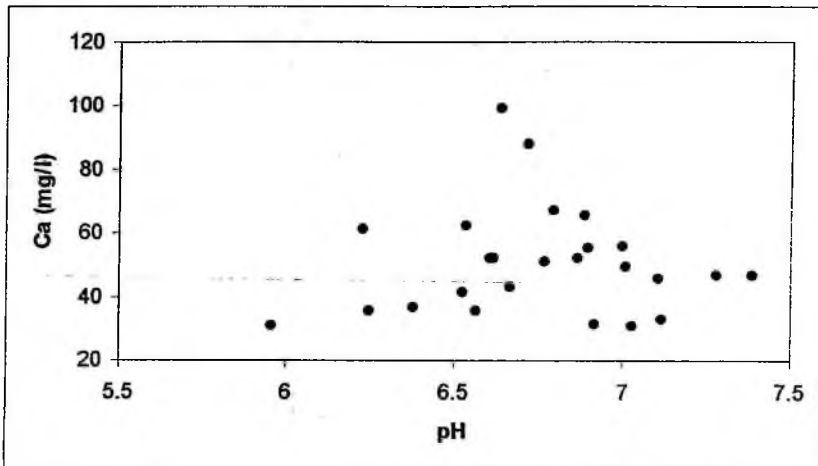


Figure 5.22 Scatter plot of Calcium and pH of the group II type in the study area.

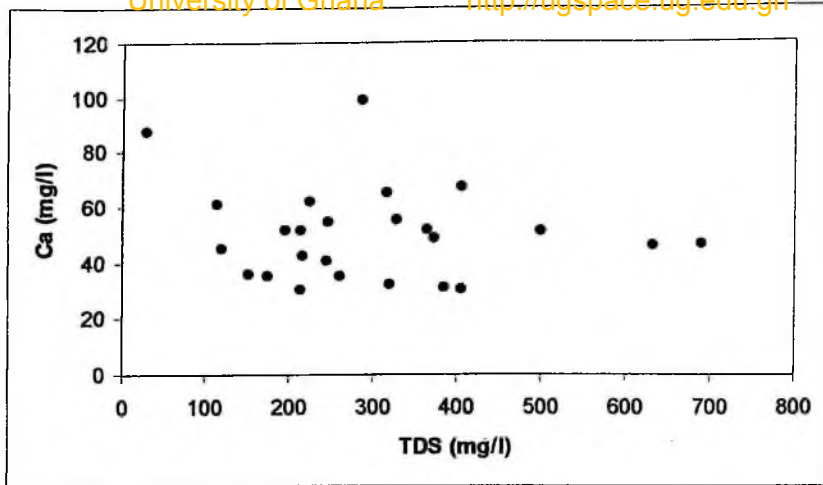


Figure 5.23 Scatter plot of Calcium and TDS of the group II type in the study area.

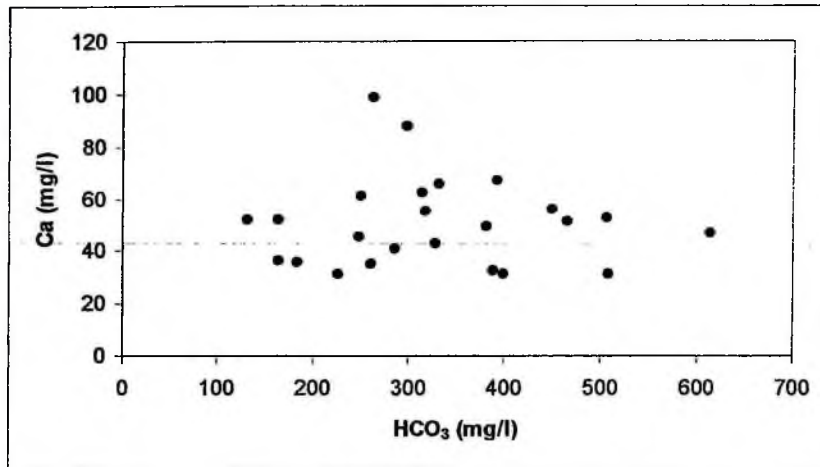


Figure 5.24 Scatter plot of Calcium and HCO₃ of the group II type in the study area.

Unlike the first group, this is formed in calcareous shales, slates or phyllite aquifers. Increase in calcium concentration in this group corresponds to a generally uniform sodium concentration and has no relationship with the magnesium concentration. The points in the plots are also widely scattered indicating the variable source of calcium in this group. The major source of the calcium is, therefore, the dissolution of

plagioclase feldspar and calcite minerals that occur in the aquifer under partially open system as shown by the following equations:

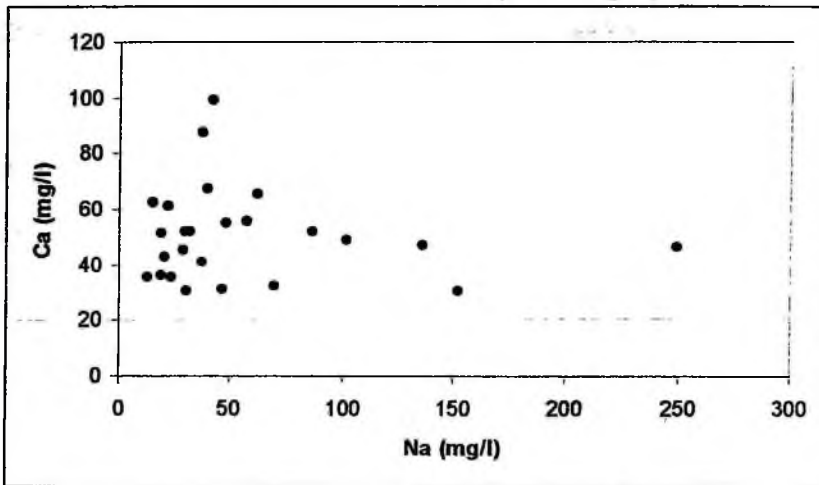
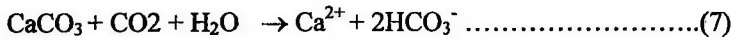
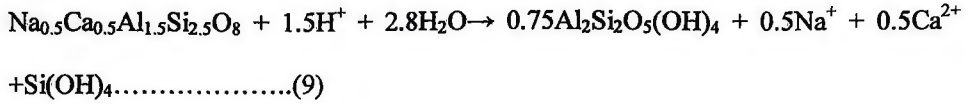


Figure 5.25 Scatter plot of Calcium and Na of the group II type in the study area.

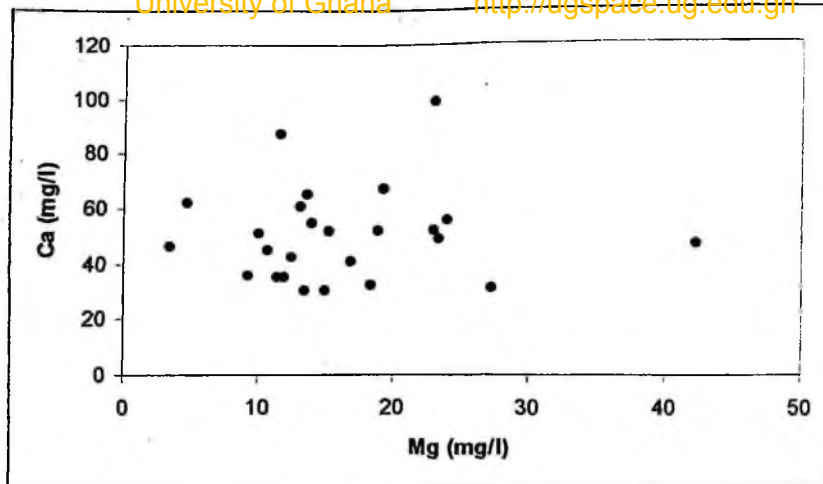


Figure 5.26 Scatter plot of Calcium and Mg of the group II type in the study area.

5.1.8 Magnesium distribution.

Magnesium is the sixth most abundant metal in surface rocks and a major constituent of common minerals found in igneous, metamorphic and sedimentary rocks such as olivine, pyroxene, mica, serpentine and dolomite. It is an essential element for plant and animals and a major dissolved constituent in natural water (Hem, 1992).

The concentration of magnesium in the groundwater in the study area ranges from a minimum of 0.62 mg/l at Guaman in the Jasikan district to a maximum of 42.30 mg/l at Dawa in the Nkwanta district with a mean concentration and standard deviation of 10.69 mg/l and 8.21 respectively. A greater part of the area has Mg concentrations lower than the average but higher concentrations occur in the southwestern and northwestern parts of the study area. Exceptionally low concentrations of less than 15

University of Ghana <http://ugspace.ug.edu.gh>
mg/l occur in the Jasikan district and the northeastern and southeastern parts of the Nkwanta district.

The plots of magnesium against pH, bicarbonate and total dissolved solids show two types of groundwater:

I. Type I of concentration less than 15 mg/l.

II. Type II of concentration greater than 15 mg/l.

The first group of groundwater has low magnesium concentration of less than 15 mg/l and shows two sub water groups when magnesium is plotted against pH, TDS and bicarbonate concentration (Figs.5.27, 5.28 and 5.29). The first sub group shows relatively low pH, TDS and bicarbonate and a low Mg. The increase in magnesium corresponds with increase in pH, TDS and bicarbonate.

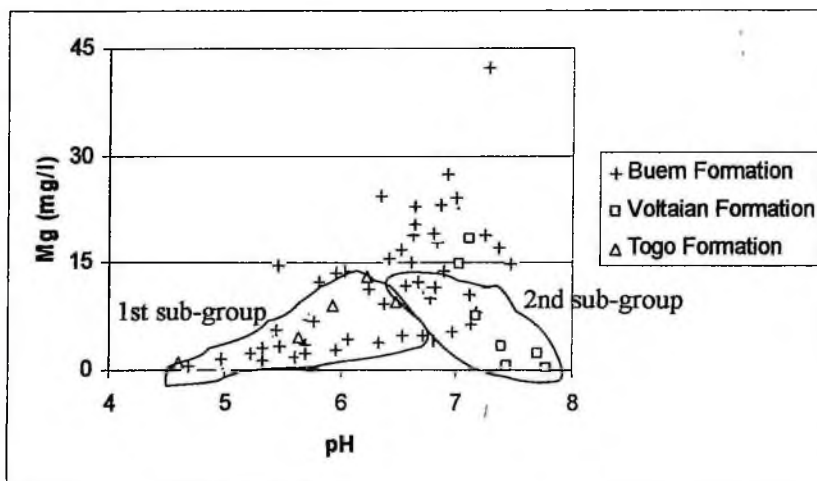


Figure 5.27 Scatter plot of Magnesium and pH in the study area.

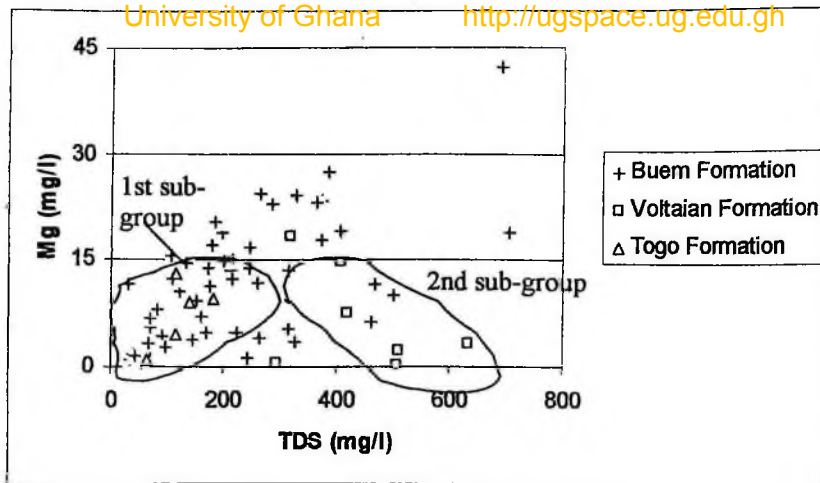


Figure 5.28 Scatter plot of Magnesium and TDS in the study area.

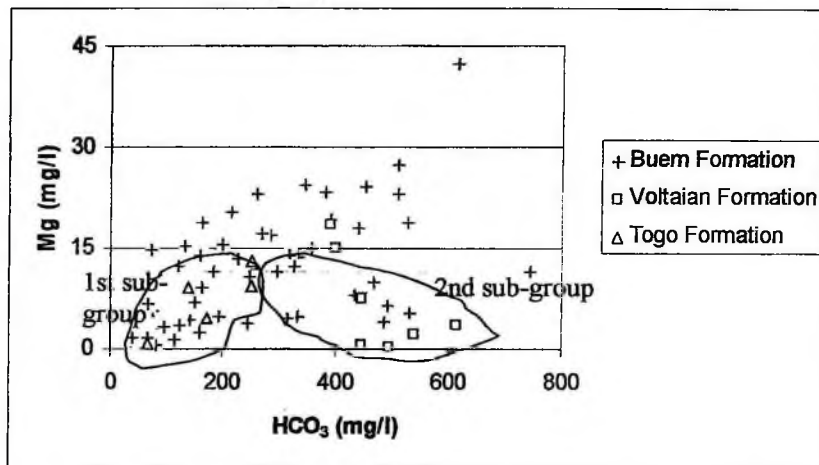
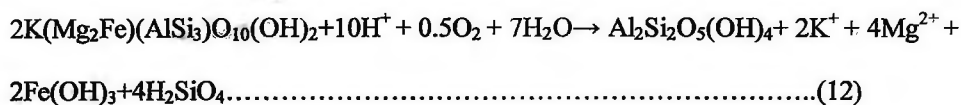


Figure 5.29 Scatter plot of Magnesium and Bicarbonate in the study area.

According to drillers lithological logs, groundwater of the first sub-group occurs mainly in the Buem sandstones and the quartzitic sandstones and Togo phyllites and the quartz-schists aquifers. Chlorite and biotite occur in small amount in the sandstones (Lashmanov, 1965). Low magnesium samples also have low bicarbonate,

pH and electrical conductivity indicating a slow dissolution kinetics of the magnesium-containing mineral in aquifer.

The mean calcium: magnesium ratio of 4 in this group is relatively high, suggesting that dolomite dissolution is not the source of magnesium. Therefore the possible source of the magnesium is the dissolution of the small amount of biotite and chlorite that occur in the aquifer. This equation is given by:



The second sub-group shows generally low Mg but relatively high pH, TDS and bicarbonate. These samples occur in the Buem and Voltaian mudstones and siltstones. Bobrov and Pentelkov (1964) noted that the mudstones are composed predominantly of clayey materials and subordinate amount of quartz, plagioclase feldspar and accessory apatite. The relationships between magnesium and pH, total dissolved solids and bicarbonate show negative correlation (Fig. 27,28 & 29). Furthermore, in Figure 5.30, as the magnesium concentration decreases, sodium concentration increases.

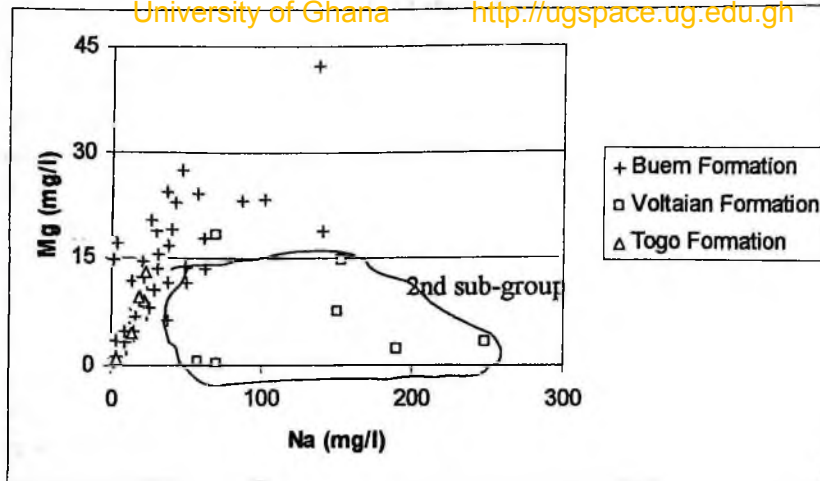
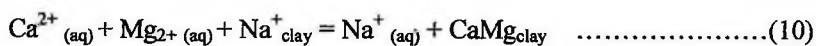


Figure 5.30 Scatter plot of Magnesium and Sodium in the study area.

The presence of mudstone and siltstone containing fine grained materials, and the negative correlation that exists between sodium and magnesium concentration probably suggest cation exchange process to be accounting for the observed water chemistry (Foster, 1950; Back, 1966; Freeze and Cherry, 1979; Thorstenson et al., 1979; Chapelle and Knobel, 1983).



This process leads to increase in total dissolved solids and bicarbonate as observed in Figures 5.28 and 5.29.

The type II (Mg concentration greater than 15 mg/l) groundwater on the other hand shows wide variation in the bicarbonate and TDS values (Fig. 5.27, 5.28 & 5.29).

These samples occur in the shales, phyllites and schists aquifers. These rocks are made up of carbonates, chlorite and biotite among others. The wide variation in the bicarbonate and TDS values on the plots indicates the variability of the source of magnesium.

5.1.9 Bicarbonate distribution.

Bicarbonate concentration ranges from 36 mg/l at Kadjebi to 746 mg/l at Agou with an average and standard deviation of 283.9 mg/l and 169.39. About 90% of the area is of concentration less than 274.5 mg/l. Concentrations of between 274.5 mg/l and 396.5 mg/l occur in the east-central and southwestern margin. Relatively higher concentrations greater than 396.5 mg/l occur to the northwestern corner of the area.

The dissolution of inorganic carbon yields CO_2 , HCO_3^- and CO_3^{2-} which is controlled by pH. Within the pH range of the groundwater in this area suggest that the dominant dissolved inorganic carbon in the groundwater is in the form of HCO_3^- . Figure 5.31 shows the strong relationship between bicarbonate and total dissolved solids which indicates the dominance of bicarbonate as the single most important anion in the groundwater in the study area.

The variation in the concentration of HCO_3^- in the area is related to the lithology and tend to control the pH distribution.

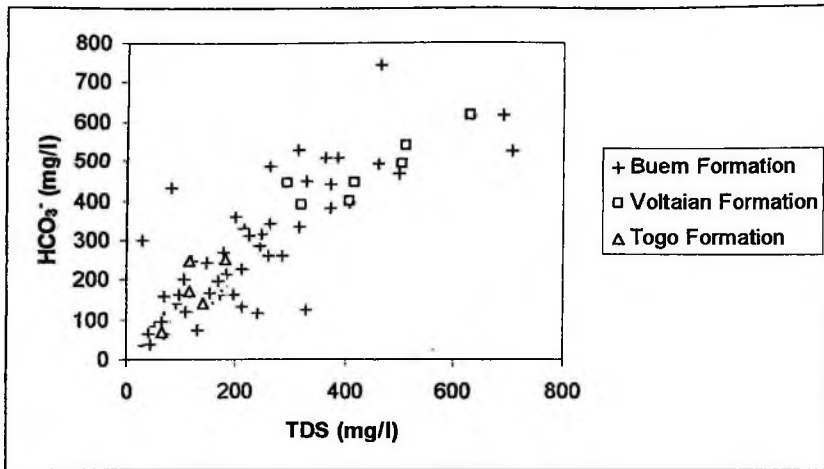


Figure 5.31 Scatter plot of bicarbonate and total dissolved solids in the area.

The scatter plot of bicarbonate and pH (Fig. 5.32) shows two relationships with different gradients:

- I. Smaller gradient with pH less than 6
- II. Greater gradient with pH greater than 6

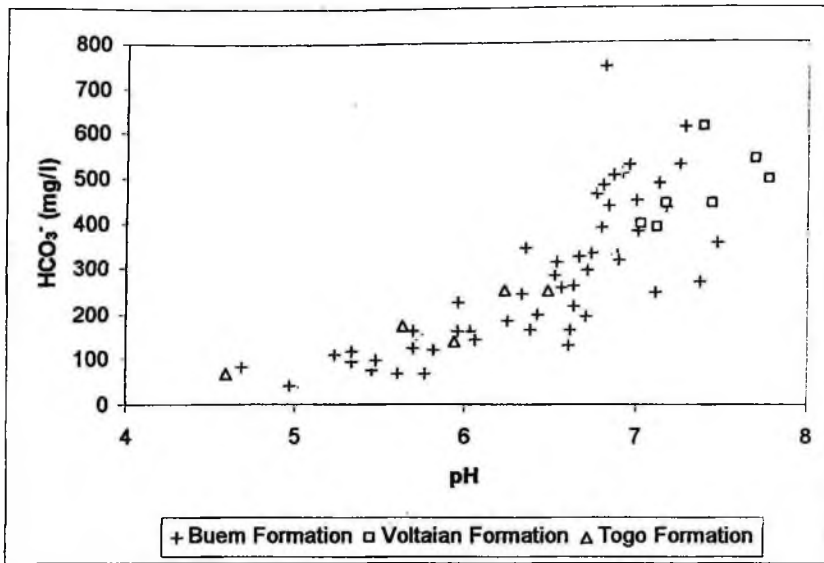


Figure 5.32 Scatter plot of bicarbonate and pH in the area.

The first group has bicarbonate occurring over a narrow range of between 40 and 200 mg/l with relatively low pH. These samples form about 43% and occur mainly in the quartzitic sandstones interlayered with minor shales aquifer. This aquifer is made up predominantly of relatively stable minerals namely quartz and plagioclase feldspar.

Consider the dissolution of carbon dioxide at pH less than 8 in the equation 1 below:



During weathering reaction, as the proton (H^+) in the soil solution is removed, equation (1) proceeds to the right hand side producing more HCO_3^- . In the quartzitic sandstones interlayered with minor shales aquifer made up mainly of stable quartz and plagioclase feldspars, consumption of H^+ in (1) is relatively slow and does not go far enough hence the relatively low cations, pH and bicarbonate.

The second group has a wide range in bicarbonate occurring over a narrow and relatively high pH range. These samples occur mainly in the shales, mudstones and siltstones aquifers composed mainly of fine grained plagioclase feldspar and calcite. The consumption of H^+ in (1) is relatively rapid as a result of the large surface area in contact with the infiltrating rainfall and the occurrence of reactive minerals. Consequently, equation 1 moves to the right-hand side releasing more bicarbonate into the groundwater. Considering this mechanism of bicarbonate increase, bicarbonate concentration is a geochemical index of weathering-cation release reaction in the area (Ohte and Asano, 1997).

Another possible explanation for the distribution of HCO_3^- in the study area is evident from figures 5.33, 5.34 and 5.35. These plots show two classes of groundwater when HCO_3^- is plotted against Sodium, Calcium and Magnesium. The first group occurs in the Buem sandstones and the quartzitic sandstones and Togo phyllites and the quartz-schists aquifers and the plots show positive correlation when HCO_3^- is plotted against sodium, calcium and magnesium. This probably indicates that the dissolution of aquifer material may be accounting for the HCO_3^- distribution. The second group on the other hand, occur in the Buem and Voltaian mudstones and siltstone. The plot shows a negative correlation when HCO_3^- is plotted against calcium and magnesium but a positive correlation against sodium. Bobrov and Pentelkov (1964) noted that the mudstones are composed predominantly of clayey materials and subordinate amount of quartz, plagioclase feldspar and accessory apatite.

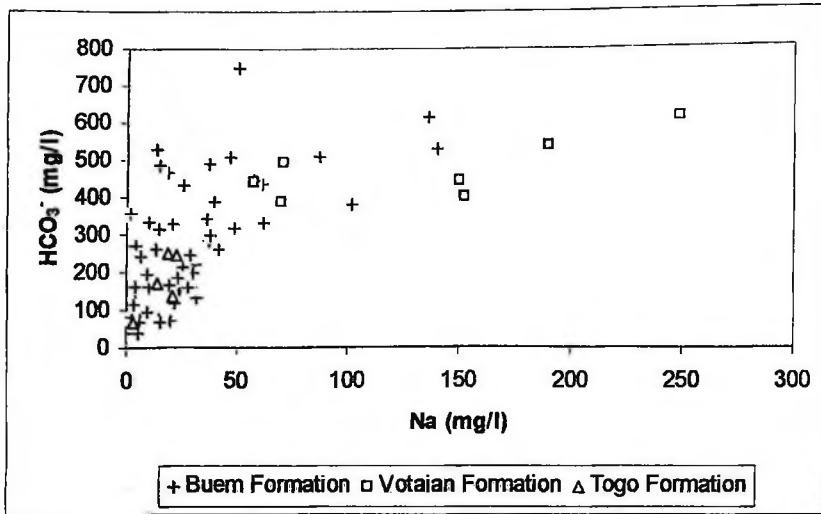


Figure 5.33 Scatter plot of HCO_3^- and Na in the study area.

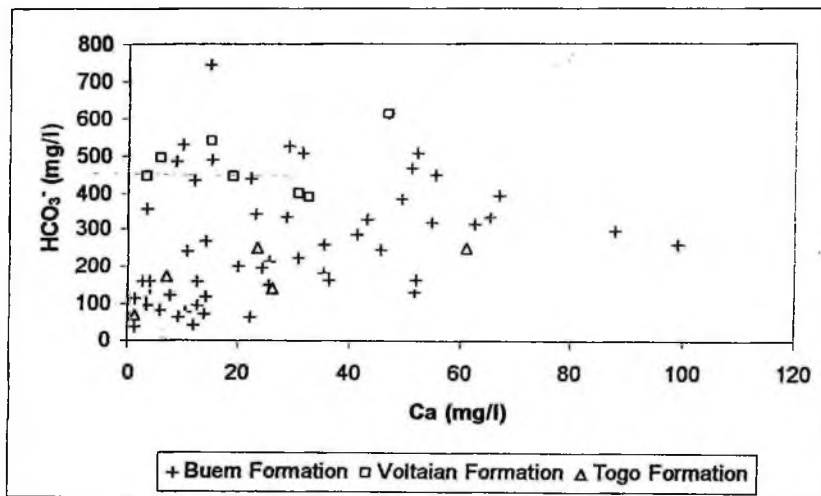


Figure 5.34 Scatter plot of HCO_3^- and Ca in the study area.

A decrease in calcium and magnesium concentration leads to an increase in sodium, pH, total dissolved solids and bicarbonate. This observed water chemistry probably indicates the dissolution of albite-rich plagioclase feldspar as the source of bicarbonate in the sample of this Formation. However, the high bicarbonate can not

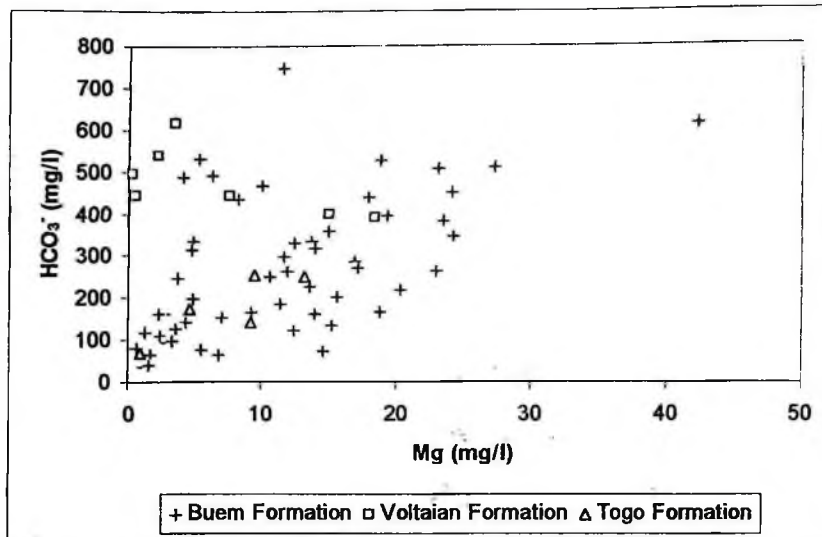


Figure 5.35 Scatter plot of HCO₃⁻ and Mg in the study area.

be accounted for by the dissolution of albite-rich plagioclase feldspar alone since it occurs in minor amount.

Another possible explanation of the water chemistry is the cation exchange of sodium for calcium and magnesium on the siltstone and mudstone surfaces. The presence of clayey materials, the relatively high pH and the negative correlation that exist between sodium and calcium makes cation exchange the likely process to explain the increase in bicarbonate in this Formation.

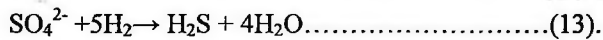
5.1.10 Sulphate distribution.

The sulphate concentrations range from 0 mg/l at Asato and Bonakye to 154 mg/l at Dawa with a mean of 8 mg/l. Most parts of study area are of concentrations less than 10 mg/l but generally increase to the northwestern part of the study area.

Based on Figure 5.36, groundwater in the area can be classified into two sets. These are:

- I. With concentration less than 10 mg/l
- II. With concentration greater than 10 mg/l

The first group forms about 83% of all the samples and occurs in both the quartzitic sandstone and shale/slate/phyllites aquifers. The generally low sulphate ion concentrations observed in the groundwaters could partly be due to reduction of sulphate to produce hydrogen sulphide gas. This is shown by the equation:



The rotten-egg smell emanating from some of boreholes especially at Dodi-Papase area confirms this fact.

Another possible reason for the low sulphate concentration is the absence of sulphate-containing minerals such as gypsum and anhydrite (Lashmanov, 1965 and Bobrov et al., 1964). On figure 5.36, the line A superimposed on the analytical data is represented by equation (14). This shows a uniform sulphate over a wide range of calcium indicating a deviation from gypsum dissolution. This probably confirms the lack of gypsum in the aquifer. Therefore the likely source of the sulphate can be attributed to atmospheric sources, sulphate impurities and/or decomposition of organic matter (Freeze and Cherry, 1979).

However, in the second set, the line B superimposed on the analytical data is represented by the linear equation (15). These samples occur in the Buem and Voltaian siltstone and mudstone aquifers in the northwestern part of the area composed of quartz, plagioclase feldspar and sericites flakes (Lashmanov, 1965).

$$SO_4^{2-} = 2 \dots \dots \dots (14)$$

$$Ca = 0.3 SO_4^{2-} - 33 \dots \dots \dots (15)$$

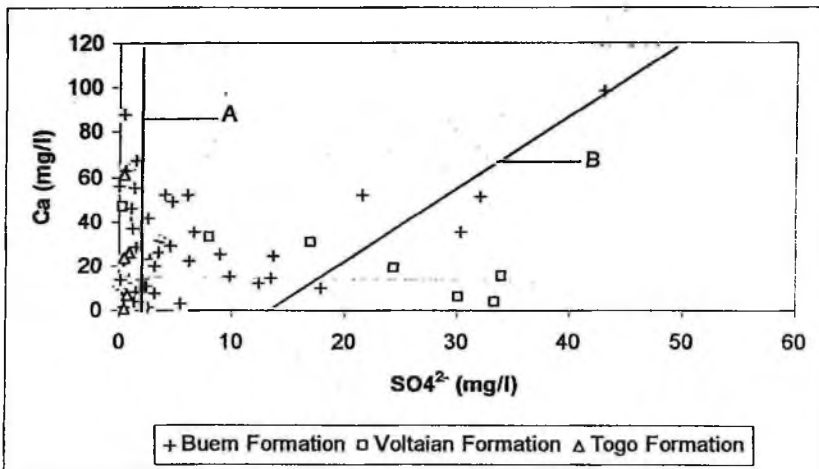


Figure 5.36 Scatter plot of Ca and SO₄²⁻ in the study area.

Even though the sulphate concentration in these samples generally increases with calcium; the ratio of calcium to sulphate is far above the stoichiometry of gypsum dissolution. This shows that the source of sulphate in the samples can not be attributed to gypsum dissolution. Figure 5.37 shows that two classes of groundwater when SO₄²⁻ is plotted against pH. One class shows low sulphate groundwater having wide

variation in pH, while the other gives wide variation in SO_4^{2-} over almost uniform pH.

This indicates probably that the oxidation of pyrite is not taking place. The source of sulphate in the aquifers can therefore be attributed to atmospheric sources, decomposition of organic matter and/ or anthropogenic sources due to the administration of fertilizer such as sulphate of ammonia.

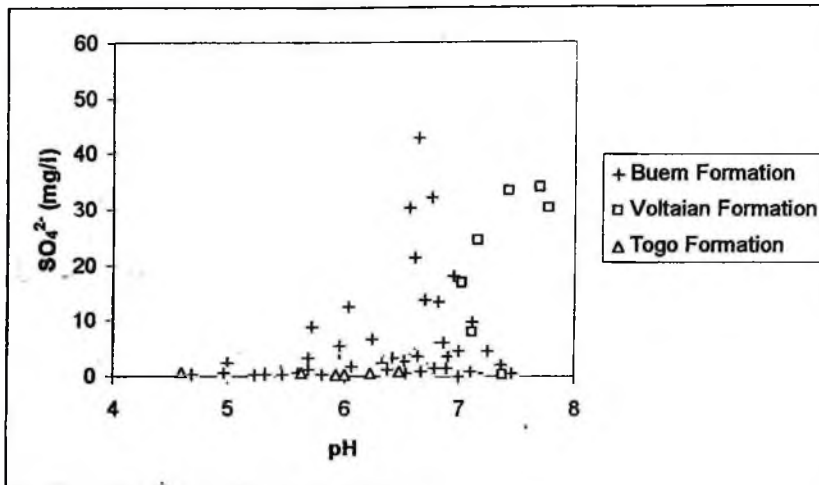


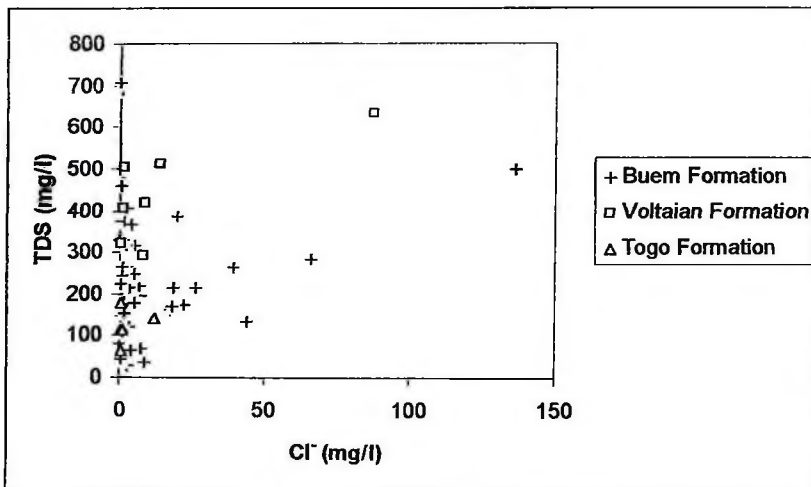
Figure 5.37 Scatter plot of pH and sulphate in the study area.

5.1.11 Chloride distribution.

Chlorine is the most abundant of the halogens. Despite the fact that chlorine has several oxidation states, chloride is the only one of major significance in aqueous geochemistry (Ebert and Lori, 2000).

The chloride concentration lies between 0.148 mg/l at Kpassa in the Nkwanta district and 136.25 mg/l at Mepasem in the Kadjebi district. The average concentration is 10.82 mg/l.

According to Horn and Adams (1966), the concentration of chloride is the lowest of all the major ions in natural water because of its lowest concentration in various rock types. Hem (1989) noted that minerals in which chloride is an essential component are not very common and chloride is more likely to be present as an impurity. However, a more important source of chloride is associated with sedimentary rocks, particularly evaporates such as halite. Figures 5.38 and 5.39 show that increase in sodium and total dissolved solids do not lead to a corresponding increase in chloride concentration. This probably indicates that the source of the chloride can not be the dissolution of evaporite. The generally high chloride concentration occurs in the shales/slates/phyllite aquifers of the Buem Formation which are composed of clay materials, chlorite or sericites and plagioclase feldspar. The relatively high chloride concentration is probably due to the occurrence of chloride as impurities in the chlorites or sericites (Kurode and Sandell, 1953) that become available to the groundwater during dissolution.



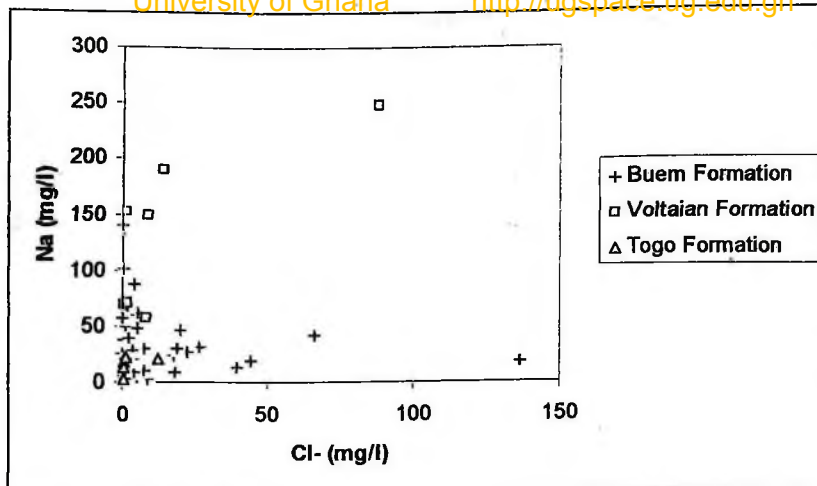


Figure 5.39 Scatter plot of Na and chloride in the study area.

The generally low chloride concentration in groundwater in the area reflects its insignificant proportion in silicate rocks. Therefore its presence in the groundwater is likely from impurities in the aquifer material (Freeze and Cherry, 1979).

5.1.12 Nitrate distribution

The concentration of nitrate in the Buem Formation varies from 0 to 17.5 mg/l with an average of 0.8 mg/l. In the Voltaian Formation on the other hand, nitrate concentration ranges between 0 and 0.1 mg/l and a mean of 0.3 mg/l. The nitrate concentration in the Togo Formation is also quite low of a mean of 0.3 mg/l and ranges between 0 and 0.06 mg/l.

All the samples in the area fall below the maximum permissible limit for nitrate concentration (45mg/l) according to WHO (1993) and are consistent with groundwater that has not undergone contamination as a result of human activity

(Bachman, 1984). High nitrate concentrations in drinking water are believed to be a health hazard because they may cause methaemoglobinemia in human infants, a potential fatal syndrome by which oxygen transport in the bloodstream is impaired (Appelo and Postma, 1993).

The sources of nitrate to groundwater have been suggested by many authors as: leaching of organic and inorganic fertilizer from agricultural land by infiltration of precipitation, animal waste, leakage from sewers and subsurface flow from upgradient areas (Hill, 1982; Flipse et al., 1984; Houzim et al., 1986; Kolaja et al., 1986; Vrba, 1986). These sources are mainly man-made and tend to increase the nitrate levels above the permissible limit. However, concentration of nitrate of the groundwater in the area rarely exceed 1 mg/l indicating that the distribution of nitrate is related to natural processes.

5.2 Hydrochemical facies

The diagnostic chemical properties of water are presented by various methods, the most common of which are the hydrochemical facies. It is more useful when presented in a Trilinear diagram (Piper, 1944) which can screen and sort large amount of chemical data. Furthermore, the Piper diagram can define the pattern of spatial change in the water chemistry among geological units (Raji and Alagbe, 1997 and Domenico and Schwartz, 1998).

In this section, the results of the chemical analysis of the groundwater in the study area based on the various Formations are plotted on a Piper diagram and the hydrochemical facies discussed. Moreover, the results are plotted on a finger print and Durov diagrams to identify the dominant ions and important reaction in the various rocks respectively.

5.2.1 Hydrochemical Facies in the study area.

The hydrochemical facies representation in the study area is based on the distribution of water types in all the geological formations and their related lithologies. From the Piper Trilinear plot (Piper 1944) (Fig. 5.40) and the water chemistry, the groundwater can be grouped into five facies. These are:

- Calcium+Magnesium- Bicarbonate (Ca+Mg-HCO_3) facies
- Calcium-Bicarbonate (Ca-HCO_3) facies
- Sodium-Bicarbonate (Na-HCO_3) facies
- Magnesium-Bicarbonate type (Mg-HCO_3) facies
- Calcium+Magnesium- Chloride (Ca+Mg-Cl) facies.

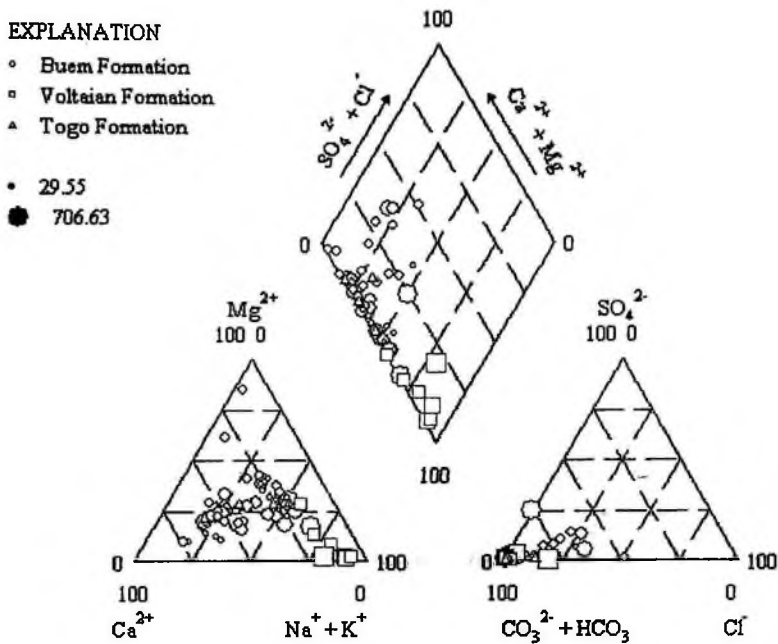


Figure 5.40 Piper plot of samples in the study area

The five water types and their summary statistics are presented in Table 5.2.

5.2.1.1 Calcium+Magnesium-Bicarbonate facies

The Calcium+Magnesium-Bicarbonate facies is predominant in the area and forms about 48% of the groundwater and occurs in the south, northeastern and pockets in the central part of the area.

The mean pH and temperature are 6.3 and 28.3°C respectively. The total dissolved solids value in this facies ranges from 35 to 407 mg/l with a mean of 210 mg/l. The electrical conductivity ranges between 68 and 1091 $\mu\text{S}/\text{cm}$ with an average of 440.3 $\mu\text{S}/\text{cm}$.

Table 5.2 Statistical Summary Of Water Types In The Study Area

Facies	Percentage of facies (%)	pH		EC ($\mu\text{S}/\text{cm}$)		TDS (mg/l)		Temperature ($^{\circ}\text{C}$)		Sodium (%)	
		Range	Mean	Range	Mean	Range	Mean	Range	Mean	Range	Mean
Ca+Mg-HCO ₃	48	5.0-7.2	6.3	68-1091	210	35-407	210	25.6-30.1	28.3	15.1-42.1	35.7
Ca-HCO ₃	24	4.7-7.1	6.2	40-924	423.2	29.6-500	170	25.9-29.8	27.8	15.4-28.1	21.1
Na-HCO ₃	17	5.7-7.8	7.2	165.8-1946	944.5	69.3-706.3	468.8	28.7-31.6	29.5	50-66.3	55.6
Mg-HCO ₃	3	7.4-7.5	7.4	414-536	475	179-201	190	27.1-28	27.4	3.6-7.4	
Ca+Mg-Cl	2	5.46		307		132.1		27.2		30.8	

Facies	Potassium (%)		Calcium (%)		Magnesium (%)		Bicarbonate (%)		Chloride (%)		Sulphate (%)	
	Range	Mean	Range	Mean	Range	Mean	Range	Mean	Range	Mean	Range	Mean
Ca+Mg-HCO ₃	0.3-3.6	1.8	19.3-49.7	33.3	1.1-42.1	30	64.5-99.9	92.9	0.1-27.5	4.6	0-13.4	2.2
Ca-HCO ₃	0.7-8.9	2.1	50.9-74.1	58.8	9.0-29.4	17.8	61-99.3	89	0.4-31.6	8	0.2-12.7	3.1
Na-HCO ₃	0.6-3.1	1.3	15.7-28	21.9	17-29.7	22.3	75.8-98.8	93.2	0.1-7.5	1.7	1.0-24.0	5.4
Mg-HCO ₃	0.2-0.8		11.2-30.4		61.4-85		95.7-99		0.7-3.4		0.3-1	
Ca+Mg-Cl	1.5		24.7		42.9		48.4		50.9		0.8	

The percentage concentration of calcium ranges from 19.3 to 49.7 % with a mean of 33.3 % of the total cation in solution. The sodium and magnesium percentages range from 15.1 to 42.1 % and 15.8 to 42.1 % with a mean of 35.7 and 30% respectively.

The bicarbonate concentration is significantly high of between 64.5 and 99.9% with a mean of 92.9 % of the total anion. The chloride and sulphate average compositions are relatively low of 4.6 and 2.2% respectively. The relative concentration of the various ions in the samples of this water type is shown on a finger print diagram (Fig 5.41).

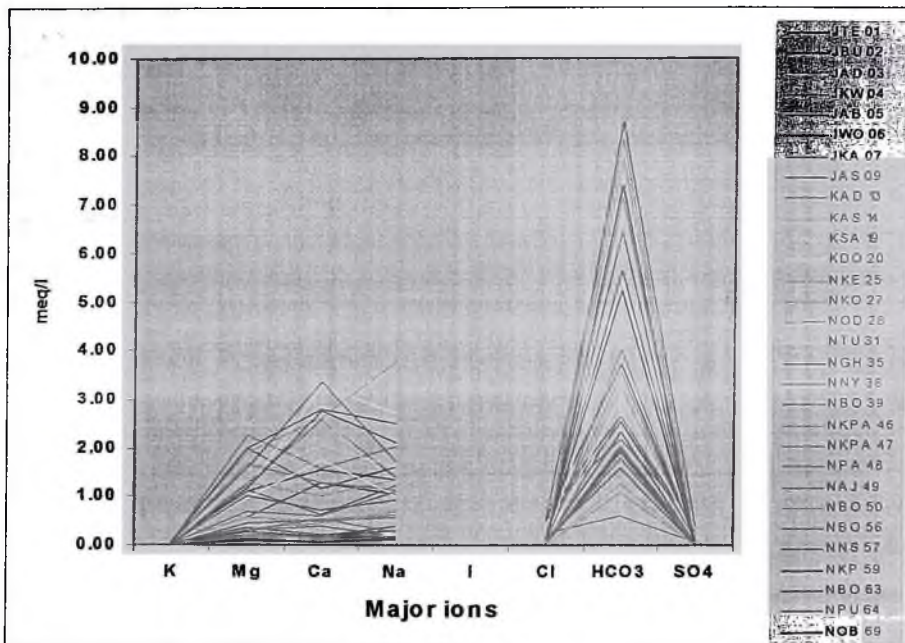


Figure 5.41 Fingerprint diagram of samples in the Ca+Mg-HCO₃ facies.

This water type occurs mainly in the quartzitic sandstones interlayered with shales aquifer. The quartzitic sandstones aquifer is composed of quartz, plagioclase feldspar and sericite matrix while carbonate minerals occur as accessory minerals in the shales. Figures 5.42a and b show that total dissolved solids and pH increase with calcium, sodium and magnesium. This increase in pH is likely due to the loss of hydrogen ions which probably results from the dissolution of aquifer materials. The dissolution reaction leads to the increase in the bicarbonate as is seen in Figure 5.41. The likely source of calcium and sodium is the dissolution of plagioclase feldspar. Magnesium probably results from the dissolution of the sericite flakes in the aquifer.

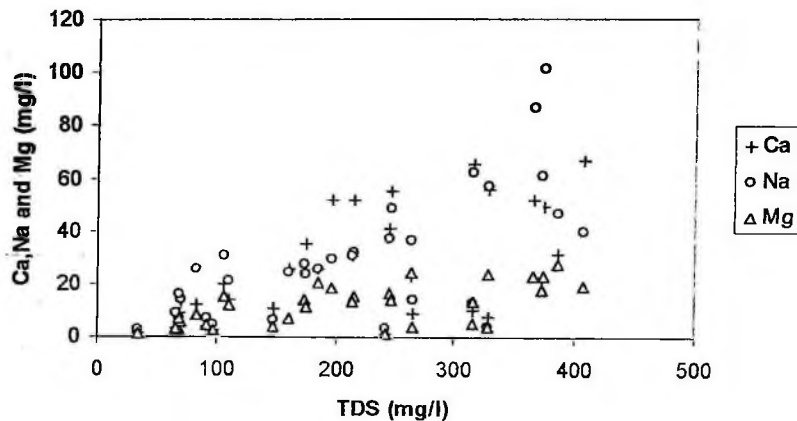


Figure 5.42a Scatter plot of TDS and Ca, Na and Mg of the Ca+Mg-HCO₃ facies

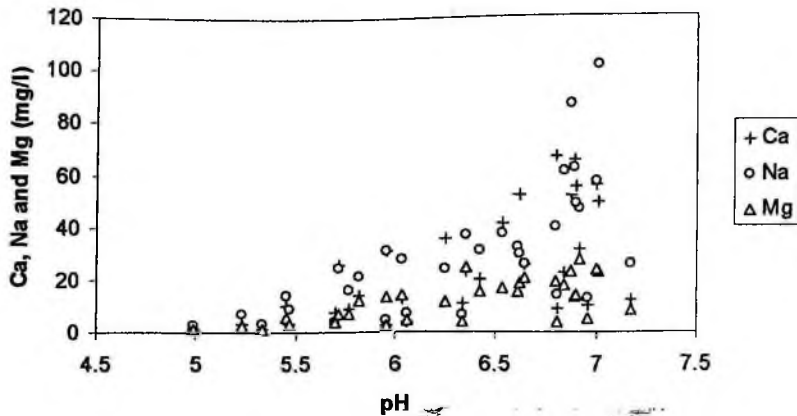


Figure 5.42b Scatter plot of pH and Ca, Na and Mg of the Ca+Mg-HCO₃ facies.

5.2.1.2 Calcium-Bicarbonate facies

The calcium-bicarbonate facies forms about 24 % of the water samples. The pH in this facies ranges between 4.69 and 7.11 with an average of 6.25. The temperature varies from 25.9 to 29.8°C and a mean of 27.8°C. The total dissolved solids value in this facies ranges from 29.6 to 500 mg/l with a mean of 170.7 mg/l. The electrical conductivity ranges between 40 and 924 $\mu\text{S}/\text{cm}$ with an average of 423.2 $\mu\text{S}/\text{cm}$.

The proportion of calcium in relation to the total cation is relatively high with an average of 58.8 % and ranges between 50.9 and 74.1%. The percentage composition of magnesium is between 9 and 29 % and a mean of 18.1%. The water has a relatively lower percentage of sodium and potassium, which varies from 15.4 to 28.1 % and 0.6 to 8.9 % respectively. The bicarbonate concentration in this water ranges between 61 and 99.3 % with a mean of 89 %. The percentage compositions of chloride and sulphate range between 0.4 to 32.5 % and 0.1 to 6.8 % and a mean of 7.8 and 1.5 respectively. This is slightly higher than the rest of water types. The relative

concentration of the various ions in the samples of this water type is shown on a fingerprint diagram (Fig 5.43).

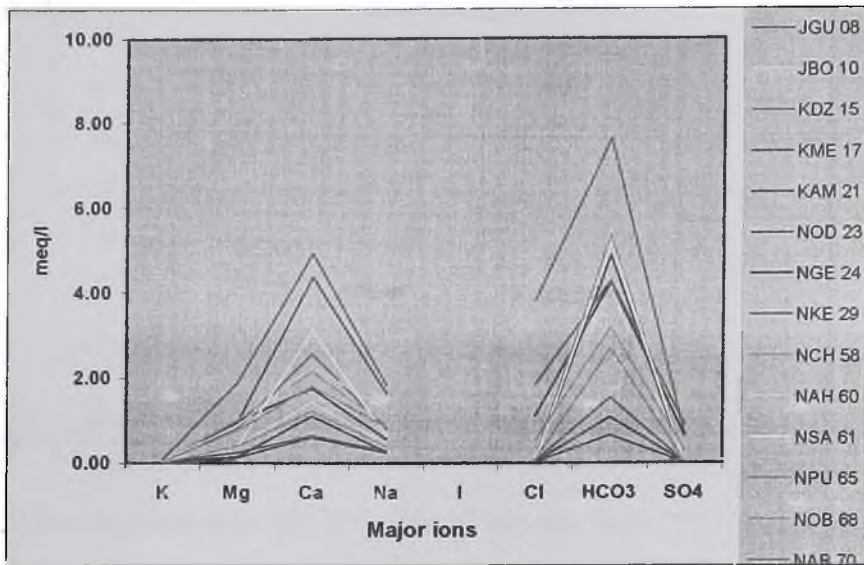


Figure 5.43 Fingerprint diagram of groundwater of the Calcium-Bicarbonate facies

The highest calcium and magnesium concentrations in this water type are 98.9 mg/l and 23 mg/l with a mean of 41.9 mg/l and 8.2 mg/l respectively. The mean concentration of sodium and potassium on the other hand are 17.2 mg/l and 1.59 mg/l respectively.

The calcium-bicarbonate water type occurs in both the quartzitic sandstones interlayered with shales and calcareous shales/ phyllites and schists aquifers.

In the quartzitic sandstones interlayered with shales the concentration of calcium, sodium and magnesium increase modestly with gradual increase in of EC, pH and HCO_3^- (Fig. 5.44a, b and c). The probable source of calcium and sodium is the dissolution of the plagioclase feldspars that occur in the quartzitic sandstones, while the magnesium is derived from sericite dissolution.

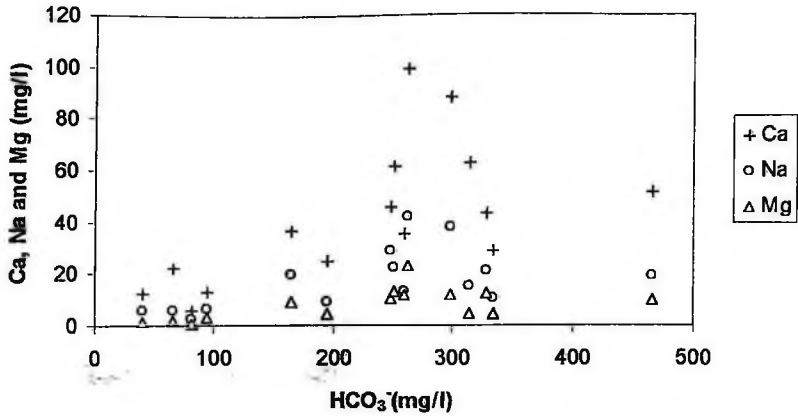


Figure 5.44a Scatter plot of bicarbonate and Ca, Na and Mg of the Ca- HCO_3 .

In the calcareous shales/ phyllites and schists aquifer on the other hand, an increase in the calcium concentration corresponds to low sodium and magnesium concentrations.

Figure 5.44a, b and c show that the EC, pH and HCO_3^- are generally high for these samples.

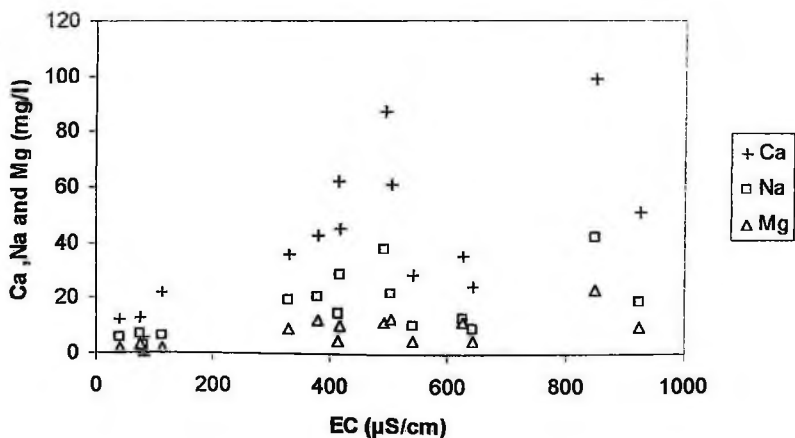


Figure 5.44b Scatter plot of EC and Ca, Na and Mg of the Ca- HCO_3 facies .

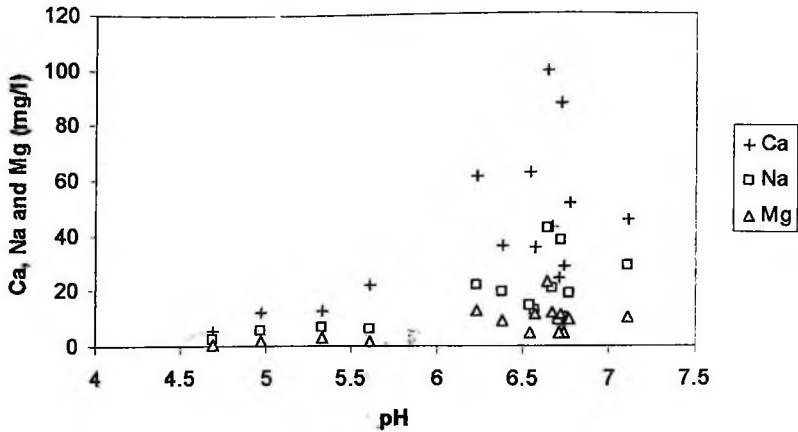


Figure 5.44c Scatter plot of pH and Ca, Na and Mg of the Ca-HCO₃ facies .

The high calcium concentration in this facies can probably result from one or both of the following processes:

- Dissolution of plagioclase feldspar and / or
- Dissolution of calcite

The dissolution of calcite seems more predominant due to the occurrence of carbonate minerals in the aquifer and generally low sodium concentration. This results in the high calcium and bicarbonate concentrations observed in the Fingerprint diagram in Figure 5.63.

The sodium-bicarbonate facies forms about 17% of the water analyzed. It occurs in pockets in the calcium-bicarbonate facies in the southeast and north western margin of the study area.

The pH in this facies ranges between 5.7 and 7.3 with an average of 6.8. The temperature varies from 28.7 to 29.9°C with a mean of 29.3°C. The total dissolved solids in this water type are the highest with a mean of 478.3 mg/l and ranges between 69.3 and 706.6 mg/l. The electrical conductivity ranges between 165.8 and 1946 $\mu\text{S}/\text{cm}$ with an average of 985 $\mu\text{S}/\text{cm}$. The total dissolved solids in this water type are the highest with a mean of 478.3 mg/l and ranges between 69.3 and 706.6 mg/l. The electrical conductivity ranges between 165.8 and 1946 $\mu\text{S}/\text{cm}$ with an average of 985 $\mu\text{S}/\text{cm}$.

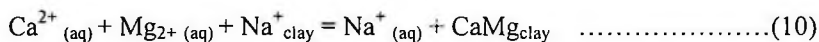
The percentage proportion of sodium in relation to the total cation is relatively high with an average of 55.6% and ranges between 50 and 66.3%. The water has a strikingly lower percentage of calcium and magnesium, which range between 15.7 to 28 % and 17 to 29.7 % with a mean of 21.9 and 22.3%, respectively. The percentage composition of potassium is very low ranging between 0.6 and 3.1 % with a mean of 1.3%.

The bicarbonate concentration in this water ranges between 75.8 and 98.8 % with a mean of 93.2%. The respective percentage compositions of chloride and sulphate range between 0.1 to 7.5 % and 1 to 24 % with mean of 1.7 and 5.4%.

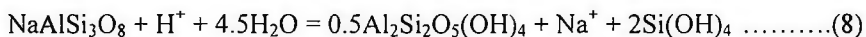
The relative concentration of the various ions in the samples of this water type is shown on a finger print diagram (Fig 5.45). This water type is found mainly in the shales/ mudstone and siltstones aquifer of the Buem and Voltaian Formations.

Mineralogically, the aquifer is composed of quartz, plagioclase feldspar, leucoxene, zircon, ilmenite and sericite flakes (Lashmanov, 1965). Unlike the Calcium+Magnesium-Bicarbonate water type, the sodium concentration is dramatically high with generally low calcium and magnesium concentration as can be observed in the scatter plot of total dissolved solids and calcium, sodium and magnesium (Fig. 5.46). This observation suggests a number of processes that may be taking place.

A high sodium and low calcium and magnesium concentration is probably due to cation exchange process because of the presence of fine grained materials, as in equation 6 (Foster, 1950; Back, 1966; Freeze and Cherry, 1979; Thorstenson et al., 1979; Chapelle and Knobel, 1983).



Another plausible reason for the high sodium concentration is the dissolution of albite- rich plagioclase feldspar:



The low calcium concentration might be due the precipitation of calcite which could be possible because of the relatively high pH of greater than 7 (Fig.5.47). The relatively high bicarbonate in this facies however, makes calcite precipitation not likely.

Finally, the relatively high sodium is sometimes attributed to the dissolution of halite, but the correlation between sodium and chloride is very poor (Fig. 5.48) and indicates that halite dissolution is not the major process controlling the increase of sodium.

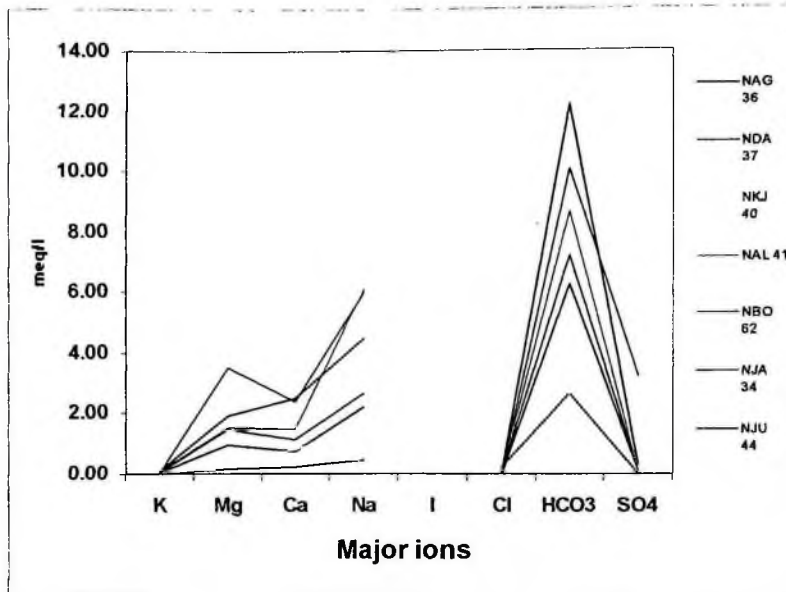


Figure 5.45 Fingerprint diagram of groundwater of the Sodium-Bicarbonate facies

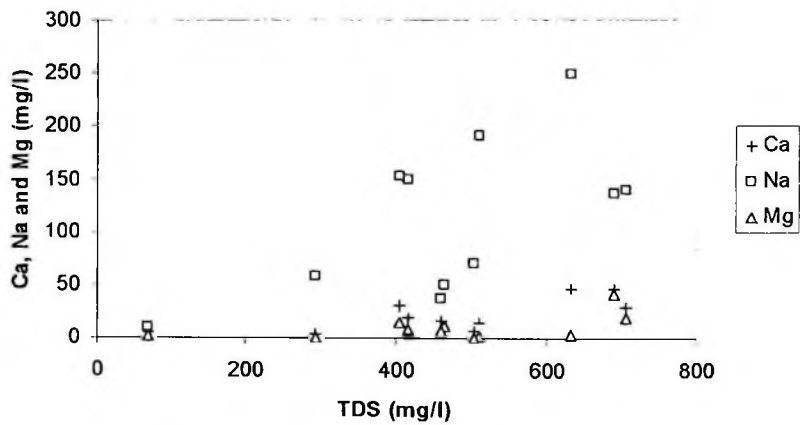


Figure 5.46 Scatter plot of TDS and Ca, Na and Mg of the Na-HCO₃ facies in the study area.

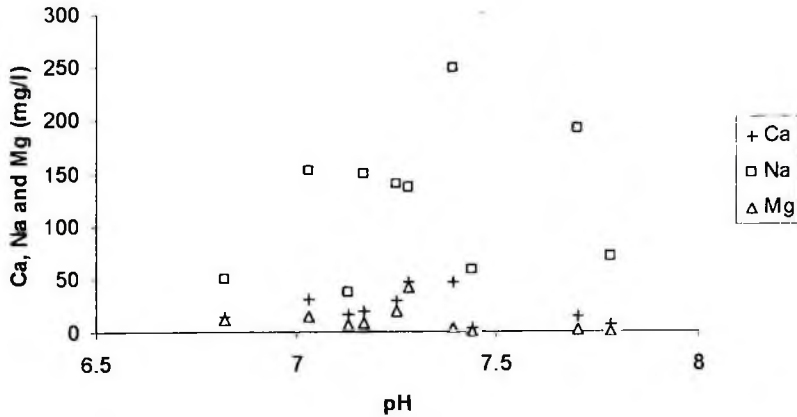


Figure 5.47 Scatter plot of pH against Ca, Na and Mg in the Na-HCO₃ facies

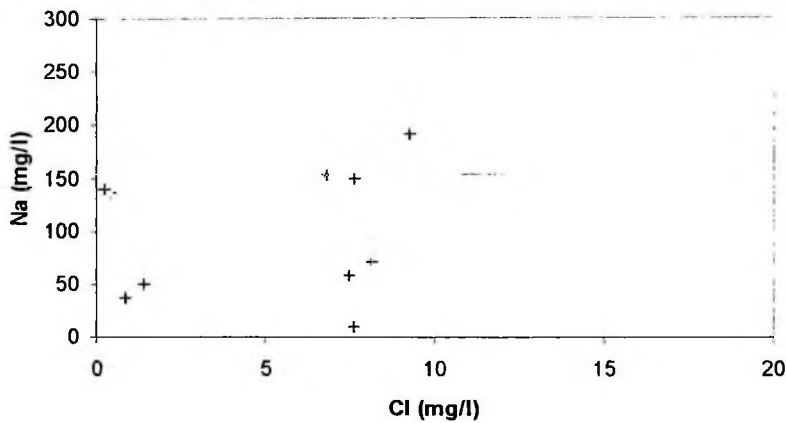


Figure 5.48 Scatter plot of sodium and chloride of the Sodium-Bicarbonate facies.

5.2.1.4 Magnesium-Bicarbonate facies.

Only two samples are of this type in this formation and forms about 3% of the water samples. It occurs in pockets in the eastern part of study area. The pH ranges between 7.37 and 7.47 with a mean of 7.42. The temperature varies from 27.1 to 28 and an

average of 27.4°C. The mean total dissolved solids and the electrical conductivity are 109.6mg/l and 225.9 μ S/cm, respectively.

The average percentage composition of calcium and magnesium are 20.8 and 73.2% respectively. Sodium and potassium forms about 48 and 4.1% of the total cation in the water, respectively. The percentage composition of bicarbonate, sulphate and chloride are 98%, 0.5% and 1.5% respectively. This facies occurs in the mudstone and siltstone of the Buem Formation which mineralogically is composed of quartz, plagioclase feldspar, leucosene, zircon, ilmenite and sericite flakes (Lashmanov, 1965). The relatively high magnesium concentration in these samples is probably due to the rapid rate of dissolution of the fine grained sericites that occur in the aquifer.

5.2.1.5 Calcium+Magnesium-Chloride Facies.

Only the sample at the Kadjebi market is of this water type. The mean pH and the temperature are 5.46 and 27.2°C respectively. The percentage composition of magnesium and calcium are 42.9 and 24.7% respectively. Sodium and potassium forms about 30 and 1.5% of the total cation in the water. The total dissolved solids and Electrical conductivity are respectively 132.1 mg/l and 307 μ S/cm. The water is made up of 48% bicarbonate with unusually high chloride percentage of 50.9%. It is worthy to note that another sample about less than 1km away also has chloride of 28.3% and bicarbonate of 68.6%. Since their corresponding nitrate concentrations are below detection limit, the source of the chloride may be due to local concentration of a chloride containing mineral in the aquifer and / or anthropogenic contamination.

5.4 Environmental Isotopes

Groundwater undergoes various processes such as evaporation from the oceans, rainout, re-evaporation and runoffs before reaching its final destination underground. These processes impart distinctive isotopic character to groundwater and help in the study of geologic processes that affect surface and groundwater. Due to this property, environmental isotopes have become invaluable tool in groundwater investigations and serve as conservative tracers of water origin.

In this section, the results of the isotopic analysis of the groundwater in the study area are discussed with respect to the Global Meteoric Water Line (GMWL). Moreover, the relationships between oxygen-18 and hydrochemistry are established.

5.4.1 Relationship between oxygen-18 and deuterium

Table 5.5 presents oxygen-18 and deuterium values including sample location, temperature, depth and chemical parameters. The groundwater isotopic data in the study area have been classified based on the three Formations found in the study area. The description of the various Formations is given in chapter two; however, the summary of the lithologies is given in Table 5.5. In the study area the stable isotopes ratios exhibit slight variations, which are unique to the various Formations. The $\delta^{18}\text{O}$ values of the groundwater samples range between -4.39 and -2.27‰ with an average of -2.95‰ . The $\delta^2\text{H}$ values on the other hand are from -26 to -8.3‰ with an average of -12.71‰ . Figure 5.49 shows that most of the samples from the Buem Formation and the Togo Formation have similar delta deuterium and delta oxygen-18 values that are relatively enriched. The samples from the Buem mudstone and siltstone and

Voltaian Formation found in the northwestern part of the area have more negative delta deuterium and delta oxygen-18. This probably suggests that the more depleted Buem mudstone and Voltaian Formation samples may be hydraulically and hydrochemically different from the Togo and most of the Buem Formation. The distribution of the delta deuterium in the study area is shown in Figure 5.50.

The relation between delta deuterium and delta oxygen-18 in Figure 5.49 shows that all the samples fall along the Global Meteoric Water Line. A line of best fit for the data gives a slope of 7.76 and deuterium excess of 10.14 ‰ giving an equation of:

$$\delta D = 7.76 \delta^{18}O + 10.14\text{‰} \dots\dots\dots(16).$$

This is generally close to the equation of the Global meteoric Water Line (Craig, 1961) in equation (3) indicating that the groundwater originated from rainfall and secondary processes, such as evaporation prior to infiltration can be rule out due in part to the high relative humidity during the rainy season and partly due to rapid rate of infiltration. Thus, the groundwater is believed to be part of the modern hydrological cycle which is continuously being renewed.

The scatter plot further shows two distinct water types based on their isotopic ratios (Fig. 5.49):

- I. Tightly clustered and relatively enriched and
- II. Scattered and relatively depleted

The first type is tightly clustered and relatively enriched in both ^2H and ^{18}O . Their mean $\delta^3\text{H}$ and $\delta^{18}\text{O}$ are -10.4 and -2.7 ‰ respectively and found in the southern and southeastern part of the study area (Fig. 5.50).

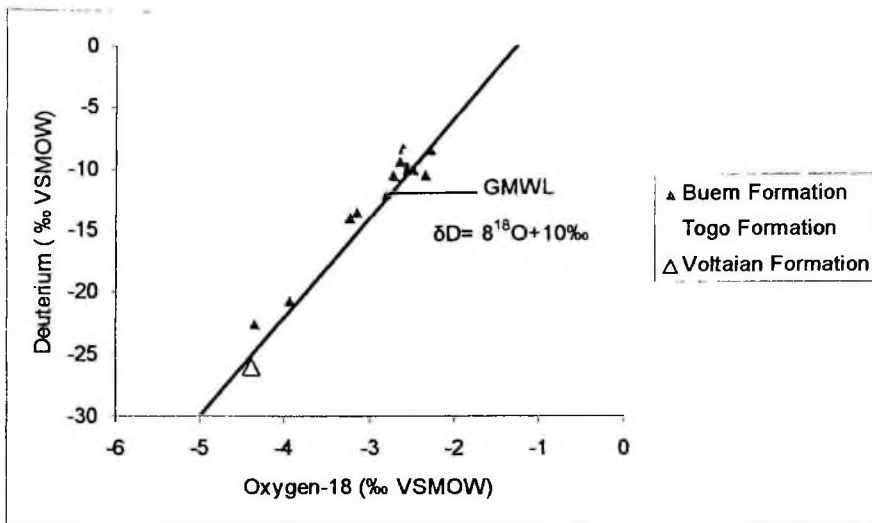


Figure 5.49 Scatter plot of Delta Deuterium and delta Oxygen-18 of groundwater samples in the study area.

The tight clustering of these samples probably shows that they have similar recharge mechanism. The second group of samples which shows some amount of scattering is relatively depleted in both ^2H and ^{18}O and has average $\delta^2\text{H}$ and $\delta^{18}\text{O}$ of -23.1% and -4.2% respectively. The two groups reveal a relatively wide spread of values probably indicating difference in aquifer and meteorological characteristics. Variations in the stable isotopic composition of water in a drainage basin are caused in part by natural variations in isotopic composition of precipitation. The isotopic content of precipitation is however, controlled in part by the particular meteorological processes acting at a given time and place and is subject to considerable variation. The hydrogen and oxygen isotopic composition of precipitation and infiltration waters are controlled by various physical factors such as latitudinal and altitudinal effects, intensity and duration of rainfall, temperature, evaporation and condensation in recharge and drainage areas (Dansgaard, 1964; Clark and Fritz, 1997).

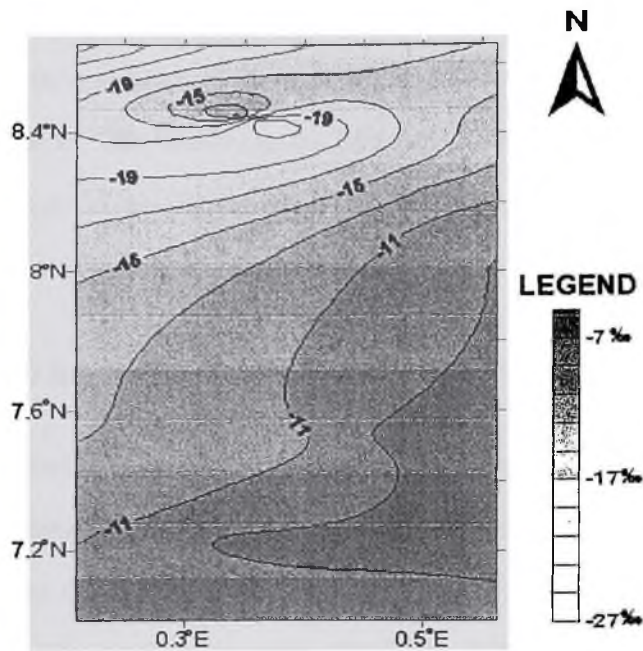


Figure 5. 50 Distribution of delta Deuterium values in the study area.

Generally both delta deuterium and delta oxygen-18 values of the groundwater showed similar trends when plotted with the physico-chemical parameters. The delta deuterium were however used for the interpretation of the isotopic values because of the minor influence of the poorly known kinetic separation factor on the overall isotope enrichment factor on deuterium (Zimmerman and Ehhalt, 1970; Friedman *et al.*, 1976).

The isotopic composition of the group I (tightly clustered and relatively enriched) groundwater found mainly in the Southern part of the area is similar to the isotopic composition of the groundwater of the South Voltaian Basin (Acheampong and Hess, 1995), the deep groundwater samples in the Dahomeyan gneiss of the Keta Basin (Jorgensen and Banoeng-Yakubo, 2001) and the groundwater of the Tarkwa-Prestea area (Kortatsi, 2004). The group II (scattered and relatively depleted) groundwater

which occur in the northern part of the area are consistent with the Upper and Northern Regions of Ghana samples (Kortatsi and Sekpey, 1993) and are slightly depleted. This implies that the difference in the groups I and II is probably due to the latitude or continental effect since the heavy isotope composition of rainwater becomes more negative as one moves from the ocean towards the continent.

5.4.2 Relationship between Deuterium and Altitude

Figure 5.51 shows that the two groups occur at different altitudes. The relatively enriched samples have wide variation in altitude while the relatively depleted samples occur at generally lower altitudes. On the average, both the enriched and depleted samples occur at the same altitude of about 198 meters. Deuterium values are different for the two groups, but within each group, deuterium composition discernibly changes with altitude (Fig. 5.1). The more depleted deuterium are associated with high altitude. Thus deuterium composition of rain that recharges each group is affected by altitude.

The scatter plot of temperature and delta deuterium demonstrates a general negative correlation (Fig.5.52). The depleted samples generally are of relatively high temperature of a mean of 29° C. Groundwater becomes more depleted with increase in temperature. The relatively enriched samples on the other hand show two clustering with different temperatures of approximately 27 and 29° C. The relatively high temperature values are associated with deeper groundwater samples probably suggesting longer residence time.

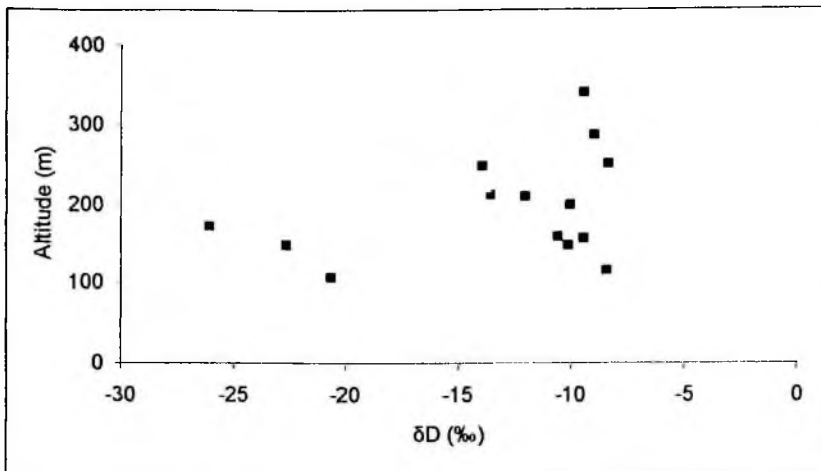


Figure 5.51 Scatter plot of Deuterium and altitude of samples site in the study area.

5.4.3 Relationship between Oxygen-18 and Hydrochemistry

Sodium, calcium and magnesium are the dominant cations present in the groundwater. The relationship between these cations and oxygen-18 demonstrate the impact of water- rock interaction. Figure 5.53 shows generally that variation in the major cations corresponds to a relatively uniform oxygen-18 values for both the depleted and enriched samples indicating probably that isotope exchange between the groundwater and the aquifer is minimal or absent. However, the relatively depleted groundwater have significantly high electrical conductivity (Fig.5.54). This means that the depleted samples may have had a longer contact period with the aquifer indicating a palaeorecharge. However, the evaluation of the possibility of palaeorecharge phenomenon must await the attempt to determine the groundwater residence times using tritium/ helium, radiocarbon or other radiometric methods.

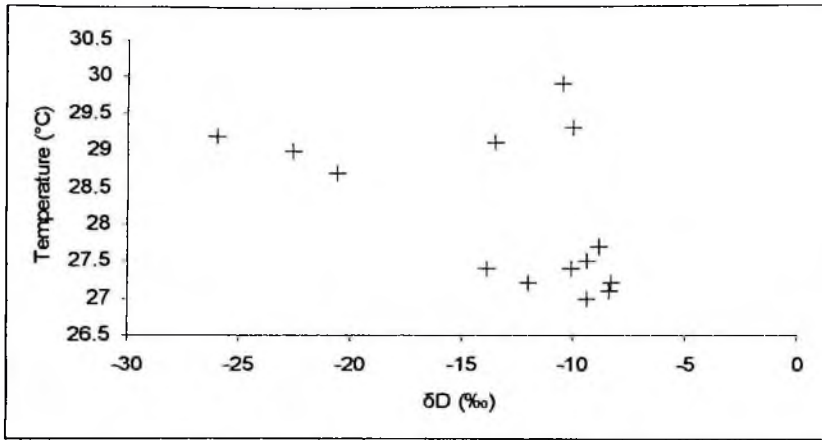


Figure 5.52 Scatter plot of Delta Deuterium and temperature of samples in the study area.

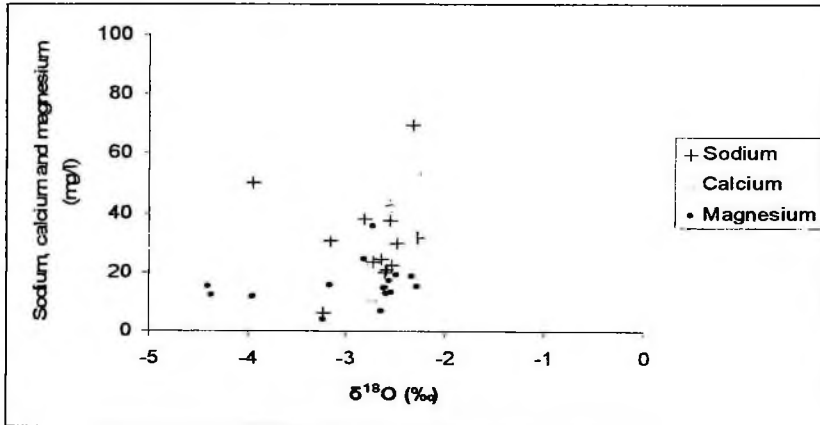


Figure 5.53 Scatter plot of Delta Oxygen-18 and sodium, calcium and magnesium in the study area.

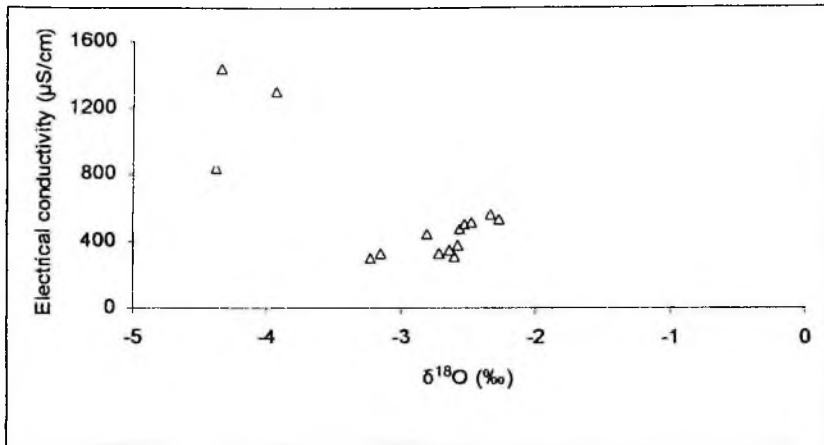


Figure 5.54 Scatter plot of Delta Oxygen-18 and electrical conductivity in the study area.

CHAPTER SIX

CONCLUSION AND RECOMMENDATION

6.1 Conclusion

The area under investigation is noted for its complex geology. The aquifers consist of crystalline, slightly meta-sedimentary and purely sedimentary rocks. This succession generally becomes purely sedimentary towards the northwestern part of the area. The study shows that the chemical composition of the groundwater of the Buem, Voltaian and Togo Formations is strongly influenced by the interaction with the geology. Based on the lithological characteristics and physico-chemical parameters, the area can be divided into two hydrochemical zones: the southern and northwestern zones. Greater part of the area falls under the southern zone. This zone is composed of both quartzitic sandstones and shales of the Buem Formation and the quartz schist of the Togo Formation. This zone is characterized by moderate to slightly acidic groundwater with generally low total dissolved solids. Within this zone, relatively low pH and low total dissolved solids occur in the mainly quartzitic sandstone aquifers while relatively high pH and total dissolved solids are found in the mainly shales aquifers. There is a general increase in the major ions with pH and total dissolved solids indicating that dissolution of plagioclase, sericites and carbonate minerals.

In the northwestern zone, the groundwater is characterized by neutral pH, high total dissolved solids, bicarbonate and sodium. There is however increasing sodium with decreasing calcium and magnesium. This observation coupled with the presence of

clay materials in these aquifers show that the groundwater composition in this zone is influenced by cation exchange of sodium for calcium on the clay material surfaces.

Different major ion associations are identified, resulting in five water types. These are the:

- I. Calcium+Magnesium-Bicarbonate
- II. Calcium-Bicarbonate
- III. Sodium-bicarbonate
- IV. Magnesium-Bicarbonate and
- V. Calcium+Magnesium-Chloride

Calcium+Magnesium-Bicarbonate water type is common to all the Formations but is generally predominant in the Buem and Togo Formations composed of quartzitic sandstone, shales and quartzitic-schist aquifers. It is however limited in the Buem and Voltaian mudstones and siltstones where the Sodium-Bicarbonate type is dominant. The likely process responsible for this water type is the dissolution of plagioclase feldspar and sericite flakes in the aquifer.

The dissolution of plagioclase feldspar and minor carbonate minerals gives rise to the Calcium-Bicarbonate facies. The Calcium-Bicarbonate water type occurs in both the quartzitic sandstones interlayered with shales and calcareous shales/ phyllites and schists aquifers. The Calcium+Magnesium-Chloride occurs in the borehole at the Kadjebi market. The high chloride is attributed to the local concentration of a chloride containing mineral in the aquifer and / or anthropogenic contamination. All the three water types mentioned above are characterized by relatively low pH, bicarbonate and

low total dissolved solids. The low pH and low total dissolved solids result as the carbon dioxide charged water interacts with the relatively stable quartz, plagioclase feldspar and sericites enroute to the water table. This reaction is generally slow, releasing small amount of ions into solution hence the low pH and low total dissolved solids.

Pure sedimentary rocks of mudstone and siltstone are found in the northwestern part of the area. The change in the lithology has a corresponding influence on the water type. The Calcium+Magnesium-Bicarbonate type gives way to the Sodium-Bicarbonate type. Mineralogically, the aquifers are composed of clay, quartz, plagioclase feldspar, leucoxene, zircon, ilmenite and sericite flakes. This water type is characterized by relatively high total dissolved solids (TDS) and high pH. The main process responsible for this facies is the cation exchange of sodium for calcium on the clay surfaces leading to a high rise in total dissolved solids (TDS) and bicarbonate.

Apart from the Kadjebi market water, the predominant anion in all the facies is the bicarbonate ion. The initial input of bicarbonate is influenced by the interaction of infiltrating rain with the atmospheric carbon dioxide and soil carbon dioxide which is likely to be uniform in the area due to similar climate and vegetation. However, results show that relatively low bicarbonate occurs in the quartzitic sandstone while higher concentration in the shales, mudstones and siltstones. This therefore indicates that the variation in the bicarbonate is influenced by the geology. The relatively low bicarbonate in the quartzitic sandstone aquifer made up of mainly silicate minerals is due to the slow dissolution kinetics of silicate minerals. There is a rise in the bicarbonate in the shales, mudstones and siltstones because of the combined effect of the dissolution of silicate minerals and cation exchange. Generally, the sulphate and

chloride do not occur in significant amount in the groundwater in all the geological formations in the area and do not show any clear trend with respect to the geology. The low sulphate and chloride shows the lack of soluble evaporate in the aquifers of all the geological formations in the area. The main source of the sulphate and chloride is attributed to atmospheric sources, decomposition of organic matter and/ or trace impurities in the aquifer material. The concentration of nitrogen-compounds (NH_4^+ , NO_3^- and NO_2^-) is generally low indicating the groundwater free of anthropogenic contamination.

The scatter plot of delta deuterium and delta oxygen-18 shows that all the water samples lie on or close to the Global meteoric Water Line (Craig, 1961) indicating that the groundwater samples originated from rainfall and secondary processes, such as evaporation prior to infiltration can be rule out due in part to the high relative humidity during the rainy season. Based on the isotopic composition of the groundwater, two types are evident. These are the:

- I. Relatively depleted delta deuterium and delta oxygen-18
- II. Relatively enriched delta deuterium and delta oxygen-18

The relatively depleted groundwater is found in the north and characterized by relatively higher pH, total dissolved solids and bicarbonate. On the other hand, the relatively enriched groundwater occur in the south and dominated by relatively low pH, total dissolved solids and bicarbonate. The observed isotopic variation is due to latitudinal, minor altitude effect and/ or palaeorecharge.

On the whole, physico-chemical parameters and isotopic data have successfully been used to describe the chemical property of the groundwater in all the geological formations namely, Buem, Voltaian and Togo Formations. Furthermore, the source of recharge to the aquifers in the Volta Region has been determined. Generally, the groundwater is less mineralized and this is reflected in the relatively low total dissolved solids. Thus groundwater in the area constitutes the main source of potable water for the local population. The groundwater in the area is generally fresh with no anthropogenic influences. Apart from the low pH in some parts of the southern zone that falls below the World Health Organisation standard for domestic use, the groundwater in the area is generally suitable for all purposes.

6.2 Recommendations

1. This work can be described as a baseline study. ~~There were several challenges~~ to this study, the main one being insufficient funds. This led to the determination of only major ions in the laboratory and only one period of sampling. Notwithstanding these limitations, this work is instructive enough.
2. In spite of the fact that the chemical composition of the groundwater falls within the World Health Organisation standards for general purposes, the low pH of between 4 and 6.5 in some parts of southern zone is a matter of concern. Though there has been no report of adverse impact on the local population, water of low pH are vulnerable to contamination and increases the mobility of heavy metals. The low pH and low bicarbonate suggest that the groundwater is of a low buffering capacity. Therefore introduction of contaminants from households may have adverse impact on the groundwater system. It is

therefore suggested that care should be exercised in siting refuse dump and septic tanks near points of discharge of groundwater such as boreholes.

3. The sampling for this research took place during the dry season. The results obtained may not necessarily reflect the general condition pertaining in the area. It is therefore recommended that both rainy and dry season sampling be conducted to ascertain the effect of the seasons on the chemical composition of the groundwater.
4. The hydrochemical facies in the northwestern zone has not been considered with respect to the southern zone facies. This is because the aquifers in the area are assumed to be unconnected with each other. However, aquifers in fractured consolidated terrain are often connected (Raju and Reddy, 1998). This therefore calls for a thorough hydrogeological work to be done in the area to assess the extent of interconnection between aquifers so as to be able to discuss the relationship between hydrochemical facies.
5. Tritium/ helium, radiocarbon or other radiometric methods should be employed to ascertain the groundwater residence times in the area. This is to explain the variation in the northwestern and southern zone.

REFERENCES

Acheampong S, Y. and Hess J, W. (1998). Hydrogeologic and hydrochemical framework of the shallow groundwater system in the Southern Voltaian Sedimentary Basin, Ghana. *Hydrogeology Journal* Vol 6 pg 527-537.

Acheampong S, Y. and Hess J, W. (1995). Major ion and stable isotope geochemistry of groundwater in the southern Voltaian sedimentary basin of Ghana. *Proceedings/ GSA 1985 International Conference*.

Afsin, M. (1996). Hydrochemical evolution and water quality along the groundwater flow path in the Sandikli plain, Afyon, Turkey. *Environmental Geology* 31 (3/4) pp 221.

Akiti, T.T. (1986). Environmental isotope study of groundwater in crystalline rocks of the Accra Plains, Ghana. 4th Working Meeting Isotopes in Nature Leipzig, September 1986 Proceedings.

Al-Agha, R.M., and El-Nakhel A.H. (2004). Hydrochemical facies of groundwater in the Gaza Strip, Palestine. *Hydrological Science Journal*. 49(3).

Appelo, C.A.J., Postma, D. (1993). From rainwater to groundwater, *Geochemistry, groundwater and pollution*. A.A Balkema, Rotterdam/ Brookfield pg. 22.

Back, W. (1966). Hydrochemical facies and groundwater flow patterns in the Northern parts of the Atlantic coastal plain. *US Geological Survey Prof. paper 498-A*, pg. 42

Bachman, L.J. (1984). nitrate in the Columbia aquifer, central Delmarva Peninsula, Maryland: USGS Water Resource investigations Report 84-4322, pg 51.

Banes, I. (1964). Field measurement of alkalinity and pH: US Geological Survey water supply paper 1535-H, pp.17.

Bates, B.A. (1953). Annual Report of the Director, Geological Survey.

Blay, P.K. (1971). The geology of field sheets 189, Baglo N.W. Report of Ghana Geological Survey Department.

Bobrov, S. and Pentelkov, V. (1964). Report on the geology and minerals of the eastern parts of the Bimbilla and Zabzugu area.

Bolt. G.H. and Bruggenwert, M.G.M. (1978). Soil chemistry- A, Basic elements: Elsevier, Amsterdam, pp 282.

Briel, L.I. (1997). water quality in the Appalachian Valley and Ridge, the Blue Ridge, and the Piedmont Physiographic Provinces, Eastern United States. Regional Aquifer-System Analysis—Appalachian Valley and Piedmont. USGS Professional Paper 1422—D30.

Bullen, T.D., Krabbenhoft, D.P. and Kendall, C. (1996). Kinetic and mineralogic controls on the evolution of groundwater chemistry and $^{87}\text{Sr}/^{86}\text{Sr}$ in a sandy silicate aquifer, northern Wisconsin, USA *Geochimica et Cosmochimica Acta*, 60: pp 1807-1821

Chapman, Deborah (1992). Water quality assessments. A guide to the use of biota sediments and water in environmental monitoring. Second Edition

Chappelle, F.H., and Knobel, L.L., (1983). Aqueous geochemistry and the exchangeable cation composition of glauconite in the Aquia aquifer, Maryland. *Ground Water*, v.21, #3, pp. 343-352.

Chebotarev, I.J. (1955). Metamorphism of natural water in the crust of weathering. *Geochim et Cosmochim Acta*. Vol.8 pp 22-212.

Colby, B.R., Hembree, C.H and Jochens, E.R. (1953). Chemical quality of water and sedimentation in the Morean River drainage basin, Wyoming: US Geological Survey water supply paper 1373 pp336.

Clark, I.D and Fritz, P. (1997). Environmental isotopes in hydrogeology. Lewis publishers, New York.

Collins, W.D. (1923). Graphic representation of analyses: Industrial and Engineering Chemistry V.15, pp.395.

Craig, H. (1961b). Isotopic variation in meteoric waters. *Science*, 133: 1702-1703

CWSA Drilling report, (2002). Daily drilling log, lithological and borehole design and development reports. Unpublished. CSIR and Ho offices database.

Dansgaard, W. (1964). Stable isotopes in precipitation. *Tellus* 16. 436-468.

Darling, W.G and Bath A.H. (1988). A stable isotope study of recharge processes in the English Chalk. *Journal of Hydrology* 101: pp 31-46.

Davies, S.N and DeWiest, R.C.M. (1966). Hydrogeology. Wiley & Sons, New York, pp148, 463.

Dela, O. Careno, Alfonso. (1951). Las provincias geohidrologicas de Mexico. (Primera parte): Universidad Nacional de Geologia Boletin. V.56, pp. 137.

Derickson, R. (2003). Study shows Regional variation in the pH of Kentucky Groundwater. [www. Uky.edu/PR/News/Achives/2003/Jan 2003/pH-groundwater.htm](http://www.Uky.edu/PR/News/Achives/2003/Jan%2003/pH-groundwater.htm).

Deutsh, W. J. (1997). Groundwater geochemistry; Fundamentals and Applications to contamination; Groundwater geochemical system pp.3, 43.

Dickson, K.A. and Benneh, G. (1988). A New Geography of Ghana. Revised Edition. Longman Group UK Ltd. Pp. 17-29

Domenico, P and Schwartz, F. (1998). Physical and chemical hydrology. Second edition. John Wiley and Sons Inc., New York, USA.

Ebert, S. M and Lori, L.G. (2000). Regional groundwater flow and geochemistry in the Midwestern basin and arches aquifer system in parts of Indiana, Ohio, Michigan and Illinois, USGS professional paper 1423-C pp. C56.

Eichinger, L., Merkel, B., Nemeth G., Salvamoser, J. and Stichler, W. (1984). Seepage velocity determination in the unsaturated Quaternary gravel. Recent investigations in the zone of aeration. Symposium Proceedings, Munich, 1984: pp. 303-313.

Emmons, W.H., and Harrington, G.L. (1913). A comparison of water of mine and hot springs: *Economic geology*, V.8, pp. 653-669.

Epstein, S. and Mayeda, T.K. (1953). Variations of $\delta^{18}\text{O}$ content of water from natural sources. *Geochim Cosmochim Acta*. 4: pp. 213-244.

Fetter, W.C. (1994). *Water chemistry. Applied hydrogeology*, pp. 422.

Feth, J.H, Roberson C.E. and Polzer, W.L. (1964). Sources of mineral content in water from granitic rocks, Sierra Nevada, California and Nevada. *U.S Geol. Surv. Water supply Pap. 1535 I*, pp. 170.

Flipse, W.J., Katz B.G., Linder J.B. and Markel R. (1984). Source of nitrate in groundwater in sewered housing development, Central Long Island, New York. *Groundwater* 22: pp. 418-426.

Foster, M.D. (1950). The origin of high sodium bicarbonate waters in the Atlantic and Gulf Coastal Plains. *Geochimica et Cosmochimica Acta*, Vol1 pp. 33-48.

Freeze, R.A and Cherry, J.A. (1979). *Groundwater*. Englewood Cliff, N.Y., Patience-Hall, pp. 238-297.

Friedman, I. (1953). Deuterium content of natural water and other substances. *Geochimica et Cosmochimica Acta*, 4: pp. 89-103.

Friedman, I., Redfield, A.C., Schoen, B. and Harris, J. (1976). The variation of the Deuterium content of natural water in the hydrologic cycle. *Review of geophysics* Vol. 2, No. 1, pp. 179-223.

Furon, R. (1963). *Geology of Africa*, English Edition.

Galloway, J.N and Cowling, E.B. (1978). The effect of precipitation on aquatic and terrestrial ecosystems: A proposed precipitation chemistry network *J. Air pollution. Cont. Assoc.* 28, 229-235.

Garcia, G. M., Hildalgo, V. Margarita del and Blesa, A.Maguel. (2001). Geochemistry of the groundwater in the alluvial plain of Tucuman province, Argentina. *Hydrogeology Journal* Vol. 9 pp. 597-610.

Garrels, R,M and Christ, C.L. (1965). *Solution, Minerals and Equilibria*. Harper and Row, New York. Pp 74-91.

Ghanem, M. and Merkel, B. (2000). Hydrochemical characterization of the Faria basin, Northeastern West Bank. *Groundwater: Past Achievements and Challenges*.

Gibbs, R.J. (1970). Mechanisms controlling world water chemistry. *Science* 170: 1088-1090.

Gills, H.E. (1969). A groundwater reconnaissance of the Republic of Ghana, with a description of geohydrologic provisions.

Gonfiantin,i R., Conrad, G., Fontes, J.C., Sauzay, G. and Payne, B.R. (1974). Etude isotopique de la nappe du Continental Intercalaire et de ses relations avec les autres nappes du Sahara Septentrional. *Isotope Techniques in Groundwater Hydrology* 1974, vol. 1, IAEA Symposium, Vienna: 227-241.

Guendouz, A., Moulla, A.S., Edmunds, W.M., Zouari, K., Shand, P. and Mamou, A. (2003). Hydrochemical and Isotopic evolution of water in the Complex Terminal aquifer in the Algerian Sahara. *Hydrogeology Journal* Vol. 11 pp. 483-495.

Hach, Company.(1997). Digital titrator manual. Alkalinity. Pp. 34-39.

Helgesen, J.O., Leonard, R.B and Wolf, R.J. (1993). Hydrology of the Great Plains Aquifer System in Nebraska, Colorado, Kansas and Adjacent Areas. USGS Professional paper 1414-E pp. E34

Hem, J.D. (1992). Study and interpretation of the chemical characteristics of natural water; Third edition, United States Geological Survey paper 2254 hydrogen ion activity (pH) pp.61.52.

Hill, A.R. (1982). Nitrate distribution in the groundwater at the Alliston region of Ontario, Canada. *Groundwater* 20: 696-702.

Horn, M.K. and Adams, J.A.S. (1966). Computer-derived geochemical balances and element abundances: *Geochemica et Cosmochimica Acta*, v.30 pp. 279-297.

Hounslow, A.W. (1995). *Water quality data analysis and interpretation*, Lewis Publishers, Boca Raton, New York.

Houzim, V., Vavra J., Fuska J., Pekny V., Vrba J., Stibral J. (1986). Impact of fertilizer and pesticides on groundwater quality. In: Vrba J, Romijn E (ed). *Impact of agricultura activities on groundwater*. Heinz Heise, Hannover, pp 89-132.

Ineson, J. and Downing, R.A. (1963). Changes in the chemistry of groundwater of the Chalk passing beneath argillaceous strata. Bull. Geological Survey GB 20 : 176-192.

International atomic energy agency, technical report series #s 95, 117, 129, 147, 165, 192, 226, 264 and 331.

James, M. Thomas; Alan, H. Welch and Michael, D. Dettinger. (1996). Geochemistry and isotope hydrology of representative aquifers in the Great Basin region of Nevada, Utah and adjacent states. United States Geological Survey professional paper: 1409-C pp. C3.

Jorgensen, N.O. and Banoeng- Yakubo, B.K. (2001). Environmental isotopes (^{18}O , ^2H and $^{87}\text{Sr}/^{86}\text{Sr}$) as a tool in groundwater investigations in the Keta Basin, Ghana. Hydrogeology Journal Vol. 9: 190-201.

Junner, N.R. and Service, H. (1936). Geological notes on Volta River District and Togoland under British mandate. Annual report on the Geological Survey by the Director 1935-1936. pp. 10-16.

Junner, N.R. (1940). Geology of the Gold Coast and Western Togo. Bulletin No. 11.

Kattan, Z. (1964). Chemical and environmental isotopes study of the fissured basaltic aquifer system of the Yarmont Basin. Isotopes in water resources management proceedings of a symposium, Vienna. Vol.2 pp.3-25.

Kesse, G.O. (1985). The Mineral and Rocks Resources of Ghana. A.A. Balkema Publishers. Netherlands-Rotterdam. Pp. 39-50.

Kitson, A.E. (1928). Provisional geological map of the Gold Coast and Western Togoland, with brief descriptive notes thereon. Gold Coast Geological Survey Bulletin No.2.

Koert (1910). "Begleit worte zur geologischer Karte von Togo" in Hans Meyer's das Deutsche Kolonialreich, vol.2, Leipzig and Vienna.

Kolaja V., Vrba J. and Zwirrmann K.H. 1986). Control and management of agricultural impact on groundwater. In: Vrba J, Romijn E (ed). Impact of agricultura activities on groundwater. Heinz Heise, Hannover, pp. 197-229.

Kortatsi, B.K.(2004). Hydrochemistry of groundwater in the mining area of Tarkwa-Prestea, Ghana. Unpublished Ph. D thesis. Pp 103.

Kortatsi, B.K. and Sekpey, N.K. (1993). Chemical and isotope evidence for the origin of groundwater in the crystalline basement complex of the Upper Region of Ghana. Proc African Geological Conf, Accra, Ghana, pp 221-242.

Lambert, S.J and Balsley, S.D. (1996). Stable isotopes of groundwaters from the Albuquerque, New Mexico basin: one decade later. Environmental Geology 31 (3/4) pp.199.

Langmuir, D. (1997). Aqueous Environmental Geochemistry. Prentice Hall Upper Saddle River, New Jersey.

Lashmanov, V. (1965). Geology and Minerals of the Area of the Nkwanta (Eastern parts) and Dutupene Field Sheets. MINCOM/GTZ Publication Project, Accra-Ghana.

Lerner, D.N. (1997). Groundwater recharge. Saether OM, de Caritat P (eds) Geochemical processes, weathering and groundwater recharge in catchments. AA Balkema, Rotterdam pp109-105.

Lerner, DN., Issar, AS and Simmers, I. (1990). Groundwater recharge. A guide to understanding and estimating natural recharge. IAH Int. Contrib Hydrogeol 8. Heinz Heise, Hannover, pp345.

Likens, G.E., Bormann, F.H., Pierce, R.S., Easton, J.S. and Johnson, N.M. (1977). Biogeochemistry of a forested ecosystem. Springer Verlag, Berlin, 146 pp.

Lyons, W., Lent, R.M., Djukic, N., Maletins, S., Pujin, V. and Carey, A.E. (1992). Geochemistry of surface waters of Vojvodina, Yugoslavia, J Hydrol. 137: 33-55.

MacDonald, A.M., Darling, G.W., Ball, D.F. and Oster, H. (2003). Identifying trends in groundwater quality using residence time indicators: an example from the Permian aquifer of Dumfries, Scotland. Hydrogeology Journal 11: 504-517.

Mancha, R. (1949). The graphical symbolization of the chemical composition of natural waters: Hidrologie Kozolny Vol 13, pp.117-118.

Martinez, D.E. and Bocanegra, E.M. (2002). Hydrogeochemistry and cation-exchange processes in the coastal aquifer of Mar del Plata, Argentina. Hydrogeology Journal Vol 10 #3 pp 393-407.

Mathess, G. (1982). The properties of groundwater. Wiley, New York.

Mayo, A.L and Klauk, R.H. (1991). Journal of Hydrology 127: 307-335.

McGuinness, C.L. (1963). The role of groundwater in the national water situation. U.S. Geol. Survey. Water Supply Paper 1800.

McLean, W., Jankowski, J. and Lavitt, N. (2000). Groundwater quality and sustainability in an alluvial aquifer, Australia. *Groundwater: Past Achievements and Future Challenges*.

Offiong, O.E and Edet, A.E. (1997). Water quality assessment in Akpabuyo Cross river Basin South Eastern Nigeria. *Environmental Geology* 34 p.170.

Ohte, N. and Asano, Y. (1997). Global comparison of the pH determining factor of the streamwaters in the world forest basins. *Hydrochemistry. IAHS Publ # 244*. pp253-263.

Olayinka, A.I., Abimbola, A.F., Isibor, R.A and Rafiu,. (1998). A geoelectrical-hydrogeochemical investigation of shallow groundwater occurrence in Ibadan, Southwestern Nigeria. *Environmental Geology* 37 (1-2) pp33-34.

Ophori, D.U. and Toth, J. (1989). Patterns of groundwater chemistry, Ross Creek Basic, Alberta, Canada. *Groundwater* 27: 20-26.

Petrovic, G. (1980). Physico-chemical aspect of alkaline ponds in Yugoslavia. In: Dokuli S.M., Metz M, Jewson D (ed). *Development in hydrobiology* p.89-95.

Piper, A.M. (1944). A graphic procedure in the geochemical interpretation of water samples. *Am Geophys*.

Raji, R.A. and Alagbe, S.A. (1997). Hydrochemical facies in parts of the Nigerian Basement Complex. pp 46-49. *Environmental Geology* 29 (1/2).

Raju, J N. and Reddy, T.V.K. (1998). Fracture pattern and electrical resistivity studies for groundwater exploration. *Environmental Geology* 34 (2/3) pp 175-182.

Rao, S. N. (2003). Groundwater quality: focus on fluoride concentration in thr rural parts of Guntur district, Andhra Predesh, India. *Hydrological Science Journal* 48(5). pp 845.

Reuss, J.O., Cosby, B.J. and Wright, R.F. (1987). Chemical processes governing soil and water acidification. *Nature* 329, pp 27-32.

Ridder, T.B. (1978). On the chemistry of precipitation (in Dutch). Royal Met. Inst. Rep. 78-4, 45 pp.

Robertson, T. (1921). The geology of Western Togoland. Report of the Geological Survey of the Gold Coast (Ghana).

Sergey, V.A and Ludmila, P. A. (2003). Hydrochemistry of the permafrost zone in the central part of the Yakutian diamond-bearing province, Russia. *Hydrogeology Journal* Vol. 11 #5, pp 574-581.

Shoeller, H. (1935). Utilite de la notion des exchanges de bases pour la comparaison des aux souterraines: France, Societe Geologie Comptes rendus Sommaire et Bulletin Serie 5 V.5, P651-657.

Schoella, H. (1955). *Geochemie des eaux souterraines*. Rev Inst Fr 10: 230-244.

Schoella, H. (1962). *Leseaux souterraines*. Massio et cie, Paris, France pp 642..

Sracek, O. and Hirata, R. (2000). *Geochemical and stable isotopic evolution of the Guarani Aquifer System in the state of Sao Paulo, Brazil*. Hydrogeology Journal, Vol. 10 #6 pp 643-654.

Stallard, R.F and Edmund J.M. (1983). *Geochemistry of the Amazon and dissolved load*. J.Geophysical Reistivity 88: 9671- 9688.

Stiff, H.A., Jr. (1951). *The interpretation of chemical water analysis by means of patterns*: Journal of Petroleum Technology, V. 3, # 10 pp. 15-17.

Thomas, J.M., Welch, A.H. and Dettinger, M.D. (1996). *Geochemistry and isotope hydrology of representative aquifers in the Great Basin Region of Nevada, Utah and Adjacent States*. United States Geological Survey Professional paper: 1409-C pp. C3

Thorstenson, D.C., Fisher, D.W., and Croft, M.G., (1979). *The geochemistry of the Fox Hills-Basal Hell Creek aquifer in the Southwestern North Dakota and northwestern South Dakota*. Wateer Resources Research, Vol 15, #6, pp. 1479-1497.

Todd, D.K. (1980). *Groundwater Hydrology*. Second edition, John Wiley, New York, pp 535.

Urey, H.C. (1947). *The thermodynamic properties of isotopic substances*. Journal of Chemical Society, 1947:562-581.

Whitehead, H.C. and Feth, J.H. (1964). Chemical composition of rain, dry fallout and bulk precipitation in Menlo Park, California, 1957-59: *Journal of Geophysical Research*, V.69, pp 3319-3333.

Winograd, I.J. and Thordarson, William. (1968). Structural control of groundwater movement in miogeosynclinal rocks of Southern central Nevada; *Geological Society of America Memoir* 110, pp.35-48.

World Health Organization (WHO). (1993). Guidelines for drinking water quality. Revision of the 1984 guidelines . Final task group meeting. Geneva 21-25 September 1992.

Yapp, C.J. (1985). Deuterium/Hydrogen variations of meteoric waters in the Albuquerque, New Mexico. USA. *J.Hydrol.* 76: 63-84.

Zimmerman, U and Ehhalt, D.H. (1970). Stable isotopes in the study of water balance of Lake Nusiedl, Austria. *Isotopes in hydrology*, pp 567-585.

APPENDIX A

APPENDIX A - The stratigraphy, hydrogeologic properties and diagram of boreholes in the Buem and Voltaian Formations.

